EXPERIMENTAL STUDIES OF HEAVY-MINERAL TRANSPORTATION, SEGREGATION, AND DEPOSITION IN GRAVEL-BED STREAMS

by

ROGER ALAN KUHNLE

B.S. Northeastern Illinois University
(1977)

M.S. University of Illinois, Chicago
(1981)

Submitted to the Department of
Earth, Atmospheric, and Planetary Sciences
in Partial Fulfillment of the Requirements
of the Degree of

DOCTOR OF PHILOSOPHY

at the

MASSACHUSETTS INSTITUTE OF TECHNOLOGY

January 1986

Signature of Author ______________________
Department of Earth, Atmospheric, and Planetary Sciences, January 24, 1986

Certified by ______________________
John B. Southard
Thesis Supervisor

Accepted by ______________________
Chairman, Department Committee on Graduate Students

EXPERIMENTAL STUDIES OF HEAVY-MINERAL TRANSPORTATION, SEGREGATION, AND DEPOSITION IN GRAVEL-BED STREAMS

by

Roger Alan Kuhnle

Submitted to the Department of Earth, Atmospheric, and Planetary Sciences on January 7, 1986 in partial fulfillment of the requirements for the Degree of Doctor of Philosophy

Abstract

Flume experiments were conducted to determine the mechanisms of transport and deposition of heavy minerals in a gravel-bed channel in shallow unidirectional flows. Two water-recirculating sediment-feed flumes were used: one with a channel 6 m long and 0.15 m wide and the other with a channel 11 m long and 0.53 m wide. Poorly sorted gravel with a mean size of 3 mm with 3% by weight of magnetite (density 5.2 g/cm^3), lead (density 11.4 g/cm^3), and tungsten (density 19.3 g/cm^3) was used. The magnetite and tungsten were 0.125-0.500 mm in size, while the lead was 0.500-0.707 mm in size.

Total sediment transport rate out of the channel varied in all runs, at approximate periods of 3 minutes in the runs with high transport rates to 14 minutes in the runs with low transport rates. The runs with low transport rates also showed fluctuations in total transport rate at periods of about 25 minutes.

Fractional transport rates varied in all the runs. The transport rate of the 4-16 mm size fraction tended to peak before the total transport rate, while that of the 1-4 mm fraction tended to mirror the total transport rate, and that of the <1 mm fraction peaked after the total transport rate. This pattern of fractional transport rates was present in all runs except the one with the highest transport rate, in which the 16-32 mm, 1-2 mm, and the <1 mm fractions followed the same patterns as the above three fractions.

The variations in total and fractional transport rates were found to be caused by the migration of two different types of bed forms: very long and low (0.5-3 m long, 2-4 mm high) bed-load sheets in the runs with low and moderate transport rates, and dunelike bed forms (60 cm long, 1 cm high) in the run with the highest transport rate.

The beds were armored with coarse grains in all runs except that with the highest transport rate (Run H5), in which the size distribution of the bed surface was nearly the same as that of the original sediment mix.

The heavies became concentrated into a layer (here termed the heavy sublayer) composed of nearly 100% heavy minerals and lying beneath a layer of low-density sediment. Heavies were not transported in long-term equilibrium runs in a given region of the bed until the heavy sublayer was fully developed there.

Heavies were transported at the top of the heavy sublayer only when erosion of the active layer exposed the heavy sublayer to the flow. The bed forms in the low-density sediment of the active layer controlled the exposure of the heavy sublayer to the flow and caused the transport rate of the heavies to vary over the same time scales as the total transport rate. The longer-term fluctuations in the total transport rate of the sediment in the runs with low transport rates also caused the transport rate of the heavies to vary at that period (~25 min).

Heavy minerals were found not to be transported during aggradation of the bed unless the rate of general aggradation was very low or during general degradation unless the rate of degradation was very high. Otherwise, the presence of heavy sublayers is necessary for the transport of heavy minerals under aggradation or degradation.

Thesis Supervisor: Dr. John B. Southard
Associate Professor of Geology

TABLE OF CONTENTS

Abstract ii

Table of Contents iv

List of Figures vii

List of Tables x

Acknowledgements xii

Introduction 1

Part I - Sediment Transport in a Gravel-Bed Laboratory Channel 3

Abstract 4

Introduction 5

Experiments 9

Equipment 9

Procedure 14

Data Collection 16

Results 20

General 20

Sediment Transport Rate vs. Time 22

General 22

Runs H1, H2, and L2 22

Runs L1 and H3 33

Run H5 35

Bed-Surface Grain-Size Distributions 36

Transport Rates of Individual Size Fractions 40

Processes of Transport 46

General 46

Observations on Sediment Transport 49

Fourier Analysis of Periodicity 56

Summary of Results 62

Bed Surface Textures 62

Transport Rates 63

Bed Forms 63

Discussion 64

Bed Forms 64

Comparison with Field Examples 67

Implications for Bed-load Sampling 71

Conclusions 76

References 78

Part II - Transport of Heavy Minerals 81

Abstract 82

Introduction 83

Previous Work 90

Experiments 100

Equipment 100

Procedure 109

General 109

Runs with Steady Conditions 109

Degrading-Bed Runs 111

Data Collection 112

Runs with Steady Conditions 112

Degrading-Bed Runs 113

Extraction of Heavies 115

Results 118

Introduction 118

Runs H1 and H2 118

General 118

Transport Samples 132
Bed Samples 134
Run H3 143
General 143
Transport Samples 146
Bed Samples 148
Run H5 150
General 150
Transport Samples 151
Bed Samples 153
Run H4 155
Summary of Steady-State Runs 158
Transport of Heavies during Degradation 161
General 161
Bed Samples 164
Transport Samples 168
Analysis 170
Discussion 172
Transport of Heavies during Aggradation 172
Bedrock Placers 175
Heavy Sublayers 177
Applications to Natural Systems 188
Formation of Placers 194
Conclusions 197
References 200
Biographical Sketch 206
Appendix 207

LIST OF FIGURES

Part I

FIG. 1.-- Schematic diagram of 6 m flume 10

FIG. 2.-- Schematic diagram of 11 m flume 11

FIG. 3.-- Photographs of the two flumes 12

FIG. 4.-- Grain-size distribution, lights, heavies and lights 15

FIG. 5.-- Photographs of piston sampler 18

FIG. 6.-- Total transport rate vs. time, Run L1 23

FIG. 7.-- Total transport rate vs. time, Run L2 24

FIG. 8.-- Total transport rate vs. time, Run H1 25

FIG. 9.-- Total transport rate vs. time, Run H2 26

FIG. 10.-- Total transport rate vs. time, Run H3 27

FIG. 11.-- Total transport rate vs. time, Run H5 28

FIG. 12.-- Photographs of a clast jam, Run H2 31

FIG. 13.-- Grain-size distribution of bed-surface samples. Run numbers for each sample are shown. 38

FIG. 14.-- Water-surface slope vs. time, Run H3 41

FIG. 15.-- Fractional and total transport rates vs. time, Run H1 43

FIG. 16.-- Fractional and total transport rates vs. time, Run H2 44

FIG. 17.-- Fractional and total transport rates vs. time, Run H3 45

FIG. 18.-- Fractional and total transport rates vs. time, Run H5 47

FIG. 19.-- Fractional transport rates vs. time, Run H5 48

FIG. 20.-- Cross-sectional profiles of bed forms parallel to flow direction, Run H5. No vertical exaggeration 54

FIG. 21.-- Periodogram for total transport rate vs. time data, Run L1. Peaks above horizontal line are significant. 58

FIG. 22.-- Periodogram for total transport rate vs. time data, Run L2. Peaks above horizontal line are significant. 59

FIG. 23.-- Periodogram for total transport rate vs. time data, Run H1. Peaks above horizontal line are significant. 60

FIG. 24.-- Coefficient of variation vs. sample length, Runs L1, L2, and H1 73

Part II

FIG. 1.-- Forces acting on a grain 86

FIG. 2.-- Schematic diagram of 6 m flume 102

FIG. 3.-- Schematic diagram of 11 m flume 103

FIG. 4.-- Photographs of the two flumes 104

FIG. 5.-- Photograph of tailgate on 6 m flume 105

FIG. 6.-- Grain-size distribution, lights, heavies and lights 107

FIG. 7.-- Grain-size distributions of the heavies 108

FIG. 8.-- Photographs of piston sampler 114

FIG. 9.-- Photograph of heavy sublayer through flume sidewall, Run H2. Flow direction was left to right. 123

FIG. 10.-- Photograph of heavy sublayer after erosion experiment, Run H2 124

FIG. 11.-- Three phases in the formation of a heavy sublayer. 126

FIG. 12.-- Photographs of heavy sublayer patches, plan view, Run H2. 128

FIG. 13.-- Cross-sectional profile of bed perpendicular to flow direction, Run H2. Exposed patch of heavy sublayer is designated by the solid circles. 130

FIG. 14.-- Photograph of successive heavy sublayers in the upstream 1 m of the bed, Run H2. Flow direction was left to right. 133

FIG. 15.-- Magnetite, lead, and total transport rates vs. time, Run H2, part 1 135

FIG. 16.-- Magnetite, lead, and total transport rates vs. time, Run H2, part 2 136

FIG. 17.-- Photographs of heavy sublayer patches, plan view, Run H3. Flow direction was left to right. 145

FIG. 18.-- Magnetite, lead, and total transport rates vs. time, Run H3 147

FIG. 19.-- Magnetite and 1-2 mm fraction transport rates vs. time, Run H5 152

FIG. 20.-- Bed and water surface elevations vs. time, Run H6. Locations were (A) 1.5 m, (B) 3.5 m, and (C) 5.5 m from the upstream end of the channel. Solid symbols are the bed elevation and open symbols are the water surface elevation. 163

FIG. 21.-- Cross-sectional profile of bed forms parallel to flow, Run H6. No vertical exaggeration. 165

FIG. 22.-- Concentrations of heavies in the bed for high and low values of aggradation and degradation ratios 178

FIG. 23.-- Concentration factor vs. density. Concentration factor is defined as the ratio of the concentration of a given size-density fraction in a bed sample to the concentration of that fraction in the original sediment mix. 179

FIG. 24.-- Reactive angles for three different size grains on a bed of unisize grains. As shown the reactive angle decreases with increasing grain size. (from Z. Li and P.D. Komar, unpub. manuscript) 181

FIG. 25.-- Ratio of critical shear stress for the i-th fraction to the critical shear stress of the mean size of the sediment (τ_{ci}/τ_{cm}) vs. the ratio of the size of the i-th fraction to the mean size (D_i/D_m). 182

FIG. 26.-- Grain-size distributions for 2.5 cm thick bed samples, Run H1 186

LIST OF TABLES

Part I

Table 1. Pulse Intervals for a Variety of Gravel-Bed Channels 7

Table 2. Experimental Conditions 21

Table 3. Mean, Standard Deviation, Coefficient of Variation, and Range of Transport Rates 29

Table 4. Mean and Coefficient of Variation for the Five 30-Minute Segments of the 150-Min Data 34

Table 5. Description of Bed-Load Sheets 51

Table 6. Significant Periods of Transport Fluctuations from Fourier Analysis 61

Table 7. Grain-Size Characteristics for Experimental Studies using Fine Gravel Sediment 65

Table 8. Grain Size, Flow Characteristics, and Bed Phase for This Study 65

Table 9. Grain Size, Flow Characteristics, and Bed Phase for Studies using Fine Gravel Sediment 66

Part II

Table 1. Physical Properties of the More Common Placer Minerals 84

Table 2. Observed Sites of Water-Laid Placers 91

Table 3. Reported Sizes of Detrital Gold 99

Table 4. Experimental Conditions 119

Table 5. Percentages of Heavies in Bed-Surface Samples, Runs H1 and H2 137

Table 6. Percentages of Heavies in Vertical Bed Samples, Runs H1 and H2 139

Table 7. Average Aggradation Rates of each Set, Run H1 142

Table 8. Percentages of Heavies in Bed-Surface Samples, Run H3 149

Table 9. Percentages of Heavies in Vertical Bed Samples, Run H3 149

Table 10. Percentages of Heavies in Bed Samples, Run H5 154

Table 11. Percentages of Heavies in 1.25 cm Samples, Run H4 157

Table 12. Percentages of Heavies in Vertical Bed Samples, Runs H6 and H7 166

Table 13. Percentages of Heavies in Bed-Surface Samples, Runs H6 and H7 167

Table 14. Percentages of Heavies in Transport Samples, Runs H6 and H7 169

Table 15. Values of u_*/w for Various Sizes and Densities of Heavies 192

ACKNOWLEDGEMENTS

The research of this thesis could not have been done without the help of many others.

I would like to thank John Southard for his guidance throughout this study. This study would not have been possible without his help.

The past and present members of the Center for Experimental Sedimentology provided invaluable assistance in the design and construction of the experimental equipment, and without their assistance the collection of much of the sediment transport data contained in this thesis would not have been possible. They were also good friends. Thanks again Kevin Bohacs, Bill Corea, Bill Chesterson, Bob Grazer, Chris Paola, Doug Walker, Jim Danna, Peter Wilcock, Joe Cerutti, Cathy Summa, Byron Williams, Scott Stull, Dave Klepacki, Mary Hubbard, and John Goodman. I would like to especially thank Peter Wilcock for use of his computer plotting subroutine and for the many animated discussions we had on sediment transport.

I thank the members of my committee: Dave Roy, Leigh Royden, Rudy Slingerland, and Norm Smith for carefully reading the manuscript and offering many constructive comments.

I would like to thank Dorothy Frank for much assistance in the typing and format of this document.

I would like to thank my parents for giving me encouragement and support throughout my education.

And lastly I would like to thank Mari, my wife, for a large amount of love, understanding, and support throughout the often rocky road towards finishing this degree. Mari and Alyssa, our daughter, have helped me keep my sense of humor and perspective during our time here.

This project was funded in part by a grant from Anglovaal Mining Company, South Africa and a thesis improvement grant, no. EAR 8415466, from the National Science Foundation.

INTRODUCTION

Despite many excellent studies, the transport and deposition of heavy minerals (defined here as those with density greater than 3.5 g/cm^3) in alluvial streams is still not well understood. In this study this problem has been approached by use of a mixture of heavy minerals and quartz-density sediment in a small alluvial channel in the laboratory. Quartz-density sediment in the pebble size range and heavy minerals in the fine and medium sand range were chosen for these experiments, because heavy minerals are often concentrated in gravelly sediments (Hails, 1976; Minter, 1978). Heavy-mineral transportation and deposition over a range of flow conditions and transport rates were investigated in this study.

The processes of transport of heavy minerals ("heavies") and quartz-density minerals ("lights") in a mixed-density sediment are to a substantial degree interactive; this will be dealt with in more detail in a later section. Specifically, it has been determined from this investigation that the movement of heavies in the sediment mix is strongly affected by the mechanisms by which the lights are transported. Looking at this situation from the other side, the heavies have been shown to have only a minor effect on how the lights are transported. The effect of the heavies on the lights was tested by making two runs (described in a later section) with conditions identical except that there was 3% heavies by weight in the sediment of one run and no heavies in the sediment of the other. No significant differences could be detected in the transport of the lights in the two runs.

This report is organized into two parts. Part I deals exclusively with the transport of the lights over the range of conditions studied. In Part II the mechanisms of transport of the heavies are related to those of the lights. This two-part approach is seen as a coherent way of presenting the results of this study.

PART I

SEDIMENT TRANSPORT IN A GRAVEL-BED LABORATORY CHANNEL

ABSTRACT

Flume experiments were conducted to investigate the mechanisms of transport of a gravel-sand mixture by shallow unidirectional flows. Two water-recirculating sediment-feed flumes were used: one with a 6 m long and 0.15 m wide channel and the other with an 11 m long channel with widths of 0.74 m and 0.53 m. The sediment, poorly sorted gravel with a mean size of 3 mm, was fed at the upstream end of the channel at steady rates from 0.03 kg/s·m to 1.0 kg/s·m. Sediment transport rate out of the channel varied in all runs, at approximate periods of 3 minutes in the runs with high transport rates to 14 minutes in the runs with low transport rates. The runs with low transport rates also showed fluctuations in total transport rate at periods of about 25 minutes.

Fractional transport rates varied in all the runs. The transport rate of the 4-16 mm size fraction tended to peak before the total transport rate, while that of the 1-4 mm fraction tended to mirror the total transport rate, and that of the <1 mm fraction peaked after the total transport rate. This pattern of fractional transport rates was present in all runs except the one with the highest transport rate, in which the 16-32 mm, 1-2 mm, and the <1 mm fractions followed the same patterns as the above three fractions.

The variations in total and fractional transport rates were found to be caused by the migration of two different types of bed forms: very long and low (0.5-3 m long, 2-4 mm high) bed-load sheets in the runs with low and moderate transport rates, and dunelike bed forms (60 cm long, 1 cm high) in the run with the highest transport rate.

The beds were armored with coarse grains in all runs except that with the highest transport rate (Run H5), in which the size distribution of the bed surface was nearly the same as that of the original sediment mix.

INTRODUCTION

Transport mechanisms in gravel-bed streams are not well understood, because the nature of the transport processes is complicated and gravel-bed streams are difficult to study in both the laboratory and the field.

One approach to the study of sediment transport in gravel-bed streams has been to consider large-scale channel features. Many studies have concentrated on large-scale bar and channel processes and their associated deposits (Krigström, 1962; Williams and Rust, 1969; McDonald and Bannerjee, 1971; Church, 1972; Eynon and Walker, 1974; Smith, 1974; Boothroyd and Ashley, 1975; Hein and Walker, 1977; Miall, 1977; Maizels, 1979; Ashmore, 1982). Many of these studies have noted large variations in transport rate over relatively short times.

Much work has been done recently to improve the measurement of sediment transport rates in gravel-bed streams. Measurement with hand-held basket samplers, the simplest technique in small streams, has often proved inadequate, prompting the development of sampling techniques that trap virtually all of the bed load transported past a channel cross section. Notable examples of these include: fences built across the entire width of a river (Østrem, 1975; Hammer and Smith, 1983), a vortex bed-load sampler (Klingeman, Milhous, and Heinecke, 1979), a slotted weir and basket sampling arrangement (Kang, 1982), a slot sampler (Reid, Frostick, Layman, 1985), and a conveyor-belt bed-load sampler (Leopold and Emmett, 1976). A summary of sampling techniques and problems is given by Klingeman and Emmett (1982).

With improvement in measurement techniques, new complexities in the patterns of sediment transport have been discovered. In several studies, repetitive sampling at closely spaced time intervals has shown the transport rate to vary strongly with time. Some of this variability has been related to dunes similar to those in sand-bed streams (Hubbell et al., 1981), but in other cases transport fluctuations at two or more scales have been found without any noticeable bed forms (Kang, 1982). Reid, Frostick, and Layman (1985) found variations in transport on time scales much longer than reported by others. Table 1 lists the periods, or pulse intervals, over which transport in gravel-bed streams has been found to fluctuate.

The main purpose of the experiments described here was to simulate the conditions of a small part of a gravel-bed stream in a laboratory channel. Over a wide range of conditions of flow and sediment feed rate, the transport mechanisms on the bed were characterized and the transport of sediment out of the channel was measured at closely spaced time intervals in order to be able to relate the variations in sediment transport rate to the processes operating in the channel. Water discharge, channel width, sediment feed rate, and sediment size distribution were selected before each run and held constant throughout the run. Sediment feed rate was varied by a factor of 30.

Table 1. PULSE INTERVALS FOR A VARIETY OF GRAVEL-BED CHANNELS

Reference	River	Flow	Pulse Interval (hrs)
Ehrenberger, 1931	Danube, Austria	??	0.3
Muhlhofer, 1933	Inn, Austria	??	0.1
Einstein, 1937	Rhine, Switz.	steady	20.0
Solov'yev, 1967	Mzymta and Ugam, USSR	??	0.2
Emmett, 1975	Slate Cr., Idaho, USA	steady	0.1-0.7
Kang, 1982	Hilda Cr., Alberta, Canada	unsteady	0.25, 0.5
Reid, Frostick, and Layman, 1985	Turkey Brook, England	unsteady	1.4-2.0
Whiting, Leopold, Dietrich, Collins, 1985	Duck Cr., Wyoming USA	steady	0.15-0.25
Hubbell et al., 1981	Laboratory channel	steady	0.2, 1.0
This study	Laboratory channel	steady	0.1, 0.2, 0.4

(after Reid, Frostick, and Layman, 1985)

Note: The pulse intervals tabulated above are the mean periods between peaks in the total transport rate for the indicated studies.

The conditions of flow and sediment feed rate used in the experiments were chosen to represent, as nearly as possible within the restrictions of the equipment, a longitudinal slice of a shallow gravel-bed stream. The main restriction on the flows that could be used was the resulting value of the width-to-depth ratio. Width-to-depth ratios close to or less than one cause the velocity profile of the flow to be grossly different from that present in most natural streams. Thus depths in the flumes were restriced to less than 10 cm. Transport rates per unit width were not nearly as restricted and covered most of the range that has been measured in natural streams.

Strictly, the results of this study apply directly only to steep, shallow, gravel-bed streams. However, the similarity of the results of this study when compared to studies of larger natural streams indicates that comparisons only to steep, shallow, streams is too restrictive (see Discussion section below). It appears that streams with fine gravel beds and transport rates per unit width in the same range as in this study will probably be associated with processes of transport that are at least qualitatively similar to those observed in this study.

The organization of the rest of this report is as follows: first the equipment and techniques will be described, then the experimental data will be presented, and finally data analysis and conclusions will be given.

EXPERIMENTS

Equipment

All runs were made in two tilting flumes in the Experimental Sedimentology Laboratory at the Massachusetts Institute of Technology. The larger had a channel length of 11 m and widths of either 0.74 m or 0.53 m, and the smaller was 6 m long and 0.15 m wide (Figs. 1-3). Water was recirculated, but sediment was fed at the upstream end of the channel and caught in a large box in the tailbox or sump at the downstream end of the channel. Water discharge was controlled by a gate valve in the return pipe and was measured with a calibrated Venturi meter and manometer to within ±5% in the larger flume and with a calibrated 90° bend meter and manometer to within ±4.5% in the smaller flume. The accuracy of the water discharge was determined by careful measurement of the volume of water pumped at a given valve setting during a known time interval in repeated calibration runs. Elevations of the bed surface and water surface were measured with a point gauge mounted on a platform that moved along rails attached to the channel walls.

Sediment was fed into the upstream end of the larger channel from a slowly moving conveyor belt that spilled off a uniform thickness of sediment. Feed rate could be varied by changing the belt speed or the thickness of the sediment pile. Feed rate was found to vary within ±4% over one complete cycle of the sediment feeder (2-5 hours), by taking timed samples of the sediment feed at intervals during the course of the feeder

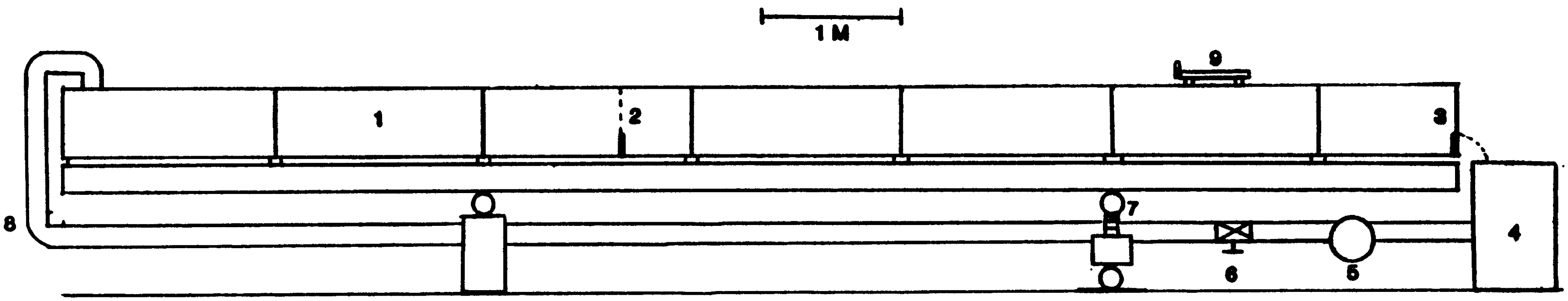

FIG. 1.-- Schematic diagram of 6 m flume

1. headbox
2. weir and baffle
3. downstream weir
4. tail barrel
5. pump
6. gate valve
7. adjustable support
8. 90° elbow meter
9. instrument platform

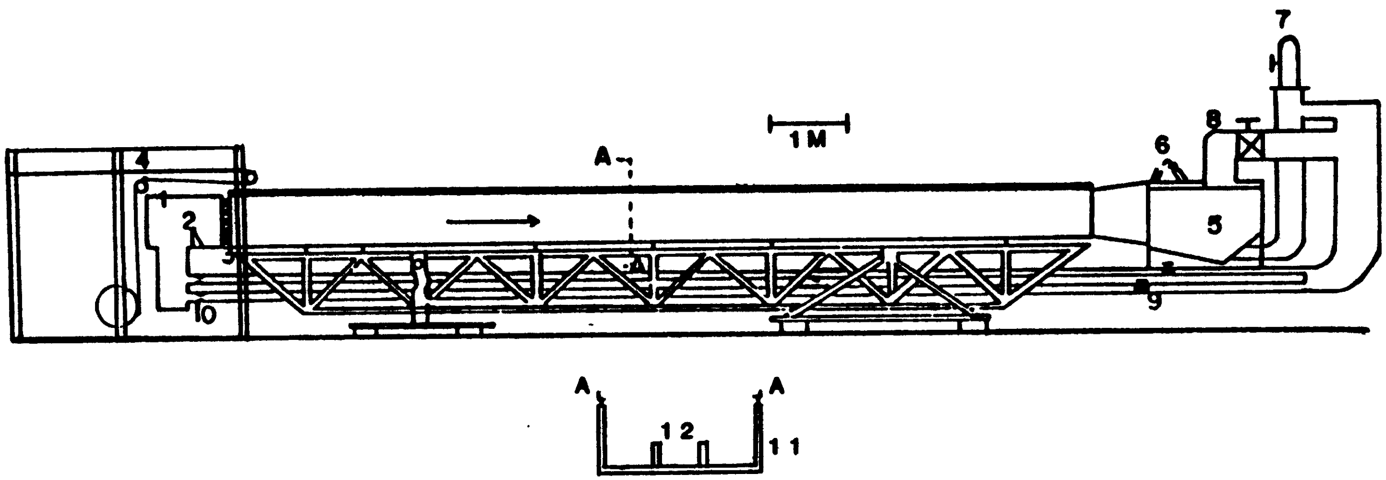

FIG. 2.-- Schematic diagram of 11 m flume

1. headbox	7. pump
2. weir	8. bypass line and valve
3. baffle	9. return lines and valves
4. sediment feeder	10. Venturi meters
5. tailbox	11. plywood channel
6. filtration system	12. 0.5 m wide inner channel

A

B

FIG. 3.-- Photographs of the two flumes.
A-- 6 m flume, B-- 11 m flume

cycle. In the smaller flume, sediment was fed by hand in a 120-second cycle; doses were spread over 90 to 105 seconds, with the remaining time used for refilling and weighing the container. The readability of the balance was such that the variation of feed was about ±4%.

In the large flume, sediment transported out of the channel was measured using a wire-mesh-covered gate on the tailramp of the channel and baskets covered with wire cloth with 0.1 mm openings. When closed, the gate caused the sediment transported out of the channel to be stored briefly on the tailramp without disrupting transport in the channel upstream. This was possible because the flow on the tailramp was supercritical and did not back up to the alluvial channel during the 30-second sample times. When the gate was opened, the flow flushed the sediment off the ramp into one of the mesh-covered baskets. The basket was then emptied through a large funnel into a sample container, one of a numbered series of three-liter metal cans. In the small flume the sampling arrangement was similar except that the channel ended in a free overfall into a sump. The sediment was caught in a sample basket, also covered with wire cloth with 0.1 mm openings, placed in the overfall, and then emptied through a large funnel into one of the sample containers.

The sediment was obtained by wet-sieving locally available outwash gravel and combining size fractions to obtain the desired size distribution. The sediment mix ranged from 0.125 to 32 mm (3.0 to $-5.0\ \phi$) with a median size of 3.03 mm ($-1.6\ \phi$)

and a standard deviation of 1.3 ϕ, where $\phi = -\log_2$(diameter in mm) (Fig. 4). The sediment in one run in the large flume and all but two of the runs in the small flume contained 3% by weight of heavy minerals (a mixture of magnetite, lead, and tungsten) ranging in size from 0.125 mm to 0.707 mm. As discussed below, by making two runs with conditions identical except for heavy-mineral content it was determined that the heavies had only a minor effect on the transport of the lights.

Procedure

The first step in preparing the flume for a run was to fill the channel with thoroughly homogenized sediment and level the bed with a channel-wide scraper suspended from the channel rails. In the large flume the next step was to adjust the speed of the conveyor-belt feeder and the height of the sediment pile to produce the desired feed rate. In the small flume the appropriate size of feed container was determined and constructed such that when full the proper weight of sediment per dose was attained. The flume was then filled with water, the pumps were started, and the water discharge was adjusted to the desired value. Each run was subdivided into a series of time intervals during which separate sets of measurements, hereafter simply called sets, were taken. Each set spanned the period of time in which the flume ran continuously. The flumes could not be run continuously for longer than about 5 hours, because the feed system in the large flume could be run only for up to 5 hours without being reset, and the tail barrel in

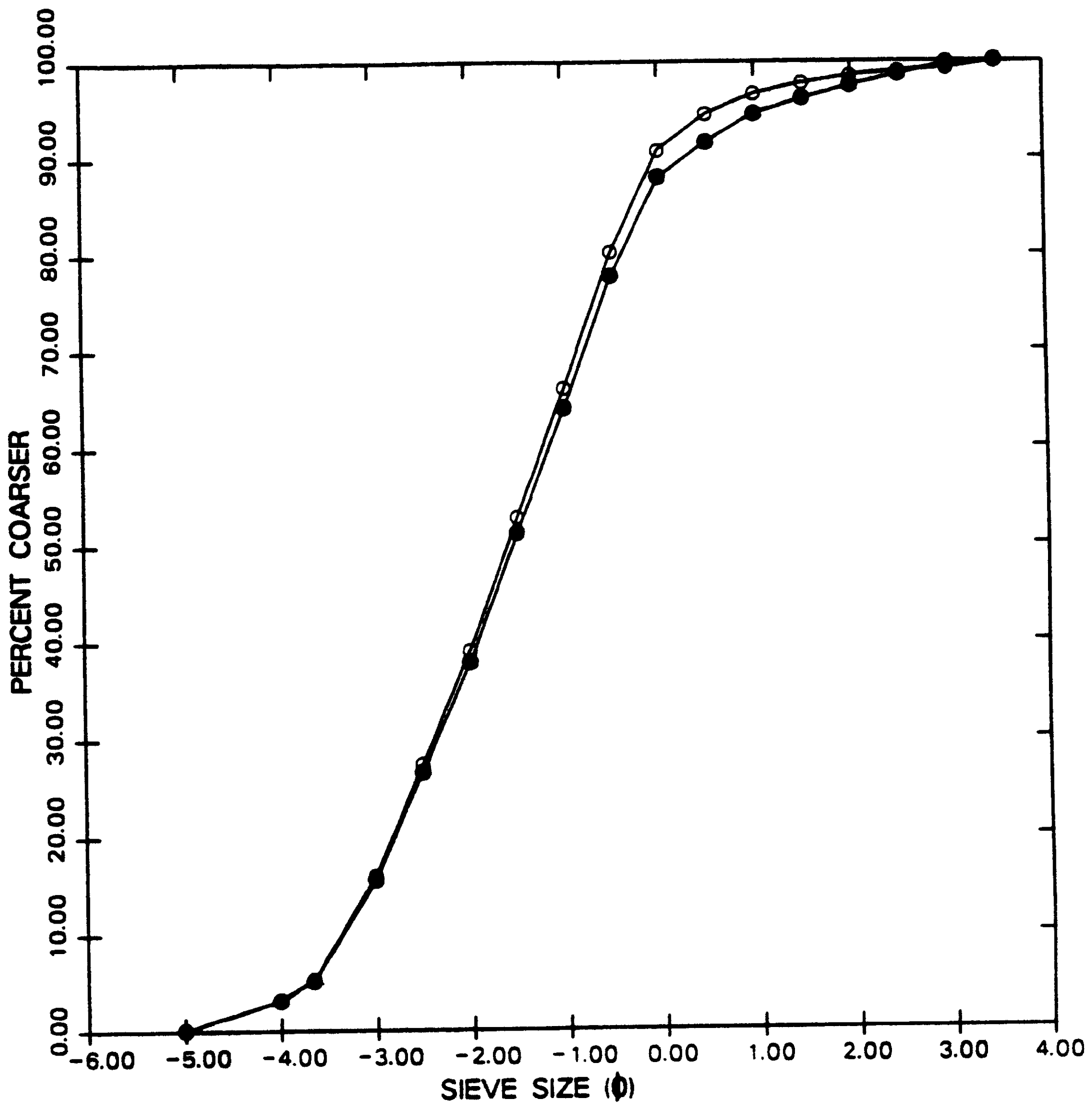

FIG. 4.-- Grain size distribution

o -- lights
● -- heavies and lights

the small flume filled with sediment in about the same time. The number of sets in each run was a function of the feed rate and total duration of the run. Water temperature and water-surface slope were measured during each set. Between sets, with the pump off, the bed-surface elevation and the quantity of sediment in the catchbox were measured. The bed-surface elevation was measured in flow-transverse traverses (with measurement points spaced 5 cm in the large flume and 1.5 cm in the small flume) at stations every 0.5 m down the channel beginning one meter downstream from the headbox. Each traverse was then averaged to give one elevation for each station, and slopes were calculated by fitting a least-squares straight line to the plot of elevation vs. position. The sediment transported out of the channel was measured volumetrically and then converted to a mass rate and compared to the sediment feed rate during the set. (Sediment volume was converted to sediment mass by filling containers with known volumes with wet sediment and then drying and weighing them. The value of the average of ten containers was used as the mass value for a given volume. The masses of these standard volumes were all within ±7%.) Equilibrium was considered to have been reached when the sediment transport rate out of the channel was nearly equal to the feed rate for two consecutive sets. The channel was then ready for sediment-transport measurements.

Data Collection

After equilibrium had been attained, sediment transport was measured by catching all sediment transported out of the channel in 30-second intervals. Data gathering in each of the three runs in the large flume lasted 150 minutes, thus generating 300 samples per run. Transport-measurement periods in the small flume were 30 to 60 minutes long. Each sample was placed in a metal can, oven-dried, and weighed. For Run H1 in the large flume, 200 of the samples were sieved to determine the transport rate of the various size fractions. Some samples from each of the sampling periods of the runs in the small flume were also sieved.

The bed surface was sampled at several locations at the end of each run. A piston sampler 13 cm in diameter modeled after one used by Dhamotharan et al. (1980) was constructed (Fig. 5). The piston was coated with a stiff mixture of clay and water, and when pushed into the bed, picked up essentially only the surface layer of grains.

To ascertain the mechanisms of grain transport and their relationship to transport rate, grain motion on the bed was observed while transport was being sampled. Since transport samples were an important source of data in this study, it was important to assess the possible errors in their measurement. Individual 30-second samples were estimated to be accurate to within ±2%, based on the accuracy in the sample times and on the mass of sediment lost to the tailbox averaged over the length of the sampling period. Average values of sediment transport rate at the channel exit, found by averaging the 150-minute sampling strings, differed from the corresponding sediment feed rates by a few percent in the large flume

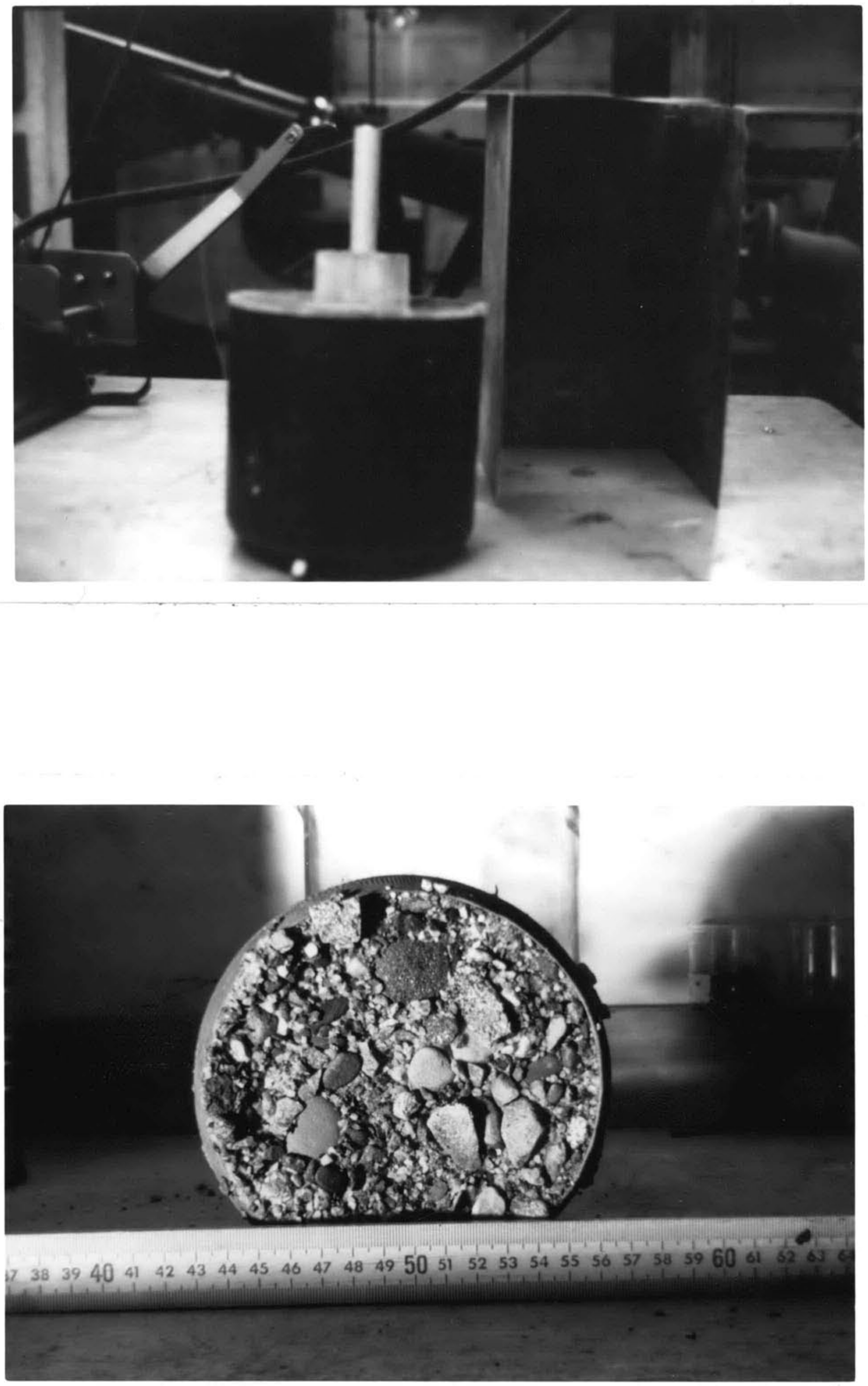

FIG. 5.-- Photographs of piston sampler

(Run L1, 5.1%; Run L2, 5.8%; Run H1, 6.4%). For the runs in the small flume in which the sample periods were 30 minutes (except Run H3) the mean measured transport rates differed from the corresponding feed rates by considerably more than for the longer sampling periods taken in the large flume. The range in differences for the shorter strings is from 7% to 36%. Only a small part of this difference can be explained by sampling errors; most is due to the shorter length of the sampling periods, which were not long enough to account for the longer-term fluctuations in the transport rate (see Table 3).

RESULTS

General

Seven runs are considered in this section: three, denoted by L in Table 2, had no heavies in the sediment mix, and the other four, denoted by H, had 3% by weight of heavies in the sediment mix. Sediment transport varied with time in all of these runs. In this section the time scales of variation in the transport rate are identified and related to the transport processes causing the variation.

In the large flume, the first two runs (Runs L1 and L2) were made with a channel width of 74 cm. The channel was then narrowed to 53 cm to eliminate alternate bars that formed in the wider channel. These alternate bars were areas where the bed on one side of the channel was higher than on the other side of the channel, although still submerged. After these features formed they did not change appreciably in shape or position. By observing these features during the runs it was concluded that they did not significantly affect sediment transport in the channel. No such stable bars were present in the run with the narrower channel (Run H1).

The approach for the rest of this section will be to consider, for all the runs, (i) total sediment transport rate vs. time, (ii) bed surface grain-size distributions, (iii) transport of individual size fractions, and (iv) the processes of transport responsible for the patterns of variation of transport rate with time.

Table 2. EXPERIMENTAL CONDITIONS

Run	Channel Width (m)	Flow Depth (m)	Fluid Discharge ($m^3/s \cdot m$)	Sediment Feed Rate ($kg/s \cdot m$)	Water Temp. (^oC)	Bed Slope	Mean Flow Velocity (m/s)
L1	0.74	0.036	0.028	0.081	13.5-16.1	0.019	0.77
L2	0.74	0.041	0.028	0.041	10.5-13.2	0.019	0.67
L3	0.15	0.046	0.035	0.034	23.4-25.8	0.024	0.77
H1	0.53	0.046	0.035	0.034	10.2-12.6	0.019	0.77
H2	0.15	0.045	0.035	0.034	18.5-23.5	0.024	0.77
H3	0.15	0.074	0.067	0.098	21.6-25.2	0.015	0.90
H5	0.15	0.069	0.089	1.073	25.4-25.5	0.021	1.29

To determine whether the heavies affected the transport of the lights in the runs with heavies, Run L3 was made with the same conditions of flow and sediment feed rate as Run H2 except that there were no heavies in the sediment. In all aspects of flow and sediment transport Run L3 was very similar to Run H2, so the heavies had only a minor effect on the transport of the lights.

Sediment Transport Rate vs. Time

General

For all of the runs except Run L3, all the sediment transported out of the channel was caught in mesh-covered baskets and placed in sample containers at 30-second intervals. In Run H5 transport was sampled for only 15 seconds out of every 30 seconds. In Runs L1, L2, and H1, transport was sampled continuously for 150 minutes, thus generating 300 discrete samples. Run H2 was sampled for 30 minutes in three separate time intervals, Run H3 for 60 minutes and Run H5 for 30 minutes. Figures 6-11, plots of total sediment transport rate with time, show that transport rate varied widely and quasi-periodically in all of the runs, with the possible exception of Run H5 (see Table 3).

Runs H1, H2, and L2

By design, Runs H1 and H2 were identical in discharge per unit width and feed rate per unit width (hereafter termed unit discharge and unit feed rate); this allows us to determine if there were any significant differences in sediment transport

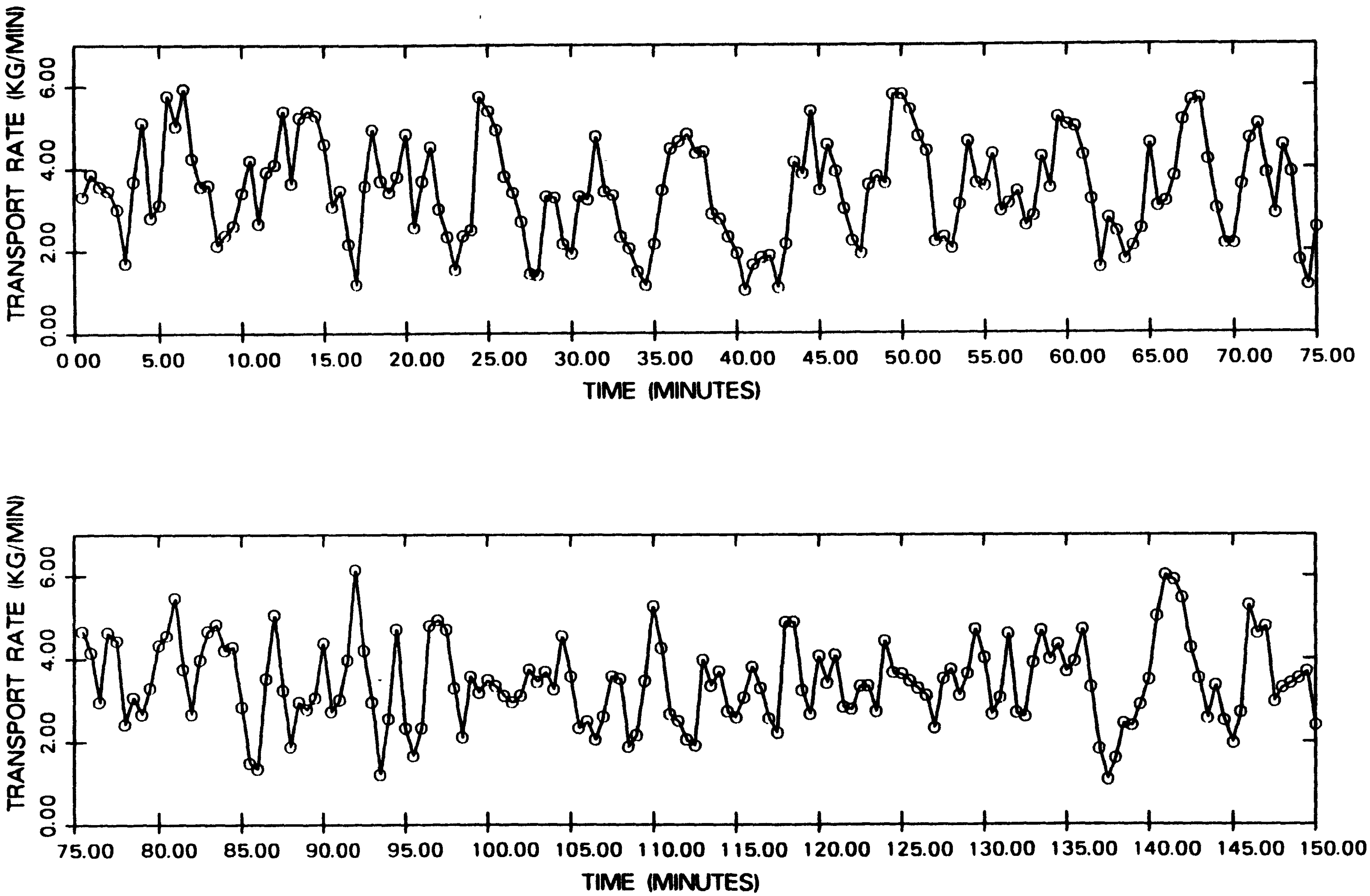

FIG. 6.-- Total transport rate vs. time, Run L1

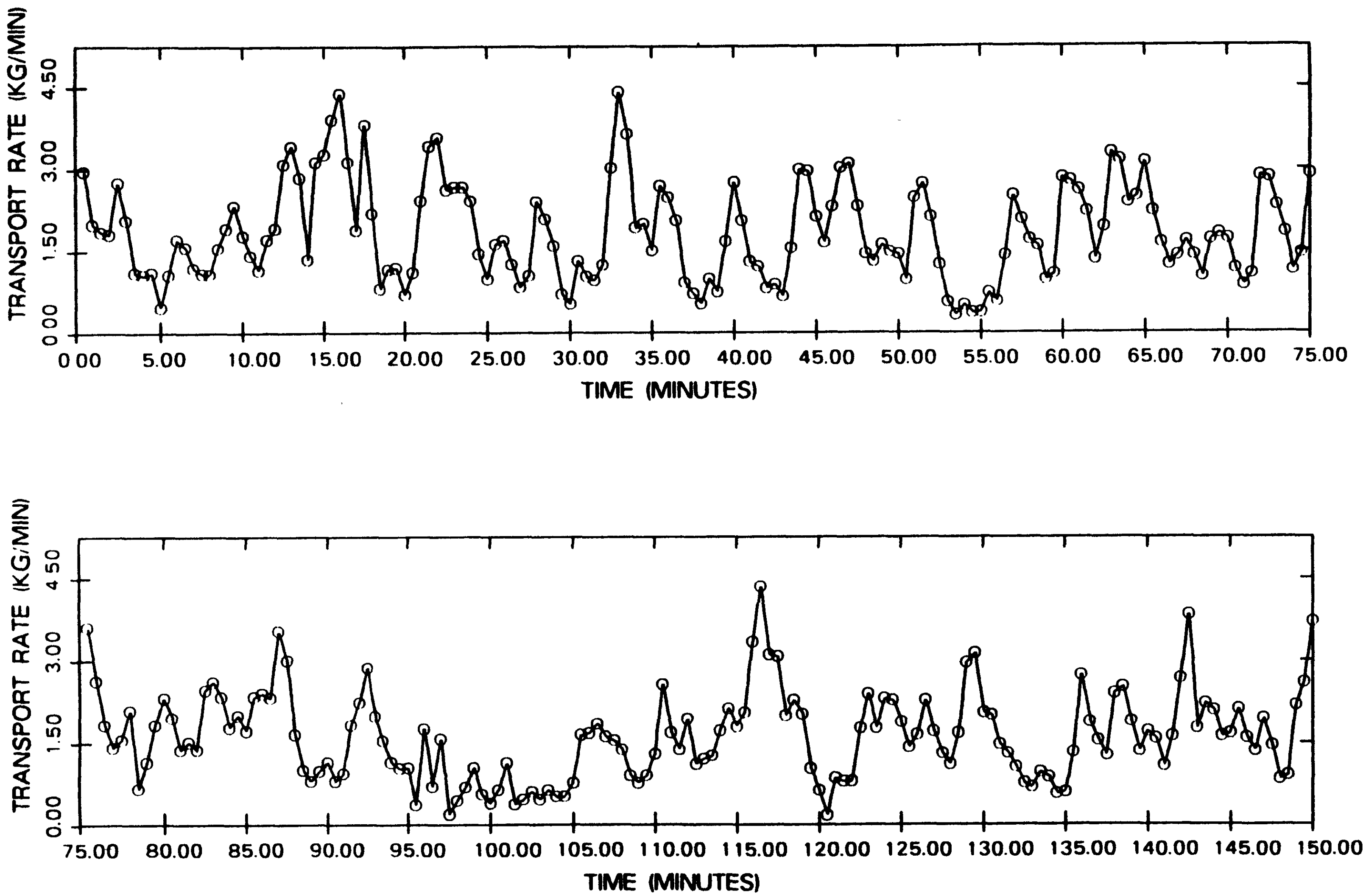

FIG. 7.-- Total transport rate vs. time, Run L2

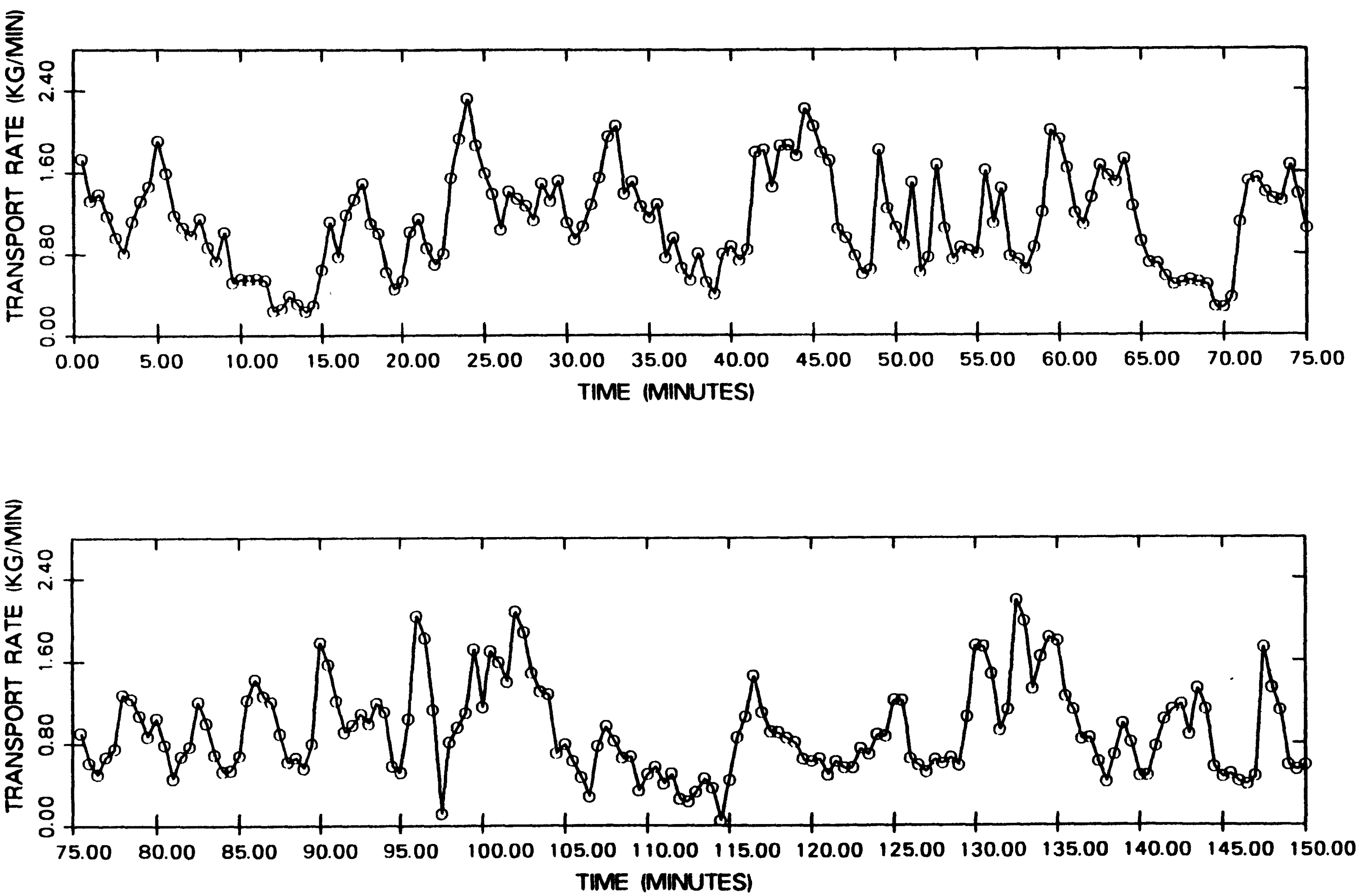

FIG. 8. -- Total transport rate vs. time, Run H1

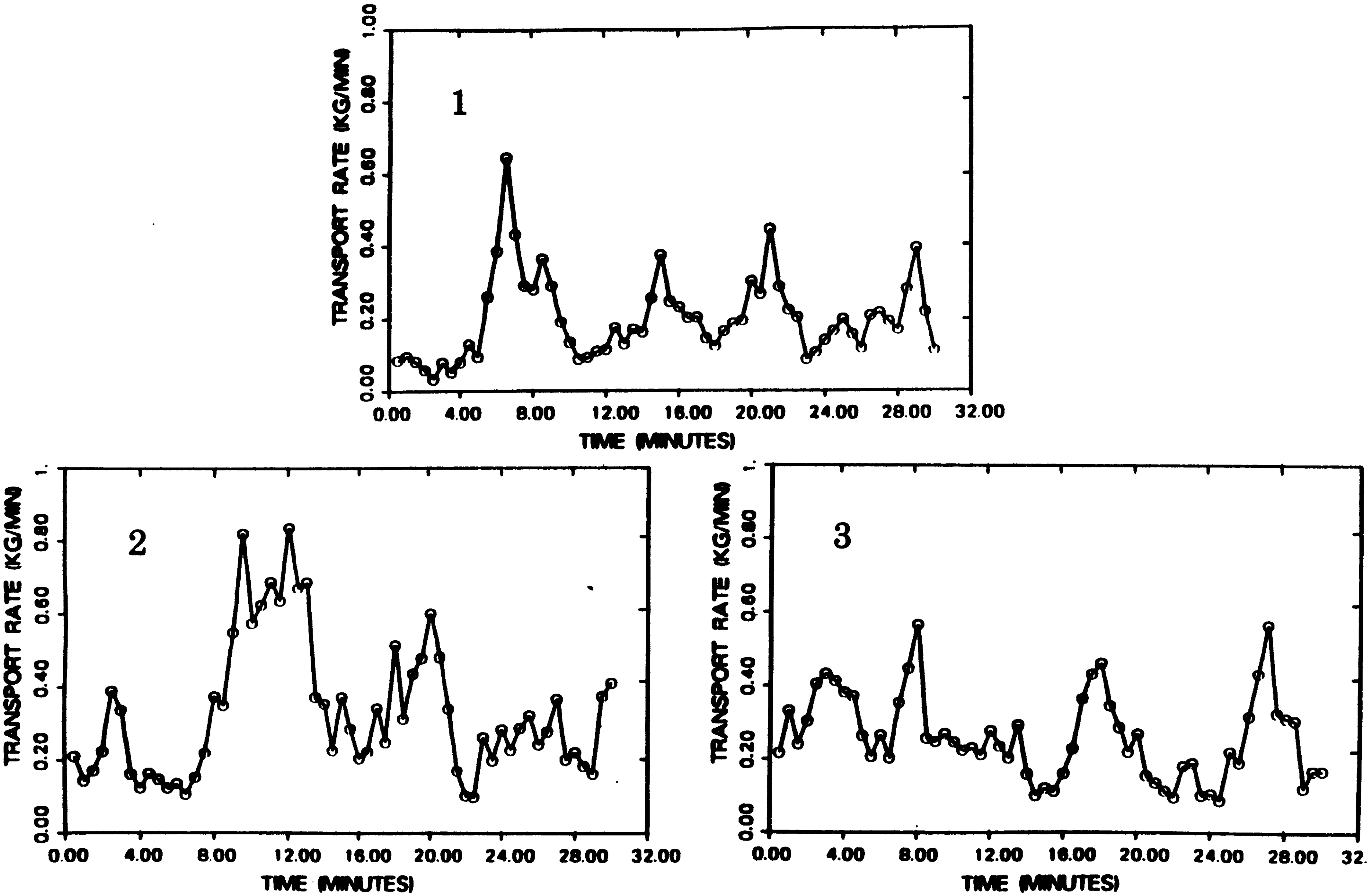

FIG. 9.-- Total transport rate vs. time, Run H2
The three sampling periods were separated
by one hour of running time.

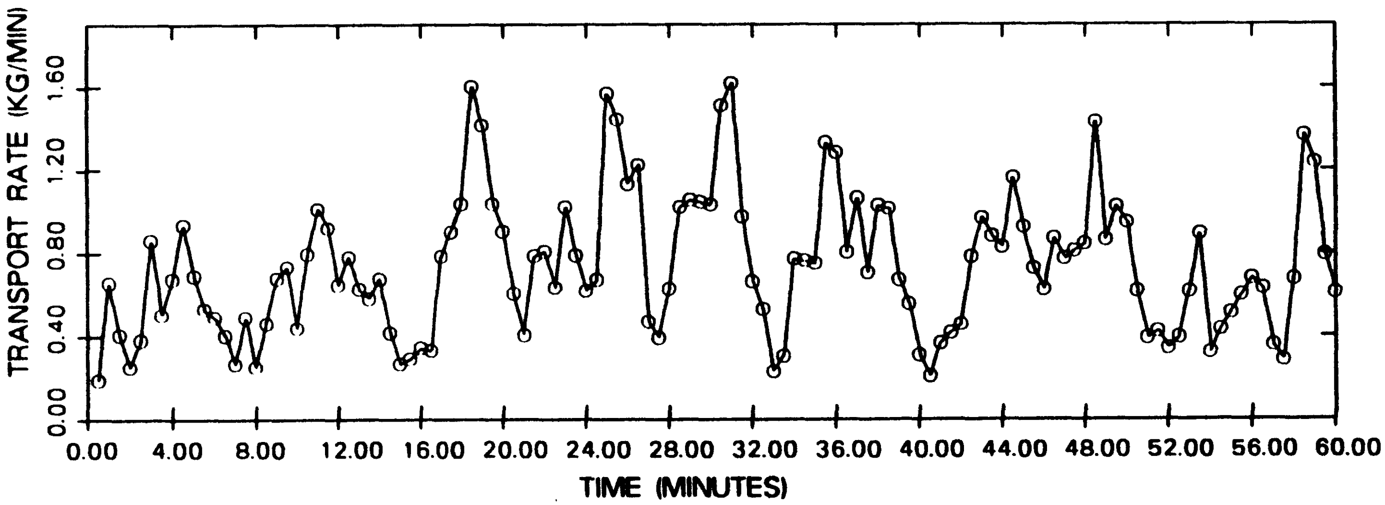

FIG. 10.-- Total transport rate vs. time, Run H3

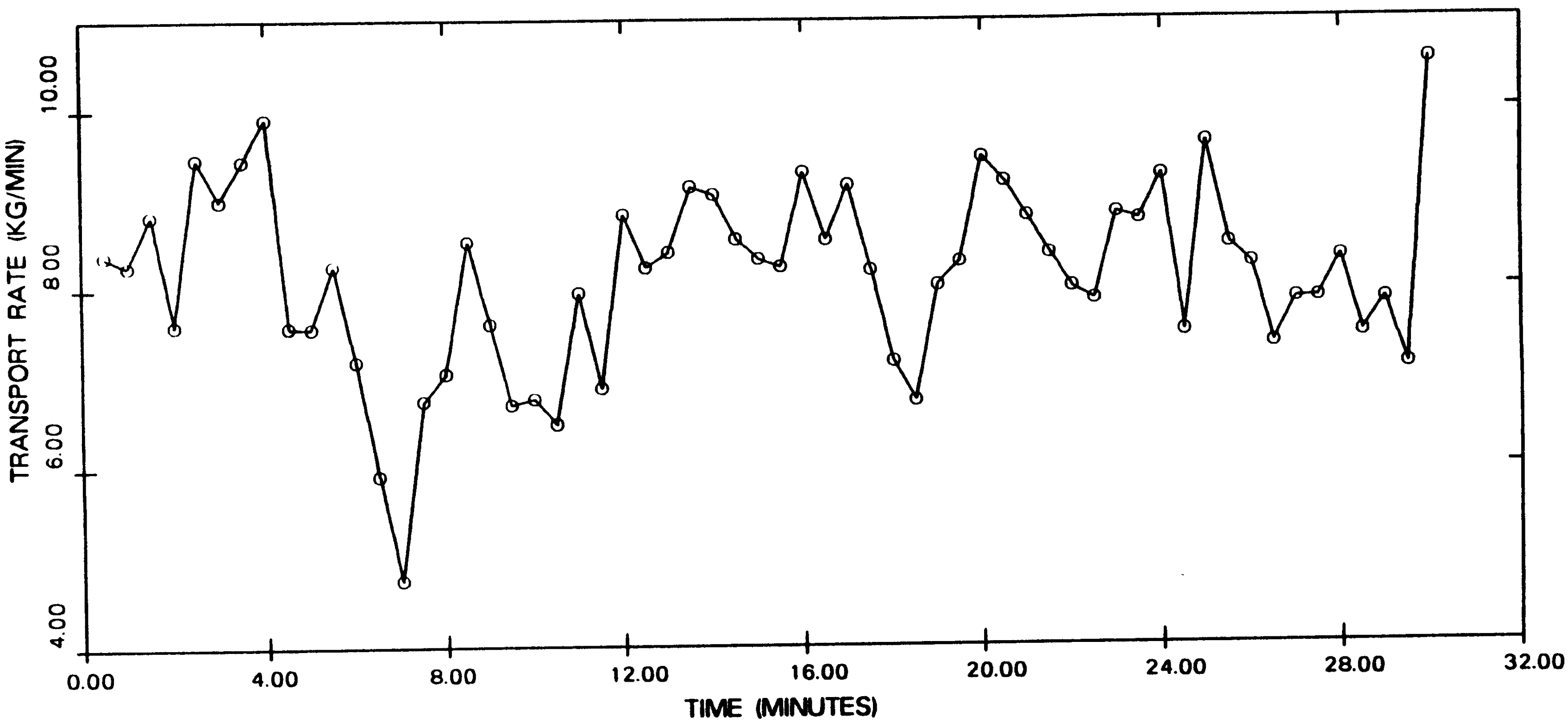

FIG. 11. -- Total transport rate vs. time, Run H5

Table 3. MEAN, STANDARD DEVIATION, COFFICIENT OF VARIATION, AND RANGE OF TRANSPORT RATES

Run		Mean transport rate from 30 sec. samples (kg/min)	Standard Deviation (kg/min)	SD * 100 / mean (%)	max. value / min. value
L1		3.41	1.12	32.8	6.0
L2		1.72	0.86	50.0	25.9
H1		1.01	0.46	45.5	57.3
	1	0.20	0.11	55.0	21.0
H2	2	0.33	0.18	54.5	8.5
	3	0.26	0.11	42.3	6.4
H3		0.73	0.33	45.2	8.7
H5		8.12	1.02	12.6	2.2

due only to channel width. Run L2 had a different unit discharge, but the unit feed rate was very close to that of the other two runs and thus Run L2 is also considered here.

At a first glance the most obvious feature of the plots of transport rate in Figures 7, 8, and 9 is the large fluctuations with time. Transport rates varied in Run H1 by a factor of more than 50, in Run H2 by a factor of 21, and in Run L2 by a factor of 26. The most striking fluctuations generally were on the order of minutes. This short-term variability was caused by the passage of long and low bed features, which will be described in detail in a later section.

Longer-term fluctuations, which appear to have periods of about 30 minutes, are also apparent in the data from Runs H1 and L2. A possible mechanism for these longer-term events, development of jams of the largest clasts extending across the entire channel, was observed in Run H2 through the transparent sidewall of the small flume. A group of 5 to 12 interlocking pebbles was enough to form a clast jam that led to aggradation upstream, which caused the upstream area to be finer in grain size and more regular in elevation (see Fig. 12). Downstream of the jam the bed was coarser and less regular due to a decrease in transport rate over the jam, causing degradation and an increase in average size of the bed sediment. Measured slopes upstream and downstream of a clast jam were 0.018 and 0.023, respectively, after Set 6 in Run H2. The clast jam and upstream aggradation sometimes lasted only minutes to tens of minutes, but could continue for up to several hours until the local slope over the jam became great enough that the flow

A B

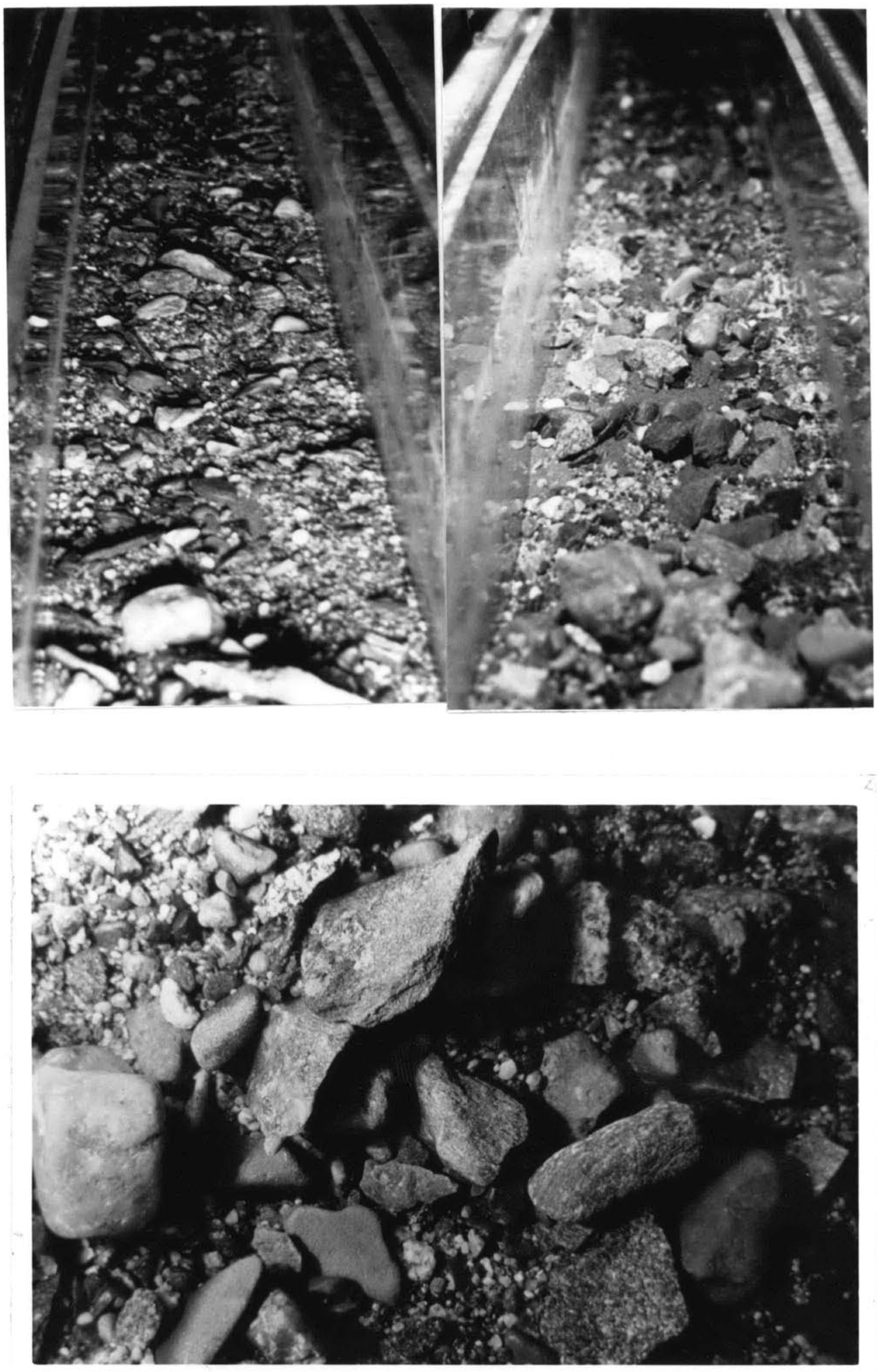

C

FIG. 12.-- Photographs of a clast jam, Run H2.
A-- view upstream, B-- view downstream,
C-- plan view of clast jam, upstream is
to the left.

could move some or all of the jammed clasts. Most jams lasted 20 to 40 minutes. Breakup of a clast jam caused the transport rate out of the channel to be higher than average. The increase in sediment transport rate was related to how long the jam had been present and how abruptly it was destroyed: rapid breakup caused one large spike in the transport record, whereas a more gradual breaching of the jam led to a slightly elevated rate for a longer time, on the order of tens of minutes. The effect of the formation and breaking of clast jams is shown by the different mean values for the three 30-minute sampling periods of Run H2 (Table 3).

Clast jams could not be observed in Runs H1 and L2, because the sidewalls in the large flume were opaque. Similar jams probably did not develop in the larger channel due to its greater width, although more localized jams could have formed and been responsible for the longer-term variability in transport rate. On the other hand, some other larger-scale channel process could equally well have been responsible for the 30-minute fluctuations observed in these two runs.

One conclusion that can be drawn from the transport-rate measurements is that accurate measurement of the mean transport rate in systems similar to ours necessitates a long sampling time. This topic will be treated in detail in a later section.

An important conclusion from comparing Runs H1, H2, and L2 is that the transport processes acting on the scale of minutes in the small flume were remarkably similar to those in the large flume for the same values of unit discharge and unit feed rate. There were also longer-term fluctuations in transport rate in both flumes; in the small flume these were caused by clast jams, but in the large flume their cause is uncertain. The key point here is that processes in both flumes were very similar, thus justifying the observations of transport made through the transparent sidewalls of the small flume. The limited width and length of the small channel as well as the slightly less uniform feed were apparently not important factors in how the sediment was transported through the system.

Runs L1 and H3

Runs L1 and H3 were made at nearly the same unit feed rate in the large and small flumes. Visual comparison of the transport-rate plots of these two runs with the runs discussed above reveals a strong similarity in the period of the short-term fluctuations, by reason of the presence of long, low bed features similar to those observed in runs with lower transport rates. One difference between these runs and those discussed earlier is that ratios of maximum to minimum measured rates (Table 3) are several times lower than for the runs with lower transport rates (Table 2). Also, for variations on the order of tens of minutes or longer, Run L1 varied less than the runs with lower transport rates (Figs. 6, 10, and Table 4). This difference is quite striking when the plots of transport rate vs. time in Run L1 are compared with those in Runs H1 and

Table 4. MEAN AND COEFFICIENT OF VARIATION FOR THE FIVE 30-MINUTE SEGMENTS OF THE 150-MIN DATA

Run #	Time of run (min)	0-30	30-60	60-90	90-120	120-150
L1	mean (kg/min)	3.54	3.36	3.49	3.27	3.50
	cv (%)	33.9	36.5	33.1	30.0	28.7
L2	mean (kg/min)	1.92	1.66	1.95	1.39	1.70
	cv (%)	48.6	54.4	37.0	60.3	43.5
H1	mean (kg/min)	1.05	1.19	0.97	0.92	0.94
	cv (%)	44.6	40.6	42.3	52.5	47.9

note: coefficient of variation = $\frac{\text{standard deviation}}{\text{mean}} \times 100.0$

L2 (Figs. 7 and 8). This lower variability was also observed in Run H3, in which events like the clast jams of Run H2 tended to be shorter-lived and less frequent.

Run H5

One of the goals of this project was to explore transport rates at the high end of the range actually measured in natural alluvial rivers. The highest measured unit transport rate of which we are aware, reported by Kang (1982) from a small glacial outwash stream in the Canadian Rockies, is about 5 kg/s•m. Much higher transport rates must certainly occur in natural streams, but to our knowledge rates higher than that reported by Kang have not been measured to date. We were able to experiment only with rates up to about 1 kg/s•m owing to the limited capacities of our flumes.

In Run H5 the feed rate was approximately ten times greater than in the run with the next lower feed rate. The data for Run H5 are markedly different from those from the runs with lower transport rates. First, the total variation in transport rate with time in Run H5 is only about a factor of 2 (Fig. 11), while for the other runs the variation is from 6 to 57 (Table 3). Second, the periodicity of the fluctuations in Run H5 is much weaker than in the other runs.

Owing to the very high transport rates in Run H5 there were two problems not encountered in the other runs. First, transport was sampled for only 15 seconds out of every 30, so only half of all the sediment transported out of the channel was caught. Also, the bed aggraded somewhat as the sampling sequence progressed, because of an unplanned decrease in water discharge in the channel. It is not known exactly what effect this aggradation had on the sampled rates, but modifications to the tail barrel before Set 2 eliminated this problem. We are confident that steady and uniform conditions were present during Set 2, as shown by the equality between feed rate and transport rate out of the channel and also by the lack of changes in the bed-surface and water-surface elevations. Although the transport record in Figure 11 was taken during a gradually aggrading bed, the results tie in well with the measurements and observations made during the other parts of the run. Bed forms observed during this run were higher and shorter and tended to disappear after they had migrated over a distance equal to about one spacing. Also, the grain-size distribution of the bed surface was much finer than that of earlier runs.

Bed-Surface Grain-Size Distributions

The evolution of the bed-surface size distribution, discussed in detail by Parker and Klingeman (1982), is an important process in gravel-bed streams. On the hypothesis that the bed evolves towards a condition in which all fractions are equally mobile, Parker and Klingeman used a transport model to explain why gravel-bed streams are usually armored. Observations reveal that the larger grains become enriched on the bed surface of a gravel-bed stream because of their lower mobility. This process of armoring was observed in all of the runs discussed here with the exception of Run H5.

The definition of armoring used here is the one recommended at the Gravel-Bed Rivers Symposium (Fort Collins, Colorado, 1985). The word armored is used to describe all bed surfaces on which coarse grains have been concentrated over their abundance in the original sediment mix. Adjectives like mobile or static are then used in conjunction with the word armor. By this classification the coarse bed surfaces that formed in these runs showed mobile armor.

The bed surfaces of Runs L3, H1, H2, H3, and H5 were sampled in this study to relate their size distributions to the conditions of flow and sediment transport in that run. A piston sampler (described above) was used to collect the samples. This sampler enabled us to sample only the surface layer of the bed (Fig. 5).

The cumulative grain-size distributions in Figure 13 show that the runs with lower transport rates tend to have coarser bed surfaces than the runs with higher transport rates: the bed of Run H3, which was formed at a higher transport rate, was somewhat finer than those of Runs H1, L3, and H2, whereas Run H5, with the highest transport rate, had a bed-surface size distribution very nearly the same as that of the original sediment mix. These results support the theory of equal mobility proposed by Parker, Klingeman, and McLean (1982) and

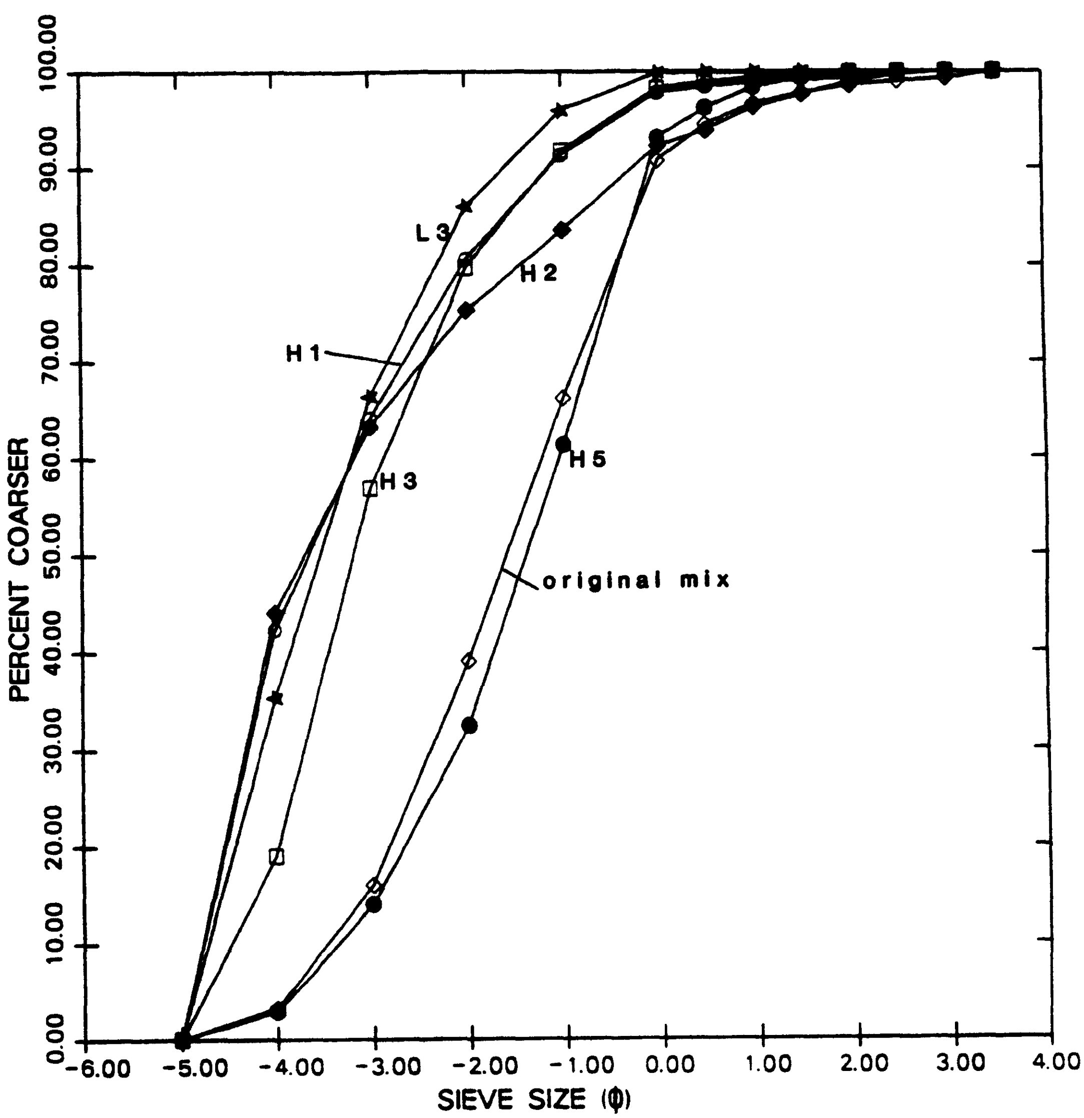

FIG. 13.-- Grain size distribution of bed-surface samples. Run numbers for each sample are shown.

Parker and Klingeman (1982). As predicted by Parker and coworkers the coarser grains appear to be less mobile than the fines at low bed shear stresses and therefore low transport rates, and the differences in mobility tend to disappear asymptotically at higher bed shear stresses.

To test how the results of this study fit into the model of Parker et al. their dimensionless bed-load transport variable W^*, defined as

$$W^* = \frac{(s-1)q_b}{(g)^{1/2}(ds)^{3/2}} \qquad (1)$$

where $s = \rho_s/\rho$, the ratio of the densities of the sediment and the fluid, respectively, q_b is the volumetric bed-load transport rate per unit width, g is the acceleration of gravity, d is the flow depth, and s is the downstream slope of the energy grade line, was calculated for Runs H2, H3, and H5. Values of W^* are 0.18, 0.52, and 3.84 for Runs H2, H3, and H5, respectively. These values plot on Figure 9 of Parker, Klingeman, and McLean (1982, p. 560) in the expected areas. In other words the value of W^* for Run H5 is well into the part of the plot where the curve flattens and all the different sizes become equally mobile without any armoring process being necessary. The W^* values from Runs H2 and H3 lie in the part of the plot where the various grain sizes would not be expected to be naturally equally mobile and thus an armored layer is necessary to render the grains equally mobile.

Another interesting observation that ties in with the formation of armored bed surfaces was made during Runs L3, H2, and H3. The initial beds, composed of the original sediment mix, eroded significantly in the beginning of the runs even though the bed slope was either nearly equal to or less than the equilibrium value eventually attained in that run (see Fig. 14). This observation can be explained by the fact that the size distribution of the original mix was much finer than that necessary to render all of the sizes equally mobile for a given flow strength and sediment feed rate. Similar observations of initial erosion in gravel-bed channels have also been made by Dhamotharan et al. (1980). This initial erosion would probably occur in most gravel-bed channels unless the bed shear stress is high enough that an armored bed need no longer form. This was the case in Run H5, in which the bed shear stress necessary to transport the sediment fed to the channel was high enough that nearly all sizes of the mix became nearly equally mobile.

Transport Rates of Individual Size Fractions

To determine the relationship between the transport rates of the individual size fractions and the total transport rate, transport samples from several runs were sieved into six size fractions: <1, 1-2, 2-4, 4-8, 8-16, and 16-32 mm. The first 200 samples of Run H1 and also selected samples from Runs H2, H3, and H5 were sieved into the above fractions, and the transport rate of each fraction was plotted on a computer-driven drum plotter. The shapes of the transport-rate

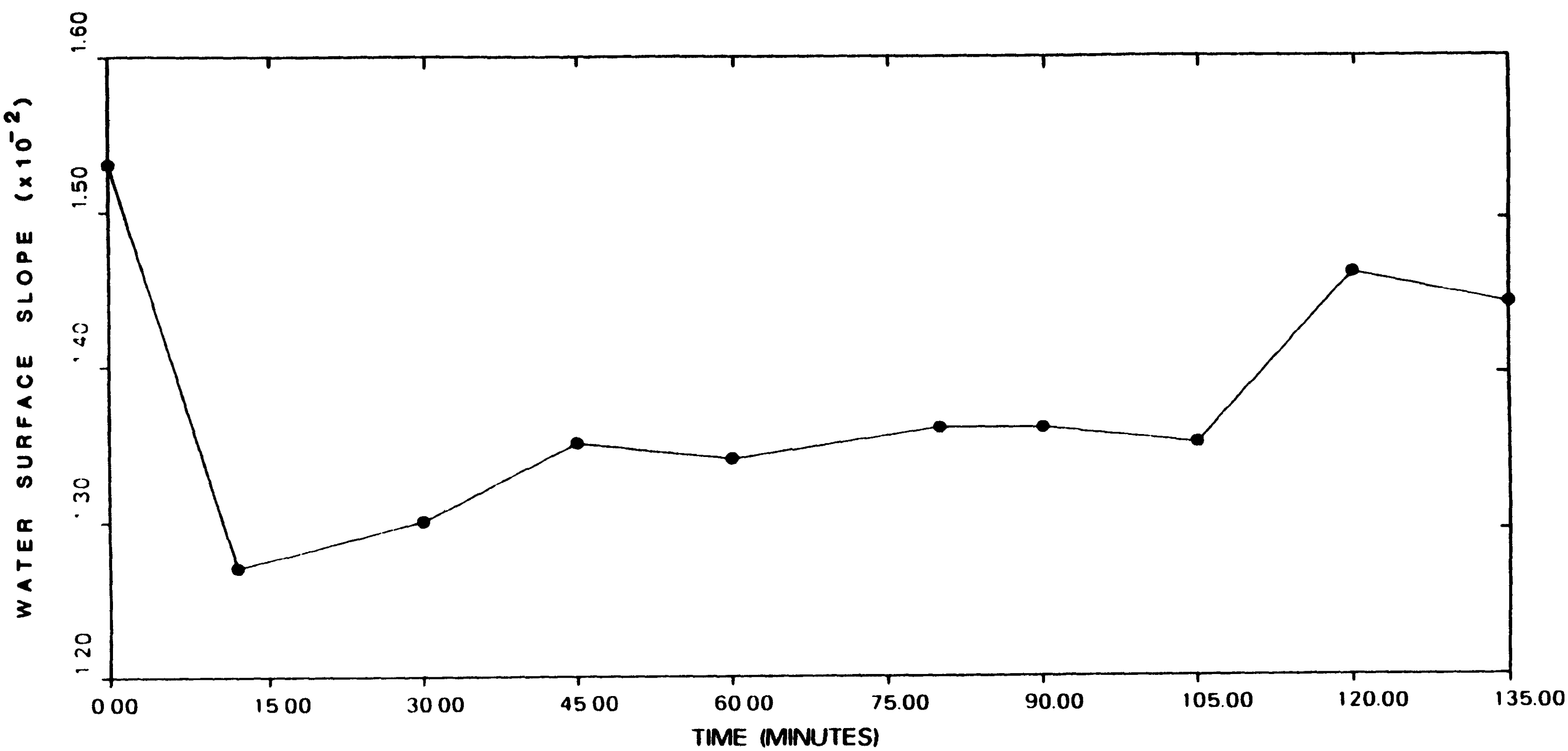

FIG. 14.-- Water surface slope vs. time, Run H3

plots of the different size fractions were compared by overlaying the plots on a light table. This exercise demonstrated that the plots of transport rate vs. time for the size ranges 4-8 and 8-16 mm were nearly the same, so these two size ranges were grouped into only one size interval, 4-16 mm. For the same reason, the size ranges 1-2 and 2-4 mm were grouped into the size interval 1-4 mm. These approximations were also found to be reasonable for Runs H2 and H3. The fractional-transport data for Runs H1, H2, and H3 will therefore be considered in the four size intervals <1, 1-4, 4-16, and 16-32 mm.

The variation of transport rate with time is significantly different for the four fractions considered. In the following, each size will be considered separately and compared to the total transport rate. In this way the contribution of each size to the total rate can be determined. Figures 15, 16, and 17 are plots of fractional transport rates for segments of Runs H1, H2, and H3. The transport rate of the 16-32 mm fraction appears to vary randomly and generally does not follow the total transport rate. This was corroborated by observations of the flume bed during the runs. The peak in transport rate of the 4-16 mm size fraction tends to precede the peak in the total transport rate and decrease thereafter even while the total rate is often still increasing. The transport rate of the 1-4 mm fraction mirrors the total rate in nearly all cases. This leaves the <1 mm fraction, whose transport rate tends to

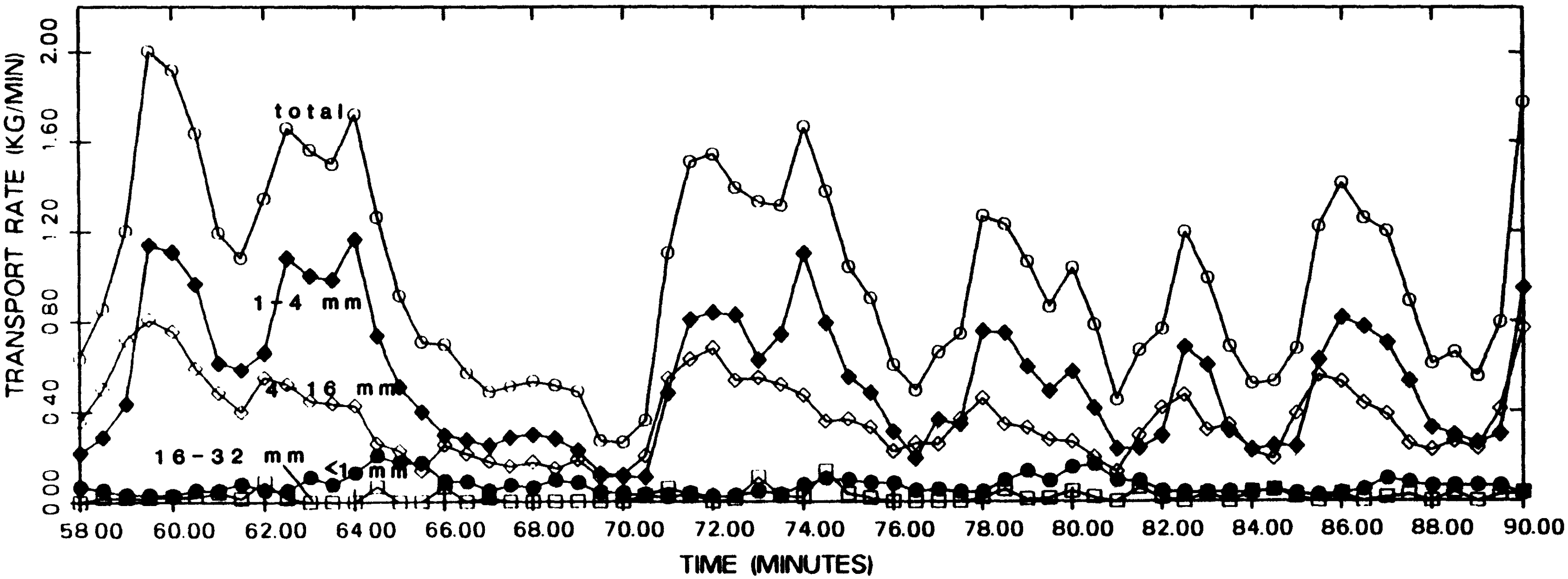

FIG. 15.-- Fractional and total transport rates vs. time, Run H1

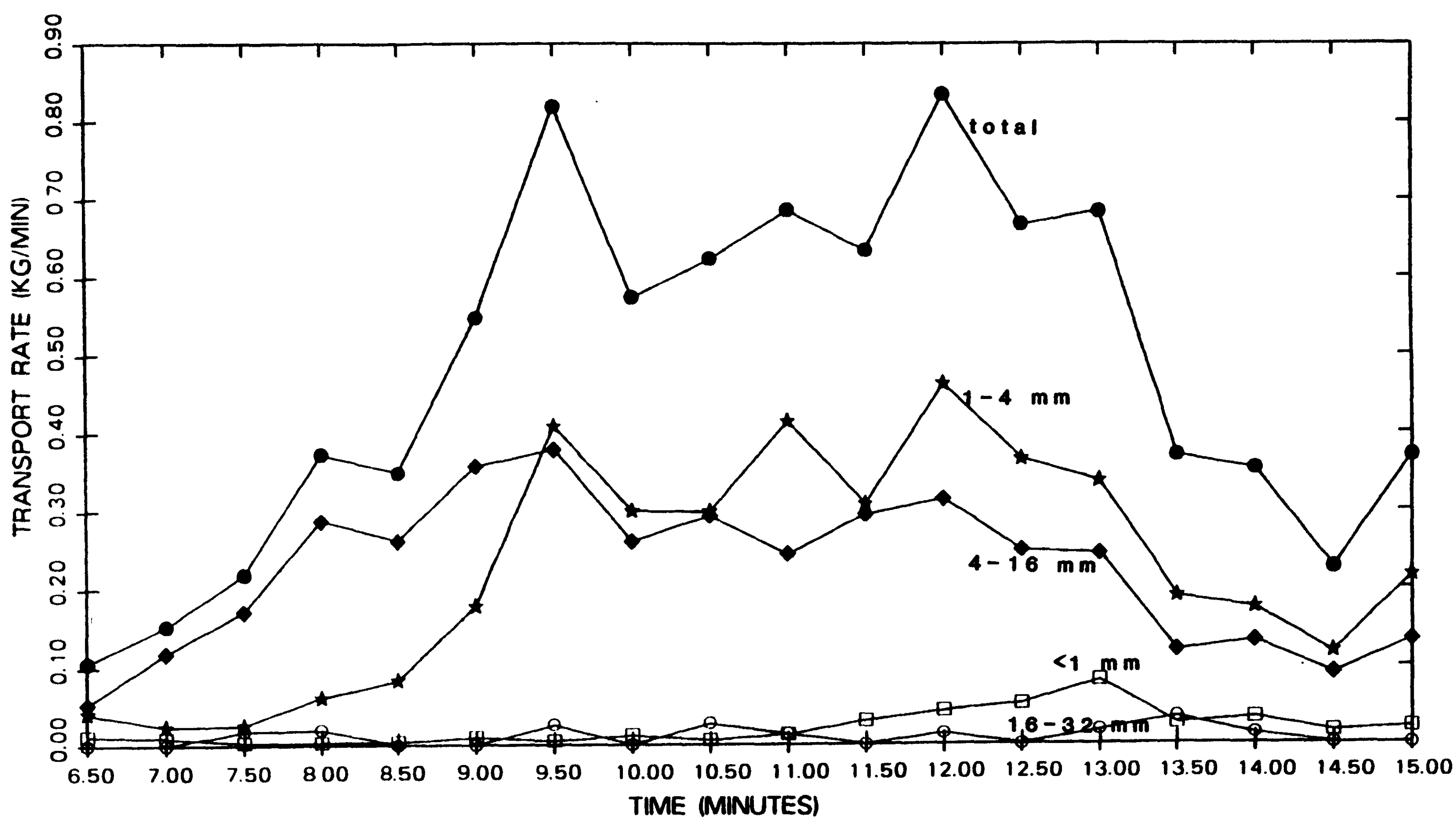

FIG. 16.-- Fractional and total transport rates vs. time, Run H2

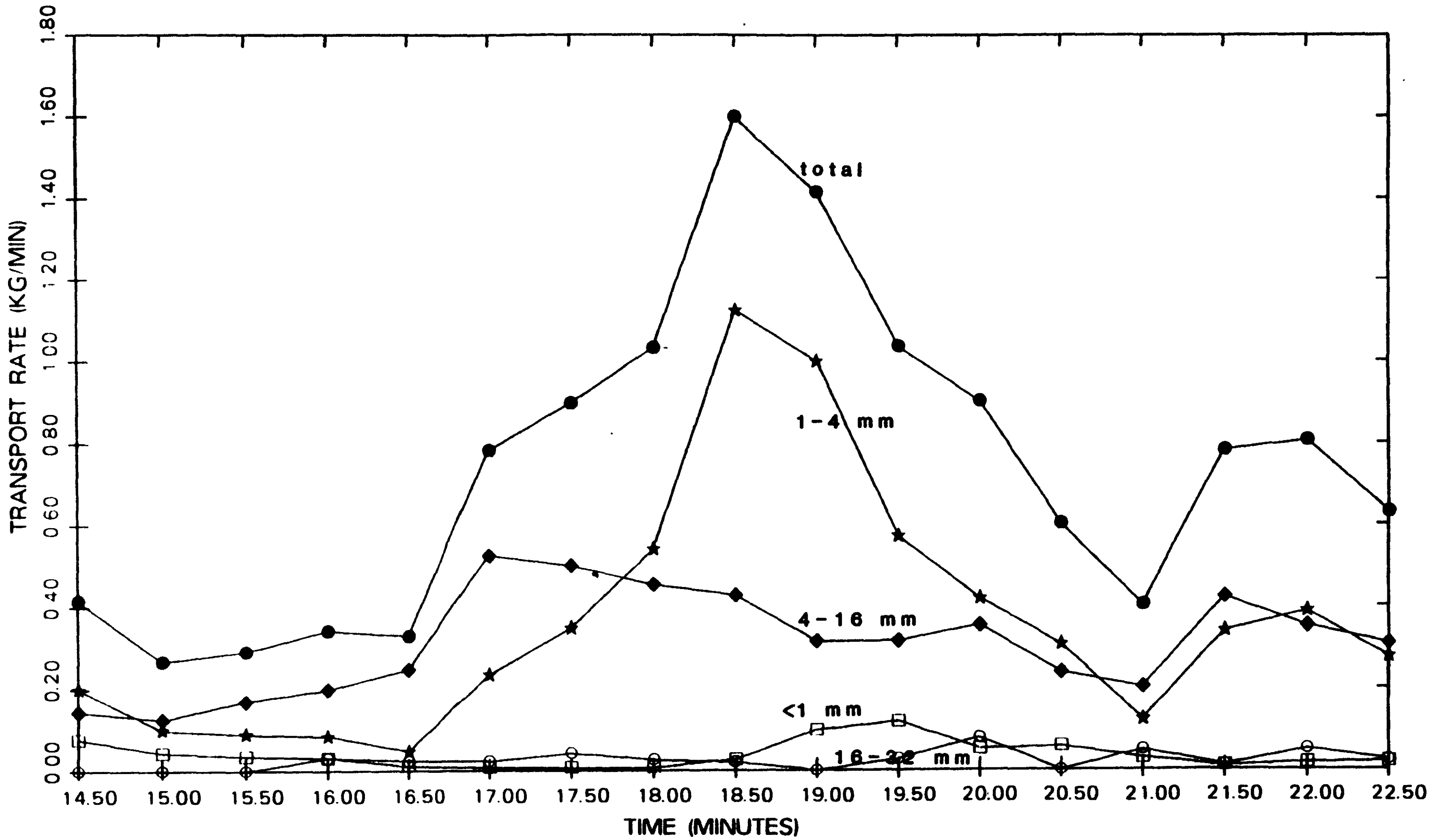

FIG. 17.-- Fractional and total transport rates vs. time, Run H3

peak after the total transport rate has peaked and is decreasing. These trends are remarkably consistent for Runs H1, H2, and H3.

The fractional-transport data for Run H5 are quite different from those for the runs with lower transport rates. The transport rates of the 8-16, 4-8, and 2-4 mm fractions vary at most by a factor of two and have no recognizable pattern to the variations (Fig. 18), but the 16-32, 1-2, and <1 mm fractions do appear to have a pattern (Fig. 19). The transport rate of the 1-2 mm fraction tends to vary quite regularly at a period of about 3 minutes. The transport peaks of the <1 mm fraction tend to follow those of the 1-2 mm fraction, similarly to what was observed in the runs with lower transport rates. The transport peaks of the 16-32 mm fraction tend to just precede those of the 1-2 mm fraction; this is also somewhat similar to the runs with lower transport rates except that in this case the 16-32 mm fraction rather than the 4-16 mm fraction shows this behavior.

Processes of Transport

General

With the transport data presented, the logical next step is to consider the processes found to be responsible for the identified transport variations. The order in which we are presenting this material corresponds to the order in which the investigation proceeded: the processes responsible for the transport fluctuations were not identified until the transport data were studied. The bed forms identified in this section

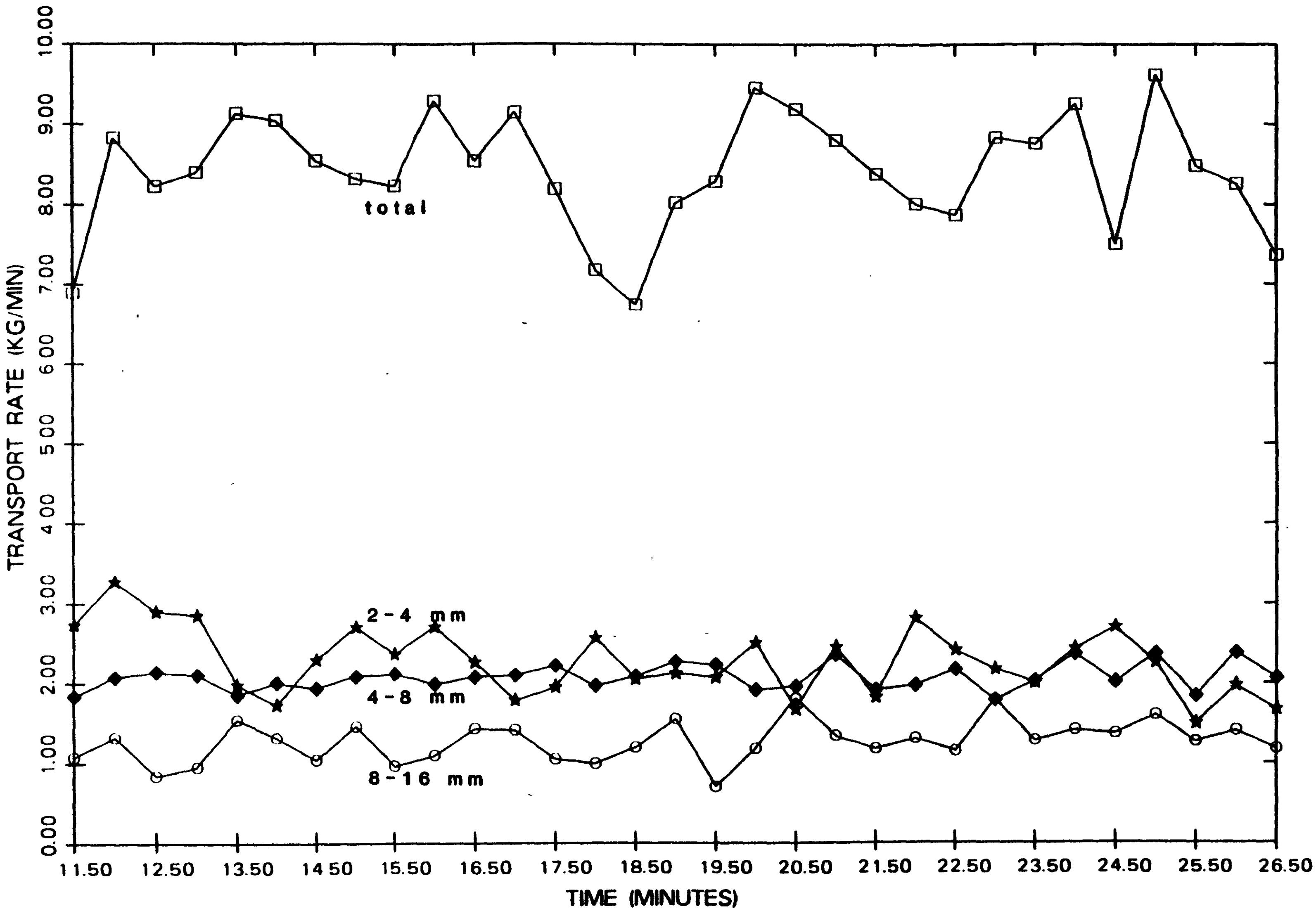

FIG. 18.-- Fractional and total transport rates vs. time, Run H5

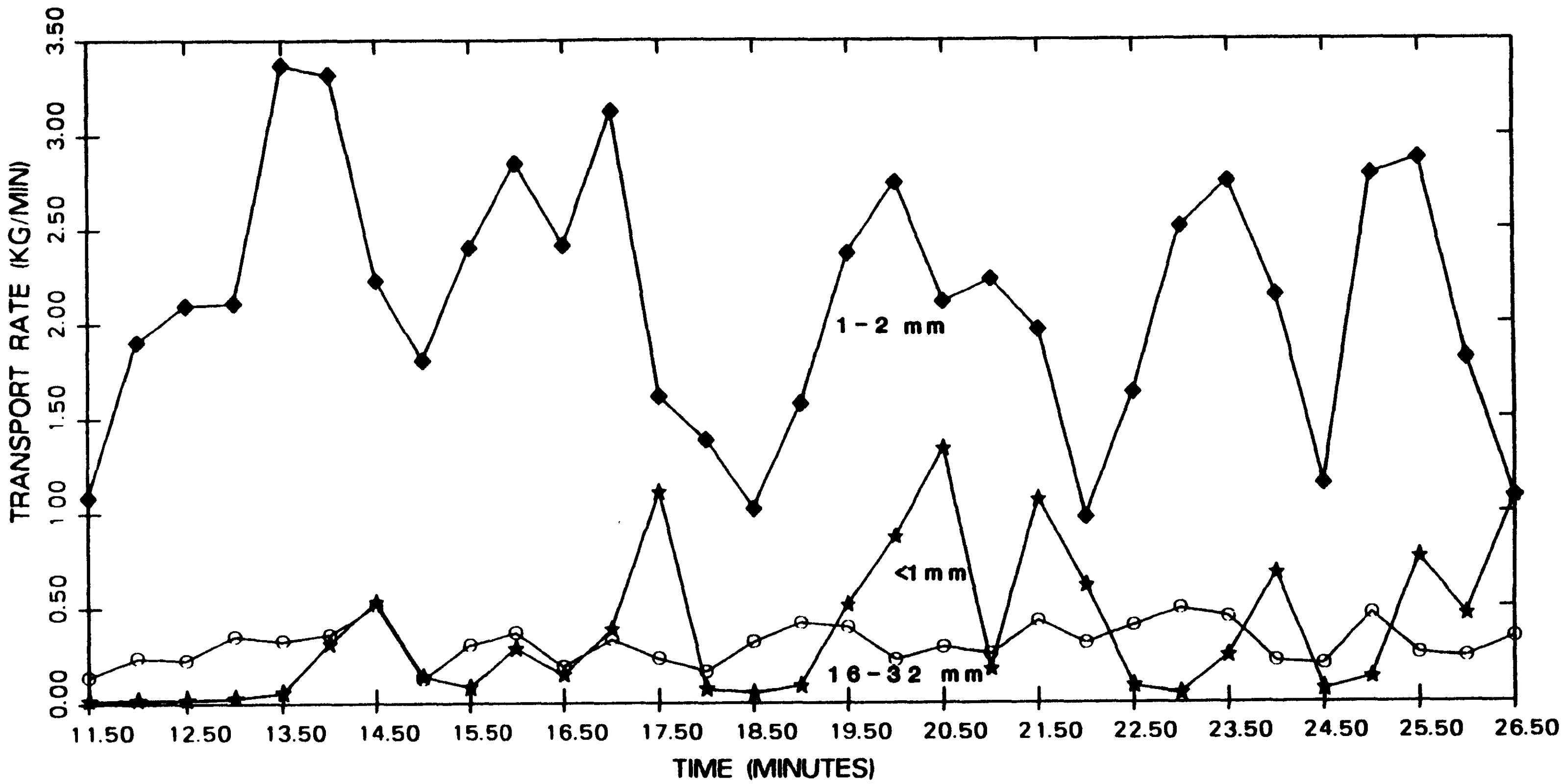

FIG. 19.-- Fractional transport rates vs. time, Run H5

were observed in Runs L3, H1, H2, H3, and H5. Although observations of the bed forms were not made in the other runs, we assume that similar processes were acting. The clast-jamming processes responsible for variations on the order of tens of minutes or longer will not be considered in this section; instead the processes responsible for the variations on the order of minutes will be considered here.

Observations on Sediment transport

In the runs with armored beds, namely Runs L3, H1, H2, and H3, observations of the transport surface confirmed what the fractional-transport data show: that the largest grains (16-32 mm) on the bed moved only infrequently and apparently at random. When these large clasts did move they were observed to be entrained in two different ways: (i) local scour of the bed around the grain caused it to move enough from its stable position (usually imbricated) that it was entrained by the flow; (ii) large grains were moved from stable positions on the bed by combinations of the forces of the impacts of many smaller grains over a short period of time and the fluid force. The grain was then moved by the force of the flow after its initial movement by grain impacts and the fluid force. Once one of these clasts was set in motion it often moved for more than one meter before it assumed another stable position on the bed. Once in a stable position, a large grain often remained in that position for an hour or more before moving again. These observations reinforce the conclusion from the transport-rate data that the large clasts tend to move randomly and at variable rates.

When the motion of the grains other than the largest ones was observed, areas of the bed where transport rates were much greater than elsewhere could readily be identified. Both from visual observations of the bed and from the data on fractional transport rates we know that most of the grains in these regions of more active transport were in the 1-4 mm size range. Areas of high transport rate did not cover the whole flume length at once. In the large flume these high-transport areas were observed to be 10 to 35 cm wide, 0.5 to 3 m long, and 2 to 4 mm high; in the small flume they were of similar dimensions but were necessarily limited in width to 0.15 m. In plan view the crests of the bed forms were straight. Hereafter these long and low bed forms will be called bed-load sheets, after the similar features given that name by Whiting and Dietrich (1986); more detail on these features will be given below. The exact positions of the downstream fronts of these bed-load sheets were often difficult to discern, but usually it was readily apparent whether the transport was strong or weak at any one location of the bed at a given time. The downstream speed of a bed-load sheet was measured by having two observers watch the transport on the bed at two points in the channel simultaneously. By this technique migration rates ranging from 0.5 to 1 cm/s were recorded in Run H1. Bed-load sheets were also readily observed on the bed of the flume with the flow off. Table 5 gives a summary of the characteristics of the bed-load sheets.

With the general mechanisms of variation of transport rate with time having been identified, an explanation of how the

Table 5. DESCRIPTION OF BED-LOAD SHEETS

Length	-	0.5 to 3.0 m
Width	-	10 to 35 cm (in 0.5 m channel)
Height	-	2 to 4 mm
Migration rate	-	0.5 to 1.0 cm/s
Grain size	-	composed primarily of 1-4 mm grains, which cause entrainment of larger grains by impacts

migration of the bed-load sheets caused the variations in transport rates of the different size fractions can now be proposed. As mentioned above, most of the grains in the gravel sheets were in the 1-4 mm size range. As the bed-load sheets moved down the channel, impacts of these grains caused 4-16 mm grains to be entrained readily by the flow. Immediately after entrainment the 4-16 mm grains moved much faster than the smaller grains in the high-transport region, but they usually traveled only 0.5 to 2.5 meters before stopping. Thus as the front of the high-transport zone migrated down the channel to within one or two meters of the end of the channel the locally entrained 4-16 mm grains began to be transported out of the channel at an increasing rate. The transport rate of the 4-16 mm size fraction thus peaked before the total transport rate, which was predominantly represented by the 1-4 mm fraction (see Figs. 15, 16, and 17). As the main part of the bed-load sheet reached the end of the channel, the total transport rate and also that of the 1-4 mm fraction peaked. After the bed-load sheet had passed out of the channel and the total transport rate was declining, the transport rate of the <1 mm fraction peaked. Our hypothesis is that the preferential entrainment of the 4-16 mm grains caused by the high-transport zone would leave an armored bed in which there were some "holes" left from the removal of these large grains. This then made some of the <1 mm grains, which were being hidden from the flow by the larger clasts, more available for transport than at other times. This enhanced transportability of the fines caused a peak in their transport rate after the main part of the pulse had passed and left them exposed.

The mechanisms of transport in Run H5 were quite different from those in the other runs. For one thing the bed surface was not armored: the larger grains did not need to become more concentrated on the bed in order to be transported at the rate at which they were fed into the channel. Unlike in the runs with lower transport rates, the coarser grains were observed to move at high velocities with few stops down the channel. The bed forms were higher and much more closely spaced than those in the runs with lower transport rates

The bed forms observed in Run H5 were about 1 cm high and 60 cm long (from the point of maximum elevation of one form to the same point on the next), and they extended completely across the channel. The forms were dominantly composed of grains of the median size of the mix, with noticeable concentrations of large clasts in the troughs just downstream of the crests (see Fig. 20). The mean migration rate for these forms was 3 cm/s measured over distances of 30 to 50 cm. Bed-form migration rates were not measured over longer distances because individual forms were very short-lived and usually did not migrate farther than 50 cm. Watching the bed forms for a period of time confirmed that they were destroyed and reformed constantly. This process of being destroyed and reformed may explain why the transport rate of the 1-2 mm grains varied on a period of 3 minutes when the measured

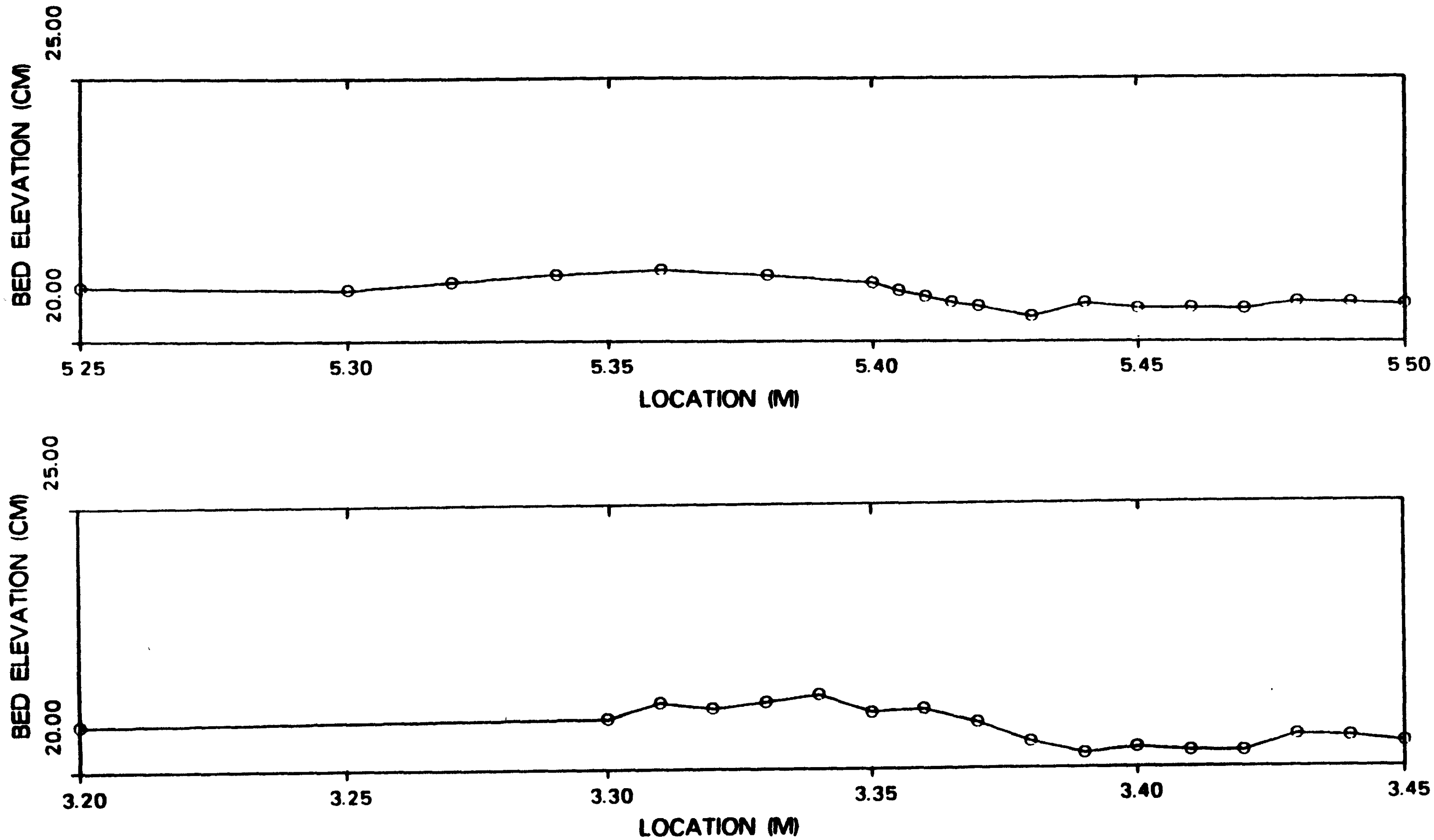

FIG. 20.-- Cross sectional profiles of bed forms parallel to flow direction, Run H5. No vertical exaggeration.

spacing and migration rate of the bed forms suggest that the transport rate of this fraction should have varied at periods of about 20 seconds. Such periods are too short for our 30-second sampling technique to resolve, but the short lives of the bed forms strongly suggests that variations in transport rate at this period were not present.

The data for the 16-32 mm grains are consistent with the observation that coarse clasts traveled at the downstream front of the bed forms in Run H5. The relative timing of the peak in total transport rate and that of the 16-32 mm fraction is similar to that observed for the 4-16 mm fraction in the runs with lower transport rates. In both cases the bed forms were responsible for causing the transport rate of the coarse fraction to peak before the total transport rate and that of the <1 mm fraction to peak after the total transport rate. The reason the transport rate of the <1 mm fraction peaked after the total transport rate in all runs seems to have been a lowering of the bed to expose more of the fine grains to the flow. The processes responsible for the timing of the peak in transport rate of the coarse fraction was not the same in all runs, however: in Run H5 the lower elevation just downstream of the crest of the form (see Fig. 20) apparently trapped some of the large grains in transport, whereas in the runs with lower transport rates the transport peak in the 4-16 mm fraction was caused by impacts and entrainment of the 4-16 mm grains by the 1-4 mm grains in the bed-load sheet.

Fourier Analysis of Periodicity

Fourier series were used as an unbiased estimator of the most prevalent periods of fluctuation in the data sets of total transport vs. time. The purpose of using Fourier analysis in this study was not to determine if there were quasi-periodic fluctuations in the sediment transport, but to identify the strongest periods of the fluctuations in the transport data sets.

The n terms of a time series, X(i),i=1,2...n, can be represented as a sum of their harmonic constituents as follows:

$$X(i) = A_o/2 + \sum_{k=1}^{m} [A_k(\cos(2\pi ki/n) + B_k(\sin(2\pi ki/n)] \qquad (2)$$

where m = (n-1)/2. The coefficients of the series are defined as

$$A_o = (2/n) \sum_{i=1}^{n} X(i)$$
$$A_i = (2/n) \sum_{i=1}^{n} X(i) \cos(2\pi ki/n) \qquad (3)$$
$$B_i = (2/n) \sum_{i=1}^{n} X(i) \sin(2\pi ki/n)$$

Fourier coefficients were generated for the data using a program modified from Davis (1973). The harmonic amplitude is defined in terms of the Fourier coefficients as

$$C_k = (A_k{}^2 + B_k{}^2)^{1/2} \qquad (4)$$

The harmonic amplitudes were plotted against the period to give an indication of which periods have the most strength in the data sets. The peaks in the harmonic amplitudes were tested for their significance using a test modified by Nowroozi (1966, 1967) from Fisher (1929) that computes the maximum magnitude that a harmonic amplitude would reach for a data set from a time series in which the variability is random. This value is then compared to the values of harmonic amplitudes generated for the data set in question. In this test the null hypothesis is that the peaks of the harmonic amplitudes were caused by random fluctuations in the data. On the assumption that the data are random the maximum significant amplitude is (Nowroozi, 1967)

$$Y = (g_p \; 2/n \sum_{i=1}^{n} [X(i)-A_o/2]^2)^{1/2} \qquad (5)$$

where g_p is a tabulated value defined as

$$g_p = (\max C_k{}^2)/(\sum C_k{}^2) \qquad (6)$$

and

$$\sum_{k=1}^{m} C_k{}^2 = 2/n \sum_{i=1}^{n} [X(i)-A_o/2]^2 \qquad (7)$$

The maximum significant amplitude from (5) was then plotted as a horizontal line on the plots of harmonic amplitude vs. period. All peaks above this line are judged to be significantly higher than would be expected from random fluctuations. The 95% confidence level was used for the calculation of the maximum significant amplitudes.

The plots of harmonic amplitude vs. period are shown in Figures 21, 22, and 23 for Runs L1, L2, and H1. There were significant peaks at 6.4 and 6.1 minutes for Run L1, at 24.9, 6.0, and nearly 11.5 minutes for Run L2, and at 26.1, 14.2, and 9.8 minutes for Run H1. Table 6 summarizes the significant

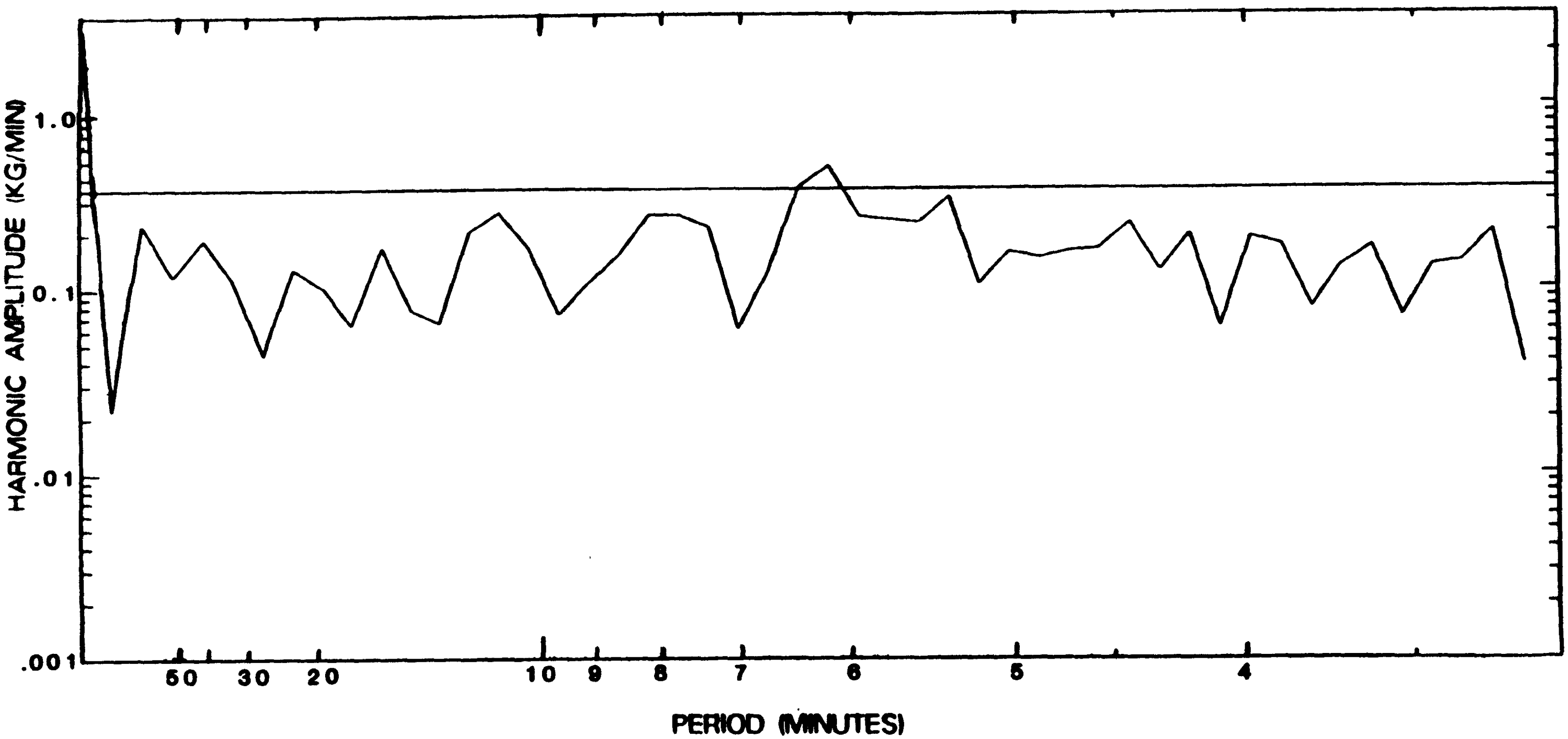

FIG. 21.-- Periodogram for total transport rate vs. time data, Run L1. Peaks above the horizontal line are significant.

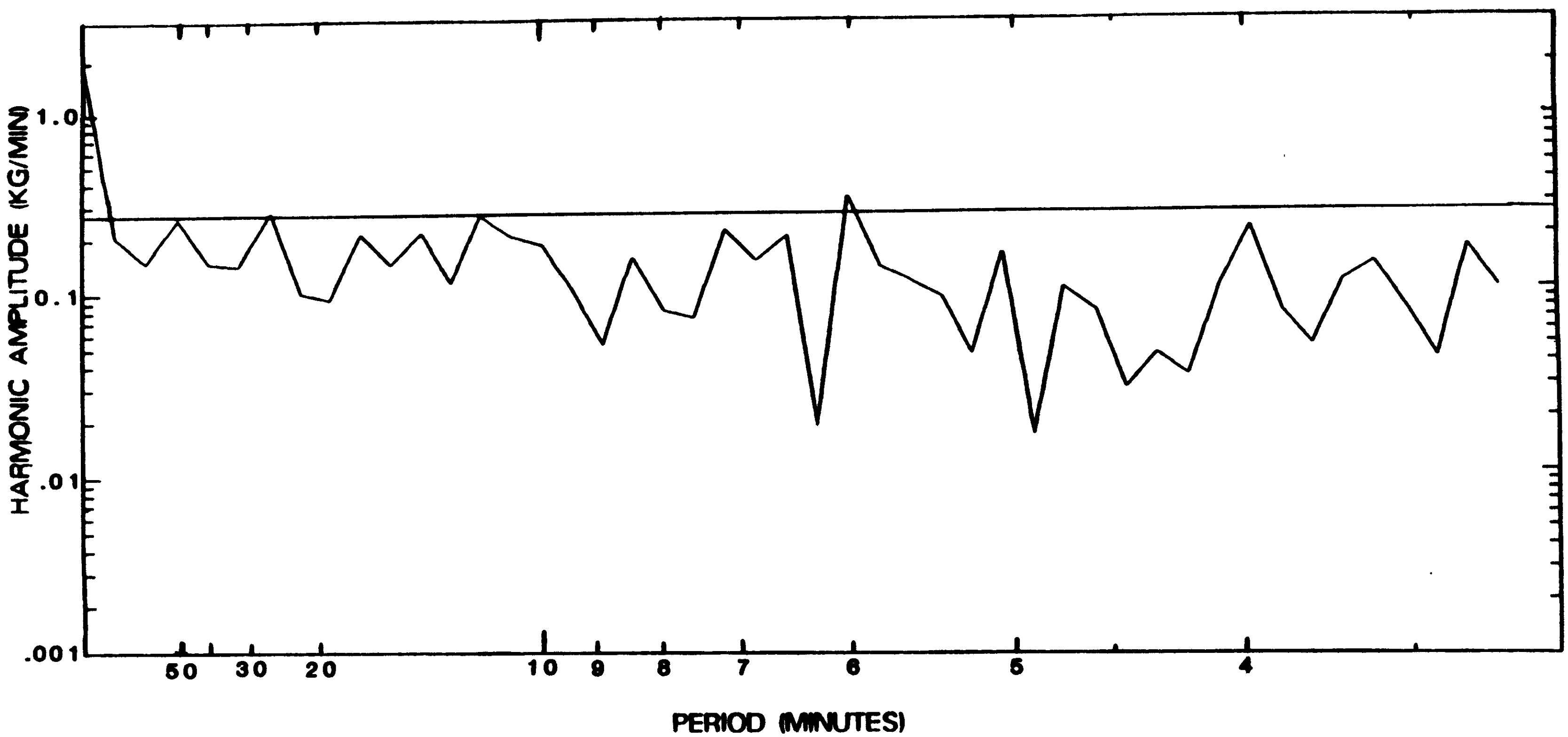

FIG. 22.-- Periodogram for total transport rate vs. time data, Run L2. Peaks above the horizontal line are significant.

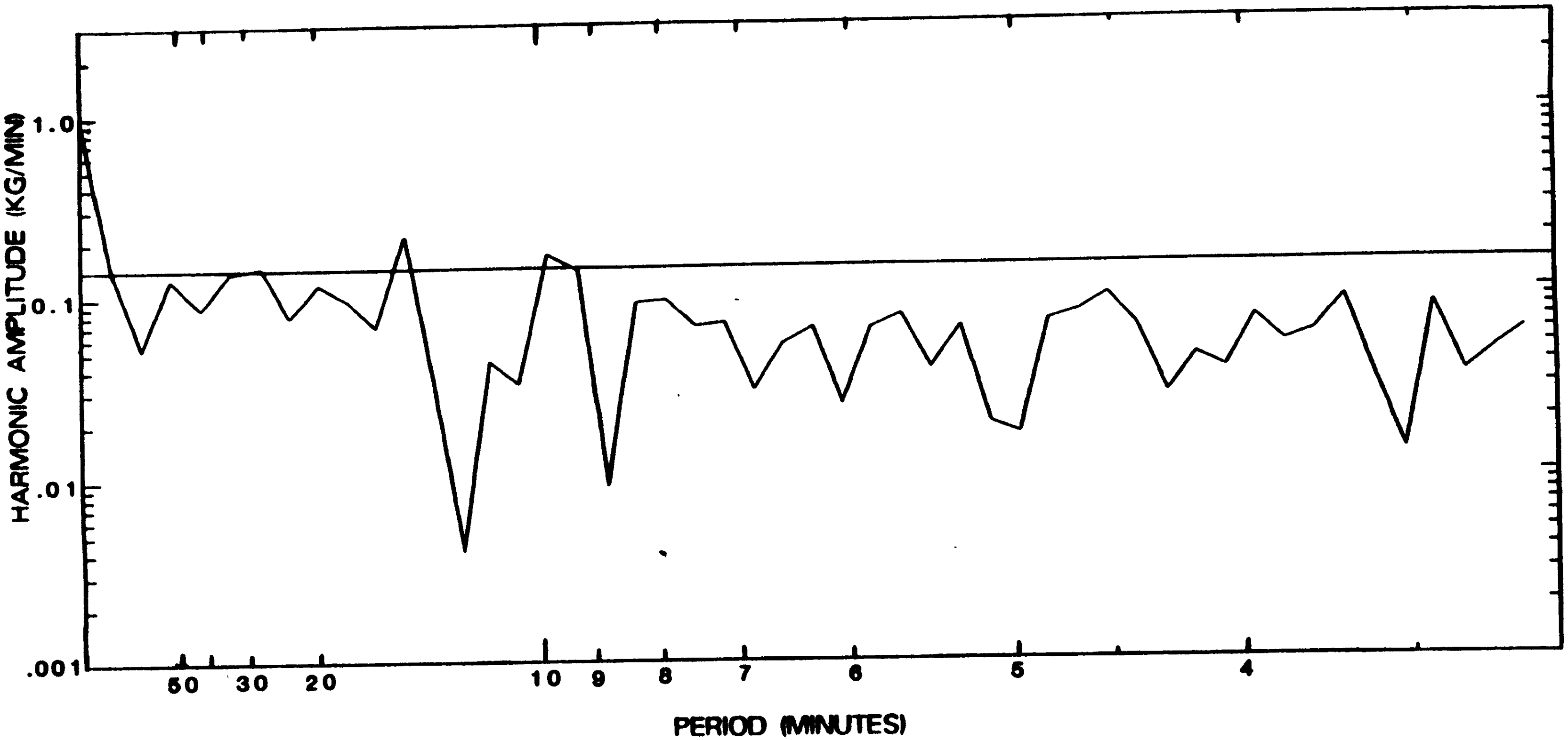

FIG. 23.-- Periodogram for total transport rate vs. time data, Run H1. Peaks above the horizontal line are significant.

Table 6. SIGNIFICANT PERIODS OF TRANSPORT FLUCTUATIONS FROM FOURIER ANALYSIS

Run		Significant periods in order of decreasing strength (minutes)
L1		6.1, 6.4
L2		6.0, 24.9, 11.5 (nearly)
H1		14.2, 9.8, 26.1
H2	-1-	7.5, 10.0
	-2-	10.0
	-3-	5.0
H3		6.7, 6.0
H5		none significant

peaks for these three runs as well as for Runs H2, H3, and H5. Because of the shorter sampling lengths of Runs H2, H3, and H5 the frequencies identified as significant are less representative than for the longer runs. Nevertheless the significant periods in these runs are close to the corresponding longer-sampled runs. The significant periods identified by this technique reinforce the observations on transport made during the runs: the data on transport vs. time for the weaker-transport runs show evidence for fluctuations on the order of tens of minutes while the stronger-transport runs do not. Also there seems to be some indication that the period of fluctuation of the shorter-term events is somewhat longer in the weaker-transport runs.

Summary of Results

Differences among the runs can be viewed in terms of the different unit feed rates used, which were varied by a factor of 30 from 0.034 kg/s·m to 1.073 kg/s·m. The data will be summarized in terms of bed-surface textures, variations in transport rate, and type of features present on the bed.

Bed-Surface Textures

The bed surface was armored in all runs except Run H5. It was coarsest in the runs with low transport rates and became finer with increasing transport rate. In the run with the highest transport rate (Run H5), the bed surface had nearly the same size distribution as the original sediment mix.

Transport Rates

Transport rates in the runs with the lowest unit feed rates (~0.03 to ~0.04 kg/s•m) were found to vary mainly at two periods: 6-14 minutes and approximately 25 minutes. For the runs with the next higher unit feed rate (~0.1 kg/s•m) the transport rate varied at periods of just about 6 minutes. At the highest unit feed rate (~1 kg/s•m), periodic fluctuations were not nearly as apparent as in the lower runs, although a periodicity of 3 minutes might have been present in the transport rate of the 1-2 mm fraction in Run H5. There was no evidence for longer-term fluctuations in transport rate at the intermediate and high unit feed rates. The range between maximum and minimum transport rates decreased with increasing mean transport rate.

Bed Forms

With increasing transport rate, bed forms ranged from very long (0.5-3 m) and low (2-4 mm) bed-load sheets to much shorter (0.6 m) and higher (1 cm) but much shorter-lived features. The processes associated with the migration of the bed forms caused the observed fluctuations in the total and fractional transport rates. All bed forms in the small flume were two dimensional in plan view because of the narrow width of the channel. In the wider channels of the large flume the shape of the bed forms in plan view was not determined due to the small height of the bed-load sheets.

DISCUSSION

Bed Forms

Data on bed configurations in gravel-bed streams are scarce. Although there seems to have been no systematic work on bed configurations in gravel-bed streams, bed configuration has been recorded in flume studies with fine gravels (Casey, 1935; Waterways Experiment Station, 1935; Mavis, Liu, and Soucek, 1937). The sediments used in these studies are summarized in Table 7. We compared our results only with runs in these three studies with nearly the same flow depths as ours (0.046 to 0.086 m; see Tables 8 and 9). Tables 8 and 9 give the grain size, flow depth, and flow velocity standardized to 10° C in addition to the measured values. Middleton and Southard (1984, p. 286) give formulas for converting bed-form data from different water temperatures to a standard of 10° C. In these three studies the transition from a plane bed (which we assume corresponds to our bed-load sheets) to dunelike bed forms took place between 0.60 and 0.67 m/s, or between 0.62 and 0.73 m/s for values scaled to 10°C (Table 9). The values shown in Table 9 are those for the maximum flow velocity with a plane bed and the minimum velocity with bed forms for depths closest to those of our study. This was considerably lower than our value of 0.90 m/s, or 1.01 m/s scaled to 10°C (Table 8). The data from the literature cited above are summarized in Figure 7.22B of Middleton and Southard (1984, p. 290). Due to an error in labeling the grain-size axis in Figure 7.22 of Middleton and Southard (1984, p. 290) the boundary shown

Table 7. GRAIN-SIZE CHARACTERISTICS FOR EXPERIMENTAL STUDIES USING FINE GRAVEL SEDIMENT

Reference	Median grain size (mm)	Size range (mm)	Sorting (%75/%25)
Casey (1935)	2.5	1.5-3.0	1.25
USWES (1935)	4.1	0.2-6.7	1.78
Mavis et al. (1937)	2.3	0.5-3.5	1.37
This study	3.0	0.1-32.0	3.74

Table 8. GRAIN SIZE, FLOW CHARACTERISTICS, AND BED PHASE FOR THIS STUDY.

Run	Md grain size(mm)	Mean flow depth (cm)		Mean flow velocity (m/s)		Bed phase
	($10^{o}C$)	(meas.)	($10^{o}C$)	(meas.)	($10^{o}C$)	
L1	3.3	3.6	3.9	0.77	0.81	bed-load sheets (plane bed)
L2	3.1	4.1	4.2	0.67	0.68	"
H1	3.1	4.6	4.7	0.77	0.78	"
H2	3.6	4.6	5.6	0.77	0.85	"
H3	3.8	7.4	9.3	0.90	1.01	"
H5	3.9	6.9	9.0	1.29	1.47	bed forms

Note: Values of depth and velocity measured are in the "meas." column, and values in the column under $10^{o}C$ have been standardized to $10^{o}C$.

Table 9. GRAIN SIZE, FLOW CHARACTERISTICS, AND BED PHASE FOR STUDIES WITH FINE GRAVEL GRAIN SIZE

Reference	Md grain size (mm) (10°C)	Mean flow depth (cm) (meas.)	Mean flow depth (cm) (10°C)	Mean flow velocity (m/s) (meas.)	Mean flow velocity (m/s) (10°C)	Bed phase
Casey (1935)	2.6	4.6	4.8	0.57	0.58	plane bed
	2.6	5.2	5.4	0.60	0.62	bed forms
Mavis et al. (1937)	3.2	8.0	11.2	0.62	0.73	plane bed
	3.2	8.4	11.6	0.62	0.73	bed forms
USWES (1935)	4.7	7.7	8.9	0.64	0.66	plane bed
	4.8	8.6	10.2	0.67	0.73	bed forms

Note: Values of depth and velocity that were measured in the above studies are under the "meas." column, and the values in the column "10°C" were scaled to that temperature.

between lower plane bed and large ripples for a sediment size of 3 mm is incorrect and should be at about 0.6 m/s in their Figure 7.22B. The boundary between plane bed and bed forms suggested by our data does not fit well with the boundary given by Middleton and Southard. One possible explanation for this is that the sorting of the sediment in our runs was much poorer (Table 7) than in the other three studies. It appears that sorting may have an important effect on the conditions for the first appearance of large ripple bed forms in gravel-bed streams.

Comparison with Field Examples

It is often asked about experimental work whether the experimental system is a good model for larger field situations. In this regard, two studies of small modern streams and one study in which gravel bed forms are described from an alluvial fan will be compared with the results of the present study.

The transport data and observations made by Whiting et al. (1985) and Whiting and Dietrich (1986) in Duck Creek, a diversion channel 5 m wide and 0.4 m deep with d_{50} = 5 mm, are very similar to those of this study. Bed-load sheets one to two grain diameters thick and dunes in stronger flows observed by Whiting and coworkers are very similar to the bed features observed in this study. The periodicity of bed-load transport rates measured with a bed-load sampler was about 10-15 minutes. Coarse grains were observed by Whiting and Dietrich (1986) to travel at the downstream front of the bed-load sheets, leading to timings of transport rates of the different fractions similar to those observed in our study: peaks in transport rate of the coarse fractions tended to precede the peaks in total transport rate, and peaks in transport rate of the fine fractions tended to follow the peaks in total transport rate. Although this pattern of variation in transport rates is very similar to that observed in our study, Whiting and Dietrich (1986) found the cause to be different: they concluded that the smooth surface of the bed-load sheet relative to the surrounding bed causes the coarse grains to travel at a high velocity over the sheet and decrease in velocity downstream of the front and therefore concentrate there. This is substantially different from the mechanisms of local entrainment of the coarse grains that we found to be the cause of the peaks in coarse fraction transport rate in the flumes.

In a field study of Hilda Creek, a small glacial outwash stream in the Canadian Rocky Mountains, Kang (1982) obtained data on sediment transport that closely resemble ours. Kang sampled the bed load of the stream with long baskets covered with 1/4" (0.64 cm) wire mesh which trapped the sediment as it passed over a spillway 6 ft (1.8 m) wide. Samples were taken for 3 to 10 seconds at intervals of 1, 2, or 5 minutes. Continuous sampling periods of several hours were achieved with this system. Kang identified two main periods of fluctuation in the bed-load transport rate. Mean periods for the short-term events were 13.2 and 15 minutes for the the 2-minute and 5-minute samples respectively. The longer-term events had mean periods of 29.2 and 30.8 minutes for the 2-minute and 5-minute data, respectively. Unit transport rates were approximately from 0.05 to 5 kg/s·m. The exact values for the unit transport rates were difficult to determine because the width of the channel varied and was not accurately known. The averages of the periods of Kang's short-term and long-term events are very close to those recorded for Runs H1 and L2 in this study. Observations of the bed when sediment was in transport were nearly impossible in Hilda Creek due to the abundant suspended load, but we believe that if the bed could have been observed the processes would have been very similar to those observed in our experiments.

One final point that needs explaining is the fact that the fluctuation period in Kang's data does not vary systematically with large changes in transport rate. One possible explanation is that the banks of the Hilda Creek channels were for the most part unconfined and freely erodible. It is our supposition that with increasing transport rates the total width of the channels at Hilda Creek would increase, thus keeping the transport of the sediment within the stability range of bed-load sheets. Our laboratory channels, however, were of fixed width and thus could not widen or braid. In the large flume, however, Run L1 especially and to a lesser extent Run L2 exhibited signs that a braided channel was on the verge of forming. The alternate bars (described above) in Runs L1 and L2 would probably have developed into a braided pattern without the contraints of the channel walls. Features similar to these alternate bars were observed by Kuhnle (1981) to be the first phase of the process by which a straight channel in gravel becomes braided.

Kang (1982) also found that half-hour averages of transport samples were the optimum length to predict the mean transport rate as determined from transport rates obtained from a bed-load fence that was constructed across the entire channel downstream of the spillway. Details of the bed-load fence can be found in Hammer and Smith (1983). Kang explained that half-hour averages were better than one-hour averages because of the rapid changes of flow characteristics in Hilda Creek. The topic of sampling problems in gravel-bed streams will be discussed in more detail later in this report.

Another study quite different from the two discussed above will be compared to our study. Wells and Dohrenwend (1985) described bed mesoforms and macroforms on alluvial-fan surfaces in southeastern California. The mesoforms are quite similar to the bed-load sheets observed in this study. These forms were found on presently inactive parts of the fans 1 to 10 meters above presently active ephemeral channels. The authors interpreted that these forms were active during shallow floods on the fan surface. The forms were composed of gravel finer (median size 2-8 mm) than the cobble-size pavement on which they rested. The spacing of the forms varied between 2 and 6 m and the height was of the order of 5 cm, or one to two grain diameters. Although these forms are larger the shapes are similar to those of the forms seen in our experiments. One difference is that the features were formed on a bed of larger clasts that were apparently not in transport when these features were deposited. All sizes were in transport in our flume experiments, but the largest sizes on the flume bed spent long periods of time motionless between movements; this makes these two situations more comparable than might be realized.

It appears that in many cases variations in sediment transport rate of streams lacking obvious bed forms may be explained by features similar to the bed-load sheets observed in this study. Subtle bed forms may be present even when the transport surface appears flat. The subtle nature of these forms may make their identification very difficult. The difficulty of identification was experienced first-hand in this study: the bed-load sheets were not discovered until the variations in transport rate had been documented and experiments in a channel with transparent sidewalls were made.

Implications for Bed-load Sampling

It is apparent from the results of this study that sediment transport in a gravel-bed channel can vary significantly even when the independent variables are held constant and the bed lacks robust bed forms. This fact demonstrates that sampling of bed-load transport in streams with similar variations in transport must be undertaken carefully in order to avoid potentially large errors in the estimate of the mean transport rate. The sampling scheme necessary to characterize the transport rates accurately for a given stream must make allowances for fluctuations in transport rate that are not related to changes in the independent variables in the system. The following exercise is an example of how to sample adequately a stream that behaves like our laboratory channel.

To demonstrate the problems of taking a transport sample for too short a time, a computer program was written (see Appendix) to combine the 30-second samples of the three 150-minute data sets of Runs L1, L2, and H1 into a complete set of 60-second samples, 90-second samples, etc., all the way up to samples half as long as the data set. Then the mean and standard deviation were calculated for each "new" data set. The coefficient of variation was then computed as a way to predict the probability of obtaining accurate results for a sample taken over a given interval of time in this system. The coefficient of variation, defined as 100 times the standard deviation divided by the mean, is an especially useful ratio in this instance: it indicates the probability of obtaining a sample representative of the mean.

Figure 24 illustrates the decreasing value of the coefficient of variation for increasing sample lengths. The zig-zag shape of the plot is an indicator of how close the sample length is to an integral multiple of the strong periods of fluctuation. In other words, if the data fluctuate at 10-minute periods, samples of 20, 30, 40 minutes, etc. will have smaller coefficents of variation than samples that do not include integral multiples of fluctuation periods.

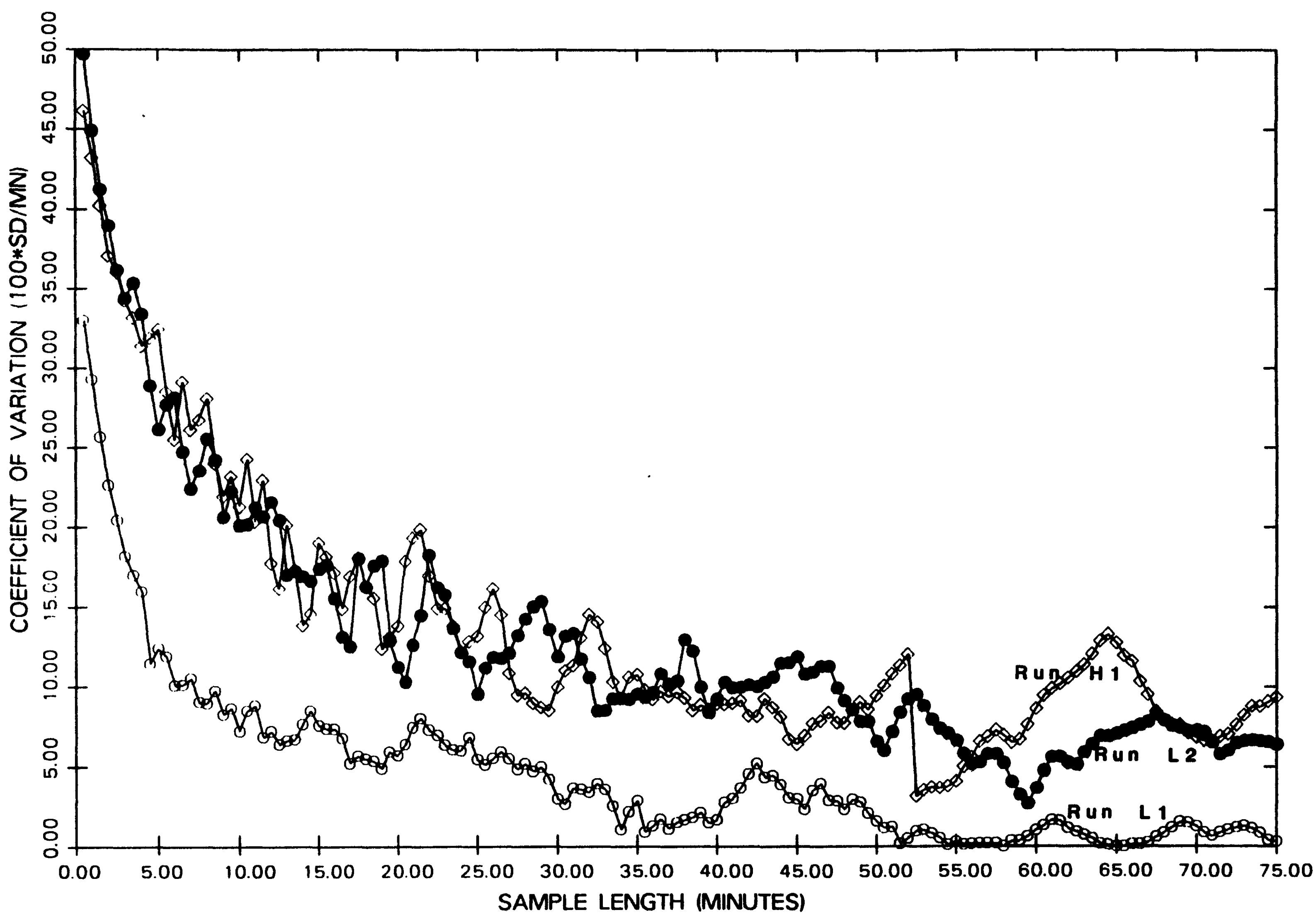

FIG. 24.-- Coefficient of variation vs. sample length,
Runs L1, L2, and H1

The worst case in this exercise would be a 30-second sample taken during Run L2. The coefficient of variation for this example is 49.6%. If we assume a normal distribution for the population of the data then the probability is 0.68 that a 30-second sample will be within 49.6% of the mean transport rate, or 0.95 that the sample will be within 99.2% of the mean. If the assumption that the data are normally distributed is a poor one, these probabilities decrease. Undoubtedly these uncertainties are too great to yield much useful information about the mean from a 30-second sample. The coefficients of variation for 30-second samples from Runs L1 and H1 are nearly as high: 32.9% and 46.1%, respectively. As sample lengths are increased the standard deviations become smaller relative to the mean transport rate. Figure 24 shows that samples on the order of 50 minutes are necessary in order to obtain the best estimates of the mean rates for Runs L2 and H1. Run L1, however, needs to be sampled for only about 20 minutes to obtain the same chance of correctly predicting the mean rate as for the other two runs. These differences in optimum sample lengths can be explained by the observation made previously that Runs L2 and H1 both had fluctuations of the order of 25 minutes whereas Run L1 did not.

Sampling the transport rate of a stream with fluctuations like those in Run H5 would undoubtedly not require as long a sample as those listed above. The above technique was applied to the data of Run H5, but the sampling length was too short to yield meaningful results. In any case this study suggests that for many gravel-bed streams sampling needs to be undertaken with caution in order to predict the mean rates accurately. Generally samples must be taken for times much longer than is often done and/or a long series of short samples must be taken. Also, averaging of a string of short samples must take into account the variability of the changing hydraulic conditions of the stream. Kang (1982) discusses this problem in terms of sampling Hilda Creek.

CONCLUSIONS

(1) Sediment transport rate was observed to vary quasi-periodically in a series of runs for which the transport rate was varied by more than a factor of 30. At the lowest transport rates (~0.03-0.04 kg/s•m) two main periods of fluctuation were observed, 6-14 minutes and 25 minutes. At higher transport rates (~0.08-0.1 kg/s•m) fluctuation periods were clustered about 6 minutes, with no evidence for longer-term variations. At the highest transport rate (~1 kg/s•m) there is some evidence for a 3-minute periodicity in the transport rates.

(2) Fractional transport rates in the runs, excluding Run H5, varied with time in the following way. The 16-32 mm size fraction moved randomly and infrequently. The transport rate of the 4-16 mm fraction tended to peak before the total transport rate. The transport rate of the 1-4 mm fraction followed the total transport rate closely. The transport rate of the <1 mm fraction tended to peak after the total rate had peaked. The run with the highest transport rate, Run H5, was different from the rest in that all sizes except the 16-32, 1-2, and <1 mm fractions moved through the channel at essentially steady rates. The transport rate of the 1-2 mm fraction showed evidence for a 3-minute fluctuation period, and the transport rates of the 16-32 mm fraction and the <1 mm fraction peaked before and after that of the 1-2 mm fraction, respectively.

(3) The migration of long (0.5-3 m) and low (2-4 mm) bed-load sheets was observed to be the cause of the 6-14 minute fluctuations in the runs with transport rates between 0.03 to 0.1 kg/s·m. The cause of the fluctuations with a 25-minute period is not known but might be related to jamming of large clasts on the bed. In the run with the highest transport rate (~1 kg/s·m), dunelike bed forms 60 cm long and 1 cm high that were constantly being destroyed and reformed are believed to have caused the 3-minute variations in transport of the 1-2 mm size fraction.

(4) The bed surface of the channel developed an armored layer much coarser than the original sediment mix in all runs except that with the highest transport rate. In the run with the highest transport rate the size distribution of the bed surface was very nearly the same as that of the original size mix.

(5) Sample lengths of 40-50 minutes were found to be necessary to predict mean transport rates with the greatest accuracy for the runs with 0.03-0.04 kg/s·m transport rates. Somewhat shorter sample lengths of 20-30 minutes were found to be necessary for the transport rates of the order of 0.1 kg/s·m.

REFERENCES

Ashmore, P. E., 1982, Laboratory modelling of gravel braided stream morphology: Earth Surface Processes and Landforms, v. 7, p. 201-225.

Boothroyd, J. C., and Ashley, G. M., 1975, Processes, bar morphology, and sedimentary structures on braided outwash fans, northeastern Gulf of Alaska, in Jopling, A. V., and McDonald, B. C., eds., Glaciofluvial and Glaciolacustrine Sedimentation, Society of Economic Paleontologists and Mineralogists Special Publication no. 23, p. 193-222.

Casey, I. H. J., 1935, Über Geschiebebewegung Mitteilungen der Preussischen: Versuchsanstalt fur Wasserbau und Schiffbau, Berlin, Helf 19.

Church, M., 1972, Baffin Island sandurs: a study of arctic fluvial processes: Geological Survey of Canada, Bulletin 216, 208 p.

Davis, J. C., 1973, Statistics and Data Analysis in Geology, John Wiley and Sons, New York, 550 p.

Dhamotharan, S., Wood, A., Parker, G., and Stefan, H., 1980, Bedload transport in a model gravel stream, University of Minnesota, St. Anthony Falls Hydraulic Laboratory, Project No. 190, 75 p.

Eynon, G., and Walker, R. G., 1974, Facies relationships in Pleistocene outwash gravels, southern Ontario: a model for bar growth in braided rivers: Sedimentology, v. 21, p. 43-70.

Fisher, R. A., 1929, Test of significance in harmonic analysis: Proceedings of the Royal Society of London, A, v. 125, p. 54-59.

Hails, J. R., 1976, Placer deposits: in Wolf, K. H., ed., Handbook of Strata-Bound and Stratiform Ore Deposits, Volume 3, Supergene and Surficial Ore Deposits; Textures and Fabrics, Elsevier Publishing Company, Amsterdam, p. 213-244.

Hammer, K. M., and Smith, N. D., 1983, Sediment production and transport in a proglacial stream: Hilda Glacier, Alberta, Canada: Boreas, v. 12, p. 91-106.

Hein, F. J., and Walker, R. G., 1977, Bar evolution and development of stratification in the gravelly, braided Kicking Horse River, British Columbia: Canadian Journal of Earth Science, v. 14, p. 562-570.

Hubbell, D. W., Stevens, H. H., Jr., Skinner, J. V., and Beverage, J. P., 1981, Recent refinements in calibrating bedload samplers, in Water Forum '81, American Society of Civil Engineers, p. 128-141.

Kang, S., 1982, Sediment transport in a small glacial stream: Hilda Creek, Alberta, unpublished M.S. thesis, University of Illinois at Chicago, 265 p.

Klingeman, P. C., Milhous, R. T., and Heinecke, T. L., 1979, 'Oak Creek vortex bedload sampler', Oak Creek Sediment Transport Report F2, Water Resources Research Institute, Oregon State University, Corvallis, Oregon.

----------------, and Emmett, W. W., 1982, Gravel bedload transport processes, in Hey, R. D., Bathhurst, J. C., and Thorne, C. R., eds., Gravel-bed Rivers, John Wiley and Sons, New York, p. 141-169.

Krigström, A., 1962, Geomorphological studies of sandur plains and their braided rivers in Iceland: Geografiska Annaler, v. XLIV (44), p.328-346.

Kuhnle, R. A., 1981, An experimental study of braiding in gravel-bed streams, unpublished M.S. thesis, University of Illinois at Chicago, 56 p.

Leopold, L. B., and Emmett, W. W., 1976, Bedload measurements, East Fork River, Wyoming: Proceedings of the National Academy of Science, v. 73, p. 1000-1004.

McDonald, B. C., and Bannerjee, I., 1971, Sediments and bedforms on a braided outwash plain: Canadian Journal of Earth Science, v. 8, p. 1282-1301.

Maizels, J. K., 1979, Proglacial aggradation and changes in braided channel patterns during a period of glacial advance: an alpine example: Geografiska Annaler, v. 61, p. 87-101.

Mavis, F. T., Liu, T. Y., and Soucek, E., 1937, The transportation of detritus by flowing water-- II: University of Iowa Studies in Engineering, Bulletin 11, 23p.

Miall, A. D., 1977, A review of the braided-river depositional environment: Earth Science Reviews, v. 13, p. 1-62.

Minter, W. E. L., 1978, A sedimentological synthesis of placer gold, uranium and pyrite concentrations in Proterozoic Witwatersrand sediments, in Miall, A. D., ed., Fluvial Sedimentology, Canadian Society of Petroleum Geologists, Memoir 5, p. 801-829.

Nowroozi, A. A., 1966, Terrestrial spectroscopy following the rat island earthquake: Bulletin Seismology Society of America, v. 56, p. 1269-1288.

---------------, 1967, Table for Fisher's test of significance in harmonic analysis: Geophysical Journal of the Royal Astronomical Society, v. 12, p. 517-520.

Østrem, G., 1975, Sediment transport in glacial meltwater streams, in Jopling, A. V., and McDonald, B. C., eds., Glaciofluvial and Glaciolacustrine Sedimentation, Society of Economic Paleontologists and Mineralogists, Special Publication 23, p. 101-122.

Reid, I., Frostick, L. E., and Layman, J. T., 1985, The incidence and nature of bedload transport during flood flows in coarse-grained alluvial channels: Earth Surface Processes and Landforms, v. 10, p. 33-44.

Smith, N. D., 1974, Sedimentology and bar formation in the upper Kicking Horse River, a braided outwash stream: Journal of Geology, v. 82, p. 205-223.

United States Waterways Experiment Station, 1935, Studies of river bed materials and their movement, with special reference to the lower Mississippi River, Paper 17, Vicksburg, Mississippi, 161 p.

Wells, S. G., and Dohrenwend, J. C., 1985, Relict sheetflood and late Quaternary alluvial-fan surfaces in the southwestern United States: Geology, v. 13, p. 512-516.

Whiting, P. J., Leopold, L. B., Dietrich, W. E., and Collins, L. M., 1985, The variability of sediment transport in a fine-gravel stream, Abstract, Third International Fluvial Sedimentology Conference, Fort Collins, Colorado.

Whiting, P. J., and Dietrich, W. E., 1986, Bedload sheets in fine-gravel: field observations and sedimentological implications: Geology (in press).

Williams, P. F., and Rust, B. R., 1969, The sedimentology of a braided river: Journal of Sedimentary Petrology, v. 39, p. 649-679.

Part II

TRANSPORT OF HEAVY MINERALS

ABSTRACT

Flume experiments were conducted to determine the mechanisms of transport and deposition of heavy minerals in a gravel-bed channel in shallow unidirectional flows. Two water-recirculating sediment-feed flumes were used: one with a channel 6 m long and 0.15 m wide and the other with a channel 11 m long and 0.53 m wide. Poorly sorted gravel with a mean size of 3 mm with 3% by weight of magnetite (density 5.2 g/cm^3), lead (density 11.4 g/cm^3), and tungsten (density 19.3 g/cm^3) was used. The magnetite and tungsten were 0.125-0.500 mm in size, while the lead was 0.500-0.707 mm in size.

The heavies became concentrated into a layer (here termed heavy sublayer)composed of nearly 100% heavy minerals and lying beneath a layer of low-density sediment. Heavies were not transported in long-term equilibrium runs in a given region of the bed until the heavy sublayer was fully developed there.

Heavies were transported at the top of the heavy sublayer only when erosion of the active layer exposed the heavy sublayer to the flow. Bed forms in the low-density sediment of the active layer controlled the exposure of the heavy sublayer to the flow and caused the transport rate of the heavies to vary over scales of minutes. Longer-term fluctuations in the total transport rate of the sediment in the runs with low transport rates also caused the transport rate of the heavies to vary at that period (~25 min).

Heavy minerals were found not to be transported during aggradation of the bed unless the rate of general aggradation was very low or during general degradation unless the rate of degradation was very high. Otherwise, the presence of heavy sublayers is necessary for the transport of heavy minerals under degradation or aggradation.

INTRODUCTION

Deposits in which heavy-minerals particles have been mechanically concentrated from regolith are common in modern and ancient sediments. (Our arbitrary definition of heavy minerals, hereafter called "heavies", is any detrital mineral with a density of 3.5 g/cm^3 or greater.) Such deposits are usually alluvial but can also be marine, eolian or even glacial (Hails, 1976). Most are known from relatively recent sediments. When the concentrated heavy mineral is an economic mineral the deposit is called a placer. A variety of minerals occur as placers (Table 1). Most minerals recovered from placers are near the primary source (Hails, 1976).

Placer deposits and other heavy-mineral concentrations have been divided into three groups based on their properties and environment of deposition. These are "heavy heavy" minerals (gold, tin, platinum), which occur mainly in alluvial streams; "light heavy" minerals (ilmenite, rutile, zircon, and monazite) which occur on beaches; and gems (mostly diamonds), which are chiefly alluvial placers (Hails, 1976). Alluvial placers, especially of "heavy heavy" minerals, are usually found in gravel-bed streams.

The increasing scarcity of high-grade placer mineral reserves has provided a powerful incentive for studies aimed at understanding the processes that concentrate them (Crampton, 1937; Cheney and Patton, 1967; Gunn, 1968; Sestini, 1973; Minter, 1978; Smith and Minter, 1980). The above field studies have begun to solve the problem, but more experimental studies in which important variables are controlled are needed to

Table 1. PHYSICAL PROPERTIES OF THE MORE COMMON PLACER MINERALS

Mineral	Moh's Hardness	Density (g/cm^3)	Resistance to weathering
Diamond (C)	10.0	3.5	very high
Garnet ($A_3B_2(SiO_4)_3$	6.5-7.5	3.5-4.3	moderate
Corundum (Al_2O_3) (Ruby and Sapphire)	9.0	3.9-4.1	very high
Rutile (TiO_2)	6.0-6.5	4.2-4.3	high
Zircon ($ZrSiO_4$)	7.5	4.5-4.7	very high
Ilmenite ($FeTiO_3$)	5.0-6.0	4.5-5.0	high
Monazite ($(Ce,La,Y,Th)PO_4$)	5.0	4.9-5.3	high
Magnetite (Fe_3O_4)	5.5-6.5	5.1-5.2	high
Cassiterite (SnO_2)	6.0-7.0	6.8-7.1	high
Uraninite (UO_2)	5.5	7.5-9.7	moderate
Platinum (Pt)	4.0-4.5	14.0-19.0 (native)	very high
Gold (Au)	2.5-3.0	19.3	very high

(after Hails, 1976)

supplement this information. To date there have been few experimental studies dealing with this problem (e.g. Wertz, 1949; Minter and Toens, 1970; Brady and Jobson, 1973; Best and Brayshaw, 1985).

Although the density of minerals sorted by surficial transport is known to vary over a wide range, from that of diamond, 3.5 gm/cm^3, to that of gold, 19.3 gm/cm^3 (Table 1), it has not been established how (or even if) the concentrating mechanisms vary with density. As a first approximation, relatively low-density heavy minerals, like magnetite, are often used as a general example of how heavy minerals of a whole range of densities are transported and deposited. The validity of this approximation is not known.

It is logical to consider theoretically what is understood about the process of concentration of heavy minerals by unidirectional fluid flows. Although at present the physics of the forces and interactions on grains being transported by flowing fluids is too complicated to treat explicitly, the similar but simpler case of fluid flowing at a velocity below the threshold for movement of the bed grains can be considered. The forces on a single grain on the bed (Fig. 1) can be separated into those resisting transport and those driving it. The resisting force is the submerged weight of the grain acting through its center of mass:

$$F_G = V(\rho_S-\rho)g \qquad (1)$$

where V and ρ_S are the volume and density of the grain, respectively, ρ is the density of the fluid, and g is the

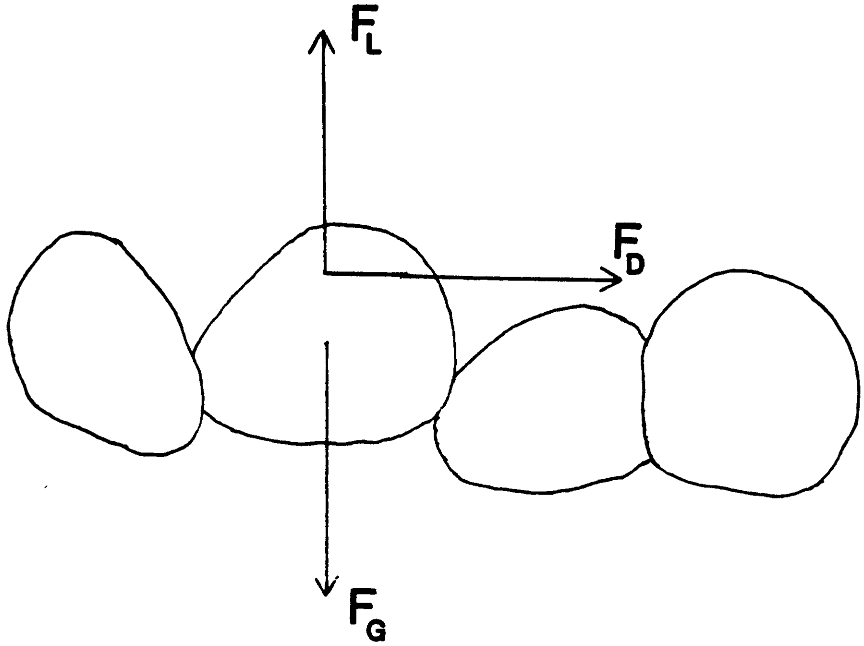

FIG. 1.-- Forces acting on a grain

acceleration of gravity. The driving forces can be resolved into the drag force and the lift force:

$$F_D = C_D(U^2/2)A \quad (2)$$

$$F_L = C_L(U^2/2)A \quad (3)$$

where C_D and C_L are coefficients of drag and lift, U is a characteristic velocity of the flow, and A is the cross-sectional area exposed to the flow. Determining the gravity force is straightforward, but certain ambiguities exist in determining the other two forces: the exposed area of the grain and the coefficient of lift and drag are variable, and it is difficult to define a characteristic velocity that can be measured readily. Thus even for the simplified case of motionless grains it is difficult to determine precisely the forces imposed by the fluid. We can look, however, at how these forces would differ for two grains of different density with all other factors being the same. It is apparent that the only difference caused by density in the forces outlined above lies in the gravity force. Due to the greater density, the gravity force acts on a larger mass for the same volume. Thus higher-density grains should be more difficult to move than lower-density ones. Also, once in transport the denser grains will probably move slower than less dense grains (Steidtmann, 1982).

Heavies tend to be smaller than the lower-density grains ("lights") with which they are associated. This is particularly true for the "heavy heavy" grains like gold (Slingerland and Smith, 1986). If heavies do occur in gravel sizes, their mass is so great that they tend to be deposited very near their source.

To sum up, then, two main factors reduce the transportability of heavy-mineral grains: (i) their large mass per volume and (ii) their small size relative to the mean size of the sediment, which causes them to be shielded from the flow because they are hidden among the larger grains. Therefore, due to the difficulty of transport the "heavy heavies" particularly tend to be found in steeply sloping gravel-bed streams. This was the principal reason that a portion of a steeply sloping gravel-bed stream was chosen for modelling in this investigation.

Although heavy minerals are known to be concentrated by transport processes operating in several different depositional environments, fluvial environments will be specifically considered here. Placer formation in a fluvial system varies over wide spatial and temporal scales. These spatial scales can naturally be divided into (i) large, $\sim 10^4$ m, (ii) intermediate, $\sim 10^2$ m, and (iii) small, $\sim 10^0$ m (Smith and Minter, 1980; Slingerland, 1984); Slingerland and Smith, 1986). These scales are related to three different scales of the fluvial system, respectively: the size of fluvial basins, the size of channels, and the size of part of a channel. The time scales associated with placer formation on these three spatial scales varies from many years for the largest scale to minutes for the smallest scale. These scales are hierarchical, in that a large-scale accumulation is made up of many intermediate-scale accumulations, each of which in turn is made up of many small-scale accumulations (Smith and Minter, 1980). An understanding of the small-scale processes is therefore necessary for an understanding of the larger-scale ones.

Perhaps the ideal approach to the problem of density sorting would be to formulate general models of transport and deposition that would apply to sediment mixtures with all percentages and sizes of lights and heavies. This has not yet been accomplished due to the great complexity of turbulent fluid flow over a loose bed. Another approach, the one taken here, is to represent as accurately as possible part of a natural system in a laboratory flume and determine how the heavies and lights respond in a representative mixture to a range of flows and transport rates. The goal of this study is to physically simulate a part of a gravel-bed river with a sediment composed dominantly of a light fraction ranging in size from 0.125 to 32 mm together with a small percentage of three different heavies ranging in size from 0.125 to 0.7 mm. In this approach the transport of heavies and lights was investigated in fixed-width channels, first with steady uniform flow and later with erosion of the sediment bed.

PREVIOUS WORK

Information on how heavy minerals are concentrated in fluvial environments comes from two main sources: field studies of recent and ancient placer deposits, and experimental studies. In the field it has generally been found that heavies are concentrated most strongly at places of reworking in a fluvial system. This often occurs at the scoured bases of sedimentary units, although there are lesser concentrations in various subenvironments within the units. These subenvironments have been summarized in a table by Slingerland and Smith (1986), reproduced here as Table 2.

Although experimental studies on density sorting have been few, much valuable information has been gained and undoubtedly much more is potentially available through this method of study. The experiments done to date have modeled fluvial processes from the scale of an entire drainage basin to that of a small part of an alluvial channel. At large scales (Adams, Zimpfer, and McLane, 1978), intermediate scales (Wertz, 1949; Shepherd and Schumm, 1974; Mosely and Schumm, 1977; Best and Brayshaw, 1985), and small scales (McQuivey and Keefer, 1969; Minter and Toens, 1970; Brady and Jobson, 1973; Steidtmann, 1982) experiments have effectively modelled parts of the fluvial system and have yielded useful information on the processes and conditions necessary to segregate minerals by density.

The foundation for the modern understanding and interpretation of density sorting by currents is the work of

Table 2. OBSERVED SITES OF WATER-LAID PLACERS

Large Scale (10^4 m)	
Bands parallel to depositional strike	Minter(1970, 1978), Sestini (1973) McGowan and Groat (1971)
Heads of wet alluvial fans	Schumm (1977)
Points of abrupt valley widening	Kuzvart and Bohmer (1978), Crampton (1937), Hall, Thomas, and Thorp (1985)
Points of exit of highland rivers onto a plain	Toh (1978)
Regional unconformities	Minter (1976, 1978)
Strand-line deposits	Nelson and Hopkins (1972), Komar and Wang (1984), Eliseev (1981)
Incised channelways	Minter (1978), Yeend (1974), Buck (1983), Buck and Minter (1985)
Pediment mantles	Krapez (1985)
Intermediate Scale (10^2 m)	
Concave sides of channel bends	Kuzvart and Bohmer (1978), Crampton (1937)
Convex banks of channel bends	Kuzvart and Bohmer (1978)
Heads of mid-channel bars	Toh (1978), Smith and Minter (1980), Kartashov (1971), Boggs and Baldwin (1970)
Point bars with suction eddies	Toh (1978), Bateman (1950)
Scour holes, esp. at tributary confluences	Kuzvart and Bohmer (1978), Mosely and Schumm (1977), Best and Brayshaw (1985)
Inner bedrock channels and false bedrock	Schumm (1977), Kuzvart and Bohmer (1978), Adams et al. (1978)
Bedrock riffles	Cheney and Patton (1967), Toh (1978)

Table 2 continued

Constricted channels between banks and bankward-migrating bars	Smith and Minter (1980), Smith and Beukes (1983)
Beach swash zones	Stapor (1973), Reimitz and Plafker (1976), Kogan et al (1975) Reid and Frostick (1985b)
Basal channel gravels	Thomas, Thorp, and Teeuw (1985), Hall, Thomas, and Thorp (1985), Camm and Hasking (1985), Aleva (1985)
<u>Small Scale (10^0 m)</u>	
Scoured bases of trough cross-strata sets	Toh (1978), McGowan and Groat (1971), Smith and Minter (1980), Buck (1983)
Winnowed tops of gravel bars	Toh (1978), McGowan and Groat (1971)
Thin ripple-form accumulations	Brady and Jobson (1973)
Dune crests	Brady and Jobson (1973)
Dune foresets	Brady and Jobson (1973), McGowan and Groat (1971), Buck (1983), Turner and Minter (1985)
Plane parallel laminae	Slingerland (1977), Clifton (1969) Buck (1983), Stavrakis (1980)
Leeward sides of obstacles	Lindgren (1911), Best and Brayshaw (1985)
Beach berms	Stapor (1973)

(from Slingerland and Smith, 1986)

Rubey (1933) and Rittenhouse (1943) on hydraulic equivalence. Hydraulic equivalence has been described as "whatever the hydraulic conditions may be that permit the deposition of a grain of particular physical properties, these conditions will also permit deposition of other grains of equivalent hydraulic value" (Rittenhouse, 1943). Although Rittenhouse and Rubey acknowledged that many factors affect hydraulic equivalence, to many workers the term became nearly synonymous with equality of settling velocity: irrespective of size, shape, and density, grains with equal settling velocities are said to be hydraulically equivalent. Settling velocities are usually calculated using a semi-empirical formula that assumes isolated grains settling under their own weight in a still and unbounded fluid, but the conditions to which grains in streams are subjected are usually far more complicated. Slingerland and Smith (1986) point out that in most placer-forming environments the water is flowing and turbulent and the concentration of suspended sediment may be high enough to significantly affect settling rates of different particles. The effect of turbulence in nearly all cases where grains are deposited from suspension should be taken into account, and in some cases the concentration of suspended grains may also be a factor. Unfortunately the effect of turbulence on settling is unclear (Slingerland and Smith, 1986), and suspended-sediment concentrations are difficult to determine unless measured during the actual depositional event. Furthermore, the importance of heavy-mineral transport in suspension is not now known. Much more information on the size of the heavies in placer deposits is needed along with experiments to resolve this question.

Entrainment equivalence is important in addition to settling equivalence in density sorting. McIntyre (1959) and Hand (1967) realized that something more than settling equivalence is needed to account for the presence of different sizes and densities of grains in a deposit. As a result Hand (1967) and Lowright et al. (1972), and later Slingerland (1977) and Burroughs (1982), have revised or extended the idea of hydraulic equivalence to take into account the differential entrainment of grains, leading to the idea of entrainment equivalence: two grains of differing density are said to be equivalent with respect to entrainment if they are set in motion from a state of rest on the same sediment bed by the same fluid forces.

Although sound, the idea of entrainment equivalence is not as readily applicable as that of settling equivalence, because the relative entrainment and bed-load transport of grains depends not only on their size and physical characteristics but also very strongly on the sizes and characteristics of all of the other grains exposed to the flow. A good first approach to this problem was made by McQuivey and Keefer (1969) and Grigg and Rathbun (1969). These workers used Shields' (1936) work on initiation of motion to demonstrate that for unisize sediments the grains with greater density need higher shear stresses to be entrained. The problem of mixed sizes of both lights and heavies, however, is not treated in their approach. Komar and Wang (1984), making use of the data of Miller and Byrne (1966), have generated plots of critical shear stress for mixed-size sediments. These relations show that grains smaller and larger than the mean size require higher shear stresses in order to be entrained. Slingerland and Smith (1986) have summarized some of the findings of Komar and Wang (1984) and have identified five different kinds of grain behavior important to entrainment sorting (hiding, trapping, armoring, overpassing, and general motion) and qualitatively illustrated them in plots of Shields parameter vs. the ratio of a given size fraction to that of the mean size. Hiding and trapping occur for grains smaller than the mean size, while armoring occurs for grains larger than the mean. Reid and Frostick (1985a) have also discussed entrainment equivalence and pointed out that interstice trapping is important for segregating minerals by density.

The sorting of grains when there is general transport of all sizes and densities is another facet of density sorting that needs to be considered. This problem is made difficult not only by all of the complications inherent in entrainment equivalence, mentioned above, but also by the transport of grains of different sizes and densities as bed load or suspended load, and also by armoring of the transport surface and the presence of bed forms that vary with flow strength. The work of Steidtmann (1982) has shed light on the effect of bed forms on transport of grains with different densities. In depositional runs in an expanding-width channel, Steidtmann found that in the presence of ripples there was virtually no downstream density sorting, but in plane-bed transport the concentration of heavies decreased rapidly downstream. This work begins to demonstrate the complexities associated with the transport states of grains of differing size and density.

Slingerland (1984) addressed the problem of transport sorting through the use of the Einstein bed-load function, by solving for the transport rates of quartz and magnetite minerals assuming a given bottom roughness size. The results of these calculations are useful as a first approximation, but the Einstein bed-load function, although it explicitly takes into account the effect of different sizes in a sediment, fails to predict measured transport rates adequately in many instances (e.g. Parker, Klingeman, McLean, 1982, Fig. 8, p. 559). The approach taken by Slingerland (1984), that of using a general transport law and solving for the transport rates of the different size and density fractions, is certainly the right approach to solving this problem, but to date no sediment-transport formula has been developed which adequately predicts transport rates for a wide range of conditions for sediment of a single density (Wilcock, Southard, and Paola, 1985). Thus predicting transport rates of sediments with mixed sizes and densities is not practical at the present time.

Slingerland and Smith (1986) also identified the dispersive pressure caused by interactions between the particles of a concentrated flow of cohesionless grains when they are sheared by gravity or fluid forces as an additional process by which grains may be sorted by density. Theoretical and experimental studies by Bagnold (1954, 1956) suggest that dispersive pressures are greater on larger and denser grains than on smaller or less dense grains in one horizon of a grain flow. This theory has not been tested for sediments of mixed sizes or densities, so the effects of dispersive pressure as a sorting agent are not known.

In summary, the main sites of heavy-mineral segregation in fluvial systems have been discovered by field studies of modern and ancient placer deposits. Processes of formation of these deposits have been illuminated through field studies of modern rivers with heavies in their sediment and experiments modeling portions of fluvial systems in the laboratory. In summarizing the status of understanding of the mechanics of density segregation, Slingerland and Smith (1986) have broken down the problem of density sorting into differential settling, entrainment, transport, and dispersive transport. To date laboratory studies have used only material with densities 5.2 g/cm^3 or less as the high-density fraction of the sediment. Also all of these studies (Wertz, 1949; McQuivey and Keefer, 1969; Minter and Toens, 1970; Brady and Jobson, 1973; Shepherd and Schumm, 1974; Mosely and Schumm, 1977; Adams, Zimpfer, and McLane, 1978; Steidtmann, 1982; Best and Brayshaw, 1985) except one (Minter and Toens, 1970) used sediments exclusively in the sand size range.

This project was designed to extend the range of experimental conditions to include heavies of three different densities (5.2, 11.4, 19.3 g/cm^3) and light minerals with a mean size in the finest gravel range. The selection of the sediment sizes for this study was a very important decision. Many studies have noted the sizes of the gravels that contain concentrations of heavy minerals (e.g. Minter and Toens, 1970; Boggs and Baldwin, 1970; Sestini, 1973; Minter, 1978; Nami, 1983; Krapez, 1985). Gravels up to boulder size have been reported. Information on the sizes of the heavy heavies, like gold, is much scarcer. The mean sizes reported for detrital gold vary from 0.025 to 1.0 mm. Table 3 lists the sizes reported by several workers. The size of the heavy fractions is very important for how the grains of a given sediment mix are transported by a given flow. The sizes of the lights and heavies in this study were chosen to the best of our knowledge to represent conditions commonly associated with natural placers.

Table 3. REPORTED SIZES OF DETRITAL GOLD

Reference	Mean size (mm)	Range (mm)
Boggs and Baldwin, 1970	0.04 - 0.7	0.03 - 1.0
Minter, 1978	--	0.005 - 0.5
Nami, 1983	0.07	0.025 - 0.3
Valls, 1985	0.17 - 0.66	0.026 - 4.63 (est)

EXPERIMENTS

Equipment

The experiments were made in the Experimental Sedimentology Laboratory at the Massachusetts Institute of Technology. All runs except one were made in a flume with a channel 6 m long and 0.15 m wide. One run, made in a flume with a channel 0.53 m wide and 11 m long, indicated that both the running times and volume of sediment needed for attainment of steady-state conditions in the larger flume were impractically large for this study, so the larger flume was abandoned for the smaller one. The smaller flume had a channel length of 10 m, but only the downstream 6 m was used, because the time necessary for the flow to come to a steady state depends not only on the transport rate per unit width but also on the channel length. Thus, if the full length of the small flume had been used, running times would not have been significantly shorter than in the larger flume, although the total volume of sediment need for a run would have been much less. The disadvantage of using the smaller flume is that only small-scale processes can be studied. Only the 0.15 m wide flume is described below. The arrangement of the larger flume was very similar to the smaller except that the sediment was fed automatically rather than manually; for more details see Part I.

The water in the flume was recirculated with a centrifugal pump, while the sediment was fed manually at the upstream end of the flume and trapped in the sump located downstream of the channel exit (Figs. 2, 3, and 4). Sediment was fed by hand at a rate that varied by ±4% at most. Water discharge was controlled by adjusting a gate valve located in the return pipe, and was measured with calibrated 90° bend meter and manometer to within ±4.5%. Elevations of bed surface and water surface were measured to within ± 0.1 mm with a point gauge mounted on a platform that slid over the flume rails.

The channel ended downstream in a free overfall that discharged into a sump. Transport samples were measured by placing a basket covered with wire cloth with 0.1 mm openings into the overfall for a measured time. When successive 30-second transport samples were being taken, three baskets were moved into the overfall sequentially and were emptied into three-liter metal sample cans through large frame-mounted funnels.

The downstream end of the channel was fitted with a movable tailgate in order to make steady rates of degradation in the channel bed possible. The tailgate, made of 3/4" thick acrylic plastic, was lowered with two 1/4" x 20 threaded rods that were mounted in tapped holes in the gate support (Fig. 5).

The light fraction of the sediment, obtained by wet-sieving locally available outwash gravels, ranged in size from 0.125 to 32 mm (3.0 to -5.0 ϕ). The gravel-sized clasts of the light fraction consisted of angular to rounded, mainly equant rock fragments and quartz with densities ranging from 2.6 to 3.0 g/cm^3.

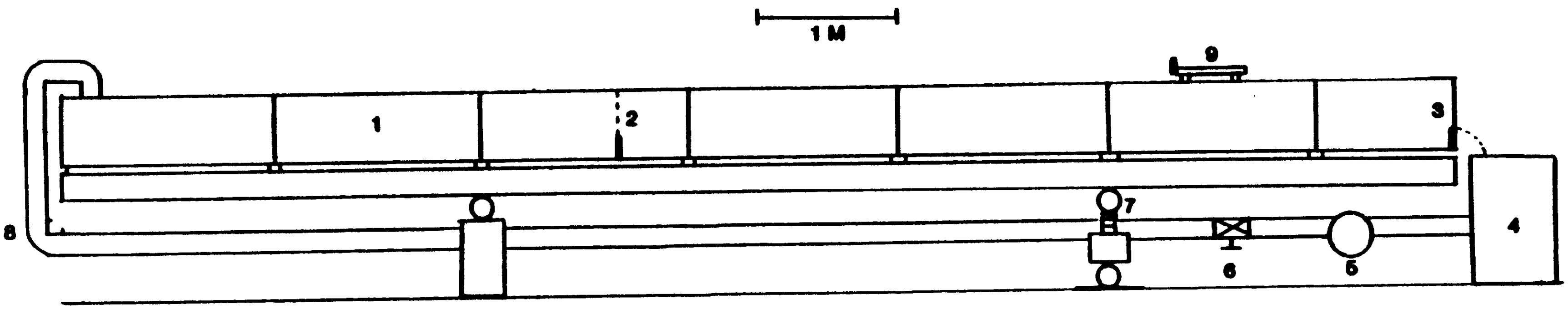

FIG. 2.-- Schematic diagram of 6 m flume

1. headbox
2. weir and baffle
3. downstream weir
4. tail barrel
5. pump
6. gate valve
7. adjustable support
8. 90^{o} elbow meter
9. instrument platform

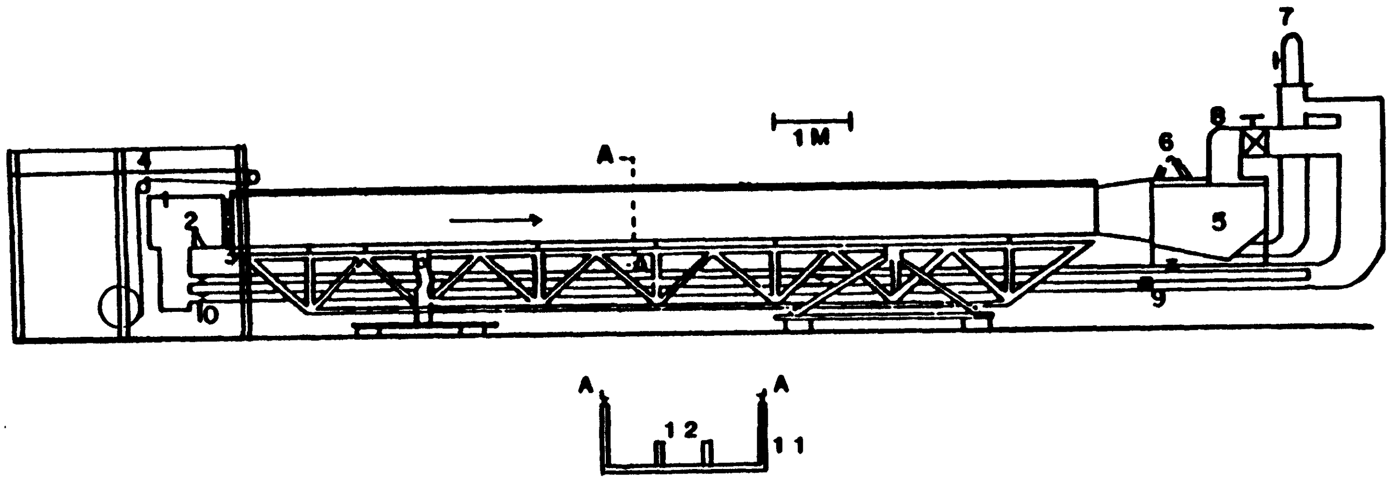

FIG. 3.-- Schematic diagram of 11 m flume

1. headbox	7. pump
2. weir	8. bypass line and valve
3. baffle	9. return lines and valves
4. sediment feeder	10. Venturi meters
5. tailbox	11. plywood channel
6. filtration system	12. 0.5 m wide inner channel

A

B

FIG. 4.-- Photographs of the two flumes.
A-- 6 m flume, B-- 11 m flume.

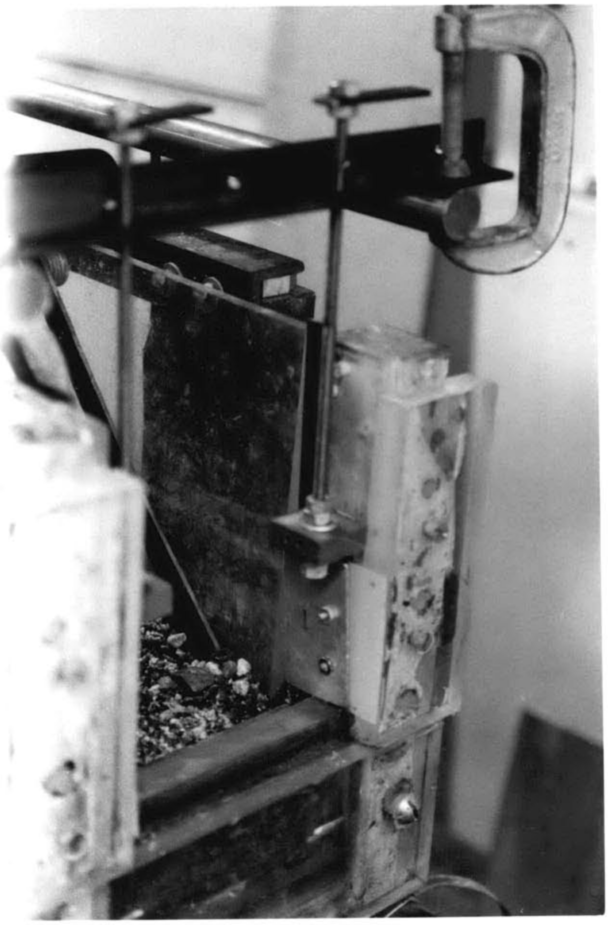

FIG. 5.-- Photograph of tailgate on 6 m flume

The heavy fraction of the sediment consisted of 0.9% magnetite (density 5.2 g/cm^3), 1.2% lead (density 11.4 g/cm^3), and 0.9% tungsten (density 19.3 g/cm^3) by weight. (All percent concentrations of heavies given in this study will be by weight.) The magnetite, sieved from a commercially available crushed product, ranged from 0.125 to 0.500 mm (3.0 to 1.0 ϕ) in size; the grains were angular and irregular. The lead consisted of spherical shot that ranged in size from 0.350 to 0.707 mm (1.5 to 0.5 ϕ). The tungsten consisted of crushed and sieved tungsten metal ranging in size from 0.125 to 0.500 mm (3.0 to 0.5 ϕ); grains were generally angular and equant. Cumulative size distributions for the total sediment mix and each of the heavies are shown in Figures 6 and 7. It was originally planned that all three heavy fractions would have the same size distribution. This would have meant that any differences in transport among the three would have been an effect only of density. As shown in Figure 7 the size distributions of the magnetite and tungsten are reasonably similar, but that of the lead was different, due to the difficulty of obtaining lead in the size range desired.

The concentrations of lead and tungsten in the sediment, 1.2% and 0.9%, respectively, are much higher than generally found in nature for minerals of similar density. These concentrations were used in order to make determinations of the percentage of heavies in a sample practical. If lower percentages had been used, unworkably large samples would have been necessary in order to reduce sampling errors to an

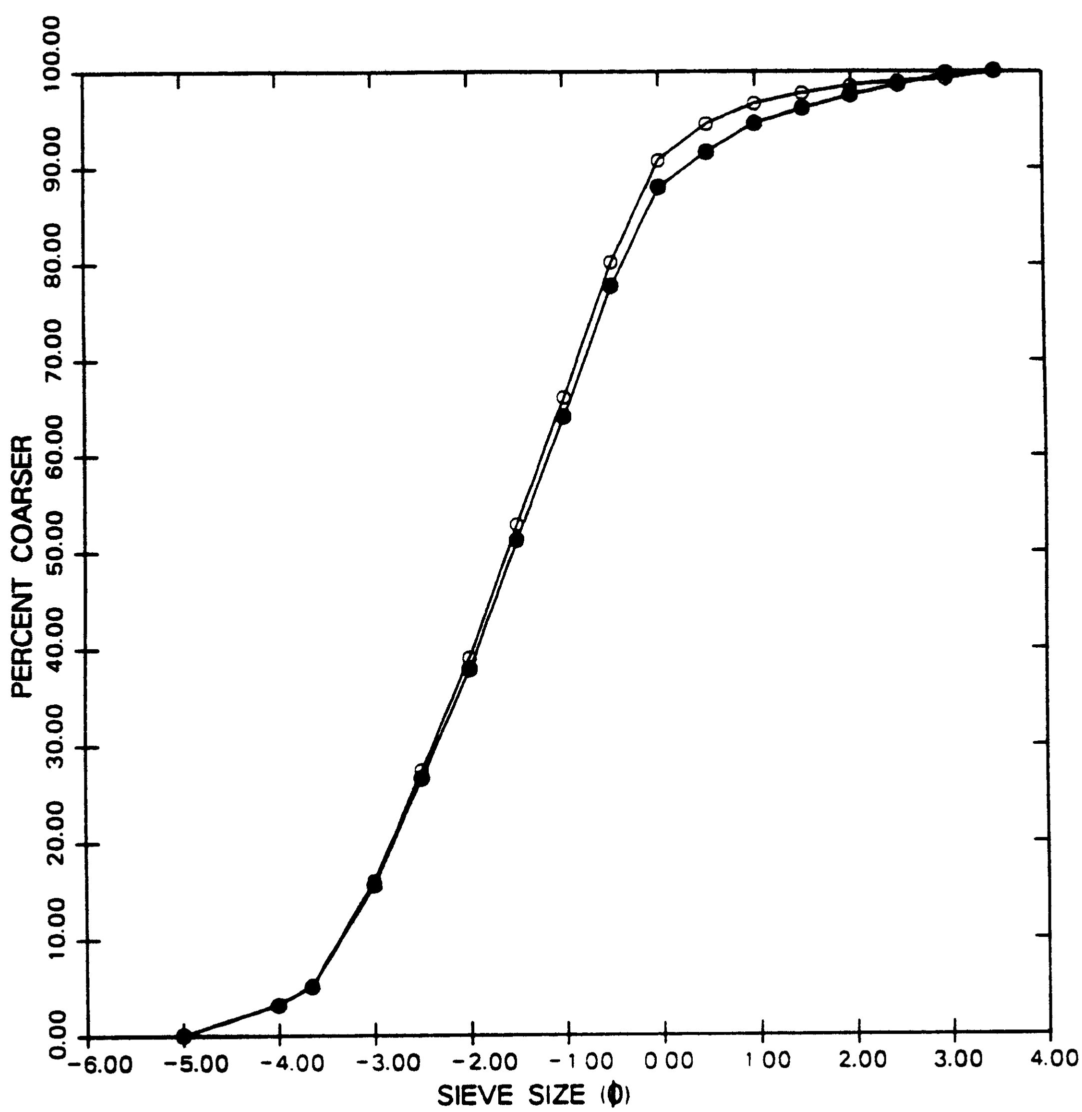

FIG. 6.-- Grain size distribution

o -- lights
● -- heavies and lights

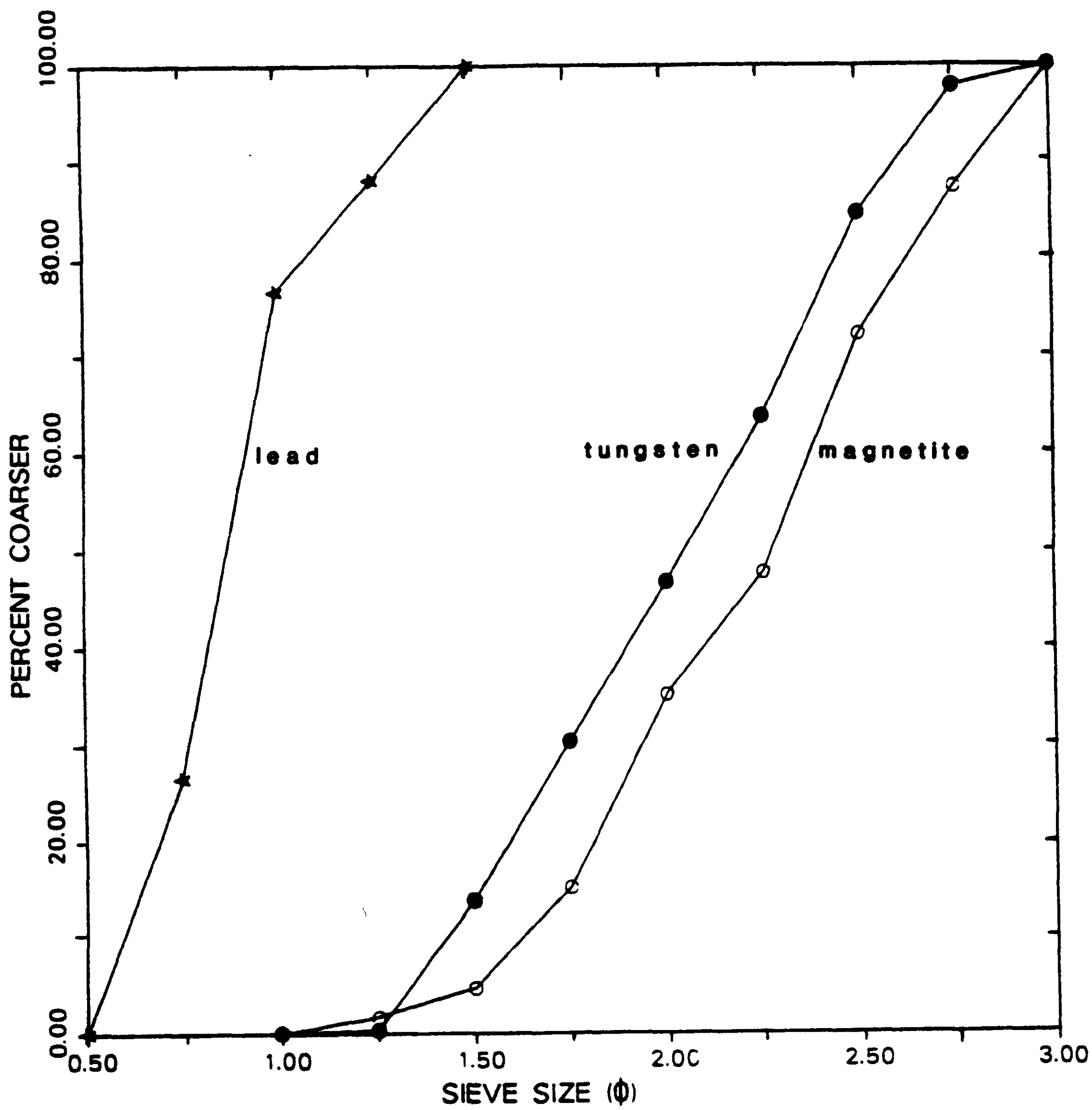

FIG. 7.-- Grain size distributions of the three heavies

acceptable level. The effect of these high concentrations on transport processes was tested in two runs, Runs H3 and H4, with the same flow and transport rates but with different percentages of heavies in the sediment mix: Run H3 had the normal value of 1.2% lead and 0.9% tungsten, while Run H4 had only one-tenth these values. The transport processes for the light fraction were indistinguishable between the two runs, and even the transport processes for the lead and tungsten themselves were very similar. This test will be discussed in more detail later in this report.

Procedure

General

Two types of runs were made in this study: six (Runs L3 through H5) were made with steady conditions of flow and sediment feed; the other two, Runs H6 and H7, were made with steay feed and no feed, respectively, and a constant rate of degradation of the bed. The procedures and methods of data collection were somewhat different between the two types of runs and are given separately below.

Runs with Steady Conditions

The first step in preparing the flume for a run was to homogenize the sediment by mixing it in a large box by hand until the concentrations of the three heavy-mineral fractions of three samples were within ±0.2% of their average values. Next a 7.5 cm sediment bed was made in the channel by adding approximately the right amount of sediment and leveling it with a channel-wide scraper suspended from the flume rails. The flume was then filled with water and the pump started. Water discharge was adjusted to the proper value using the gate valve and manometer.

For sediment feed a container of appropriate size was built according the rate needed for that run. In all runs made in the 0.15 m wide channel, except Runs H5, H6, and H7, each 2-minute sediment dose was weighed on a spring balance before being fed. Feeding was spread out as evenly as possible over 90 to 105 seconds, leaving the balance of the two-minute period for refilling and weighing the feed container. The much higher feed rates of Runs H5 and H6 necessitated prefilling the feed containers and adding sediment over 30-second intervals. In Run H7 no sediment was fed at all.

Each run was subdivided into a series of time intervals during which separate sets of measurements were taken; hereafter each of these intervals is termed a set. Each set spanned the period of time in which the flume ran continuously. Continuous running time was limited (20 minutes to 10 hours, depending on feed rate) by filling of the sump with sediment. Water temperature and water-surface slope were measured during each set. The sediment transported out of the channel was sampled for at least one 10 to 20 minute period during each set. This sample was dried, sieved, and checked for the presence of heavy minerals. In between sets, with the pumps off, the elevation of the bed surface and the volume of sediment in the sump were measured. Bed-surface and water-surface elevations were measured every 0.5 m beginning 1 m downstream from the upstream end of the channel to the 5.5 m mark. The bed-surface elevation at each location was determined by measuring the elevation every 1.5 cm across the channel and then computing the mean of the nine values. Water-surface elevations were measured in the middle of the channel at each location. Slopes were then determined from these positions and elevations by fitting a least-squares straight line. The sediment in the sump was measured volumetrically and then converted to a mass and compared with the mass of sediment fed during that set.

Equilibrium in the channel was defined as having been reached when the sediment fed into the channel nearly equaled the sediment transported out for two successive sets. Generally only the light fraction and magnetite were in equilibrium when the runs were terminated, because lead and tungsten took up to five times as long to come to equilibrium as the lower-density grains. Also, the sporadic movement of the lead and tungsten would have necessitated very long samples in order to determine whether they were in equilibrium or not. Thus closely spaced transport samples as well as bed sampling were undertaken after it had been established that lead and tungsten were being transported out of the channel.

Degrading-Bed Runs

The procedure for Runs H6 and H7 was similar to that of the other runs with a few exceptions, noted below. The initial sediment bed was 14.6 cm deep rather than 7.6 cm as in the other runs, to allow for 7 cm of degradation. In Run H6 sediment was fed in the same way as in Run H5, but no sediment was fed in Run H7. The rate of degradation in the channel was controlled by lowering the tailgate. The gate was lowered 0.19 cm/min throughout the 37 minutes of Run H6 and 0.76 cm/min during the 9.5 minutes of Run H7. A total of seven centimeters of the bed was eroded during each run. The sediment of the initial beds and the feed sediment of Run H6 was the same mix as used in the other runs (3% of heavies by weight).

Data Collection

Runs with Steady Conditions

Throughout each run the flow depth, water temperature, slope, transport mechanisms, the percentages of heavies being transported out of the channel, and the total transport rate were measured. After the flow had attained equilibrium the transport was sampled for a continuous period. All sediment was caught in consecutive 30-second samples for 30 minutes in Runs H2 and H5, and for 60 minutes in Run H3. These samples were then weighed, and selected ones were sieved and the heavies extracted in order to determine short-term variations in transport.

At several locations down the channel, two kinds of bed samples were taken at the end of each run: surface samples, to characterize the grain sizes and densities present in the bed surface at a particular location of the bed, and vertical samples 2.5 cm thick, to characterize the grain sizes and densities of the surface and subsurface layers. The surface samples were taken with a piston sampler 13 cm in diameter modeled after one used by Dhamotharan, Wood, Parker, and Stefan (1980), consisting of a 16 cm length of PVC pipe with a piston rigidly mounted 2.5 cm from one end (Fig. 8). A stiff mixture of bentonite and water was applied to the piston in a layer 2 cm thick before the sampler was used. The sampler was then driven firmly into the bed and carefully lifted out. This technique yielded samples of the bed surface essentially one grain thick. The clay was then separated from the sample by washing the mixture through a #120 mesh (0.125 mm) sieve. The sample was then dried and sieved, and the heavies were separated.

After surface sampling, the bed was sampled vertically at upstream, midstream, and downstream locations. Samples 15 cm x 15 cm x 2.5 cm thick were taken successively from the surface to the channel bottom. These samples were also oven-dried and sieved, and the heavies were extracted in order to test for variations in heavies with depth in the sediment.

Degrading-Bed Runs

Elevations of water surface and bed surface were taken at 1.5 m, 3.5 m, and 5.5 m downstream from the head of the channel every minute during the two runs. These measurements were taken to the nearest millimeter through the flume sidewalls, using rulers rigidly affixed to the outside of the walls. Run H6 was made in two sets 17 minutes and 20 minutes long, and Run

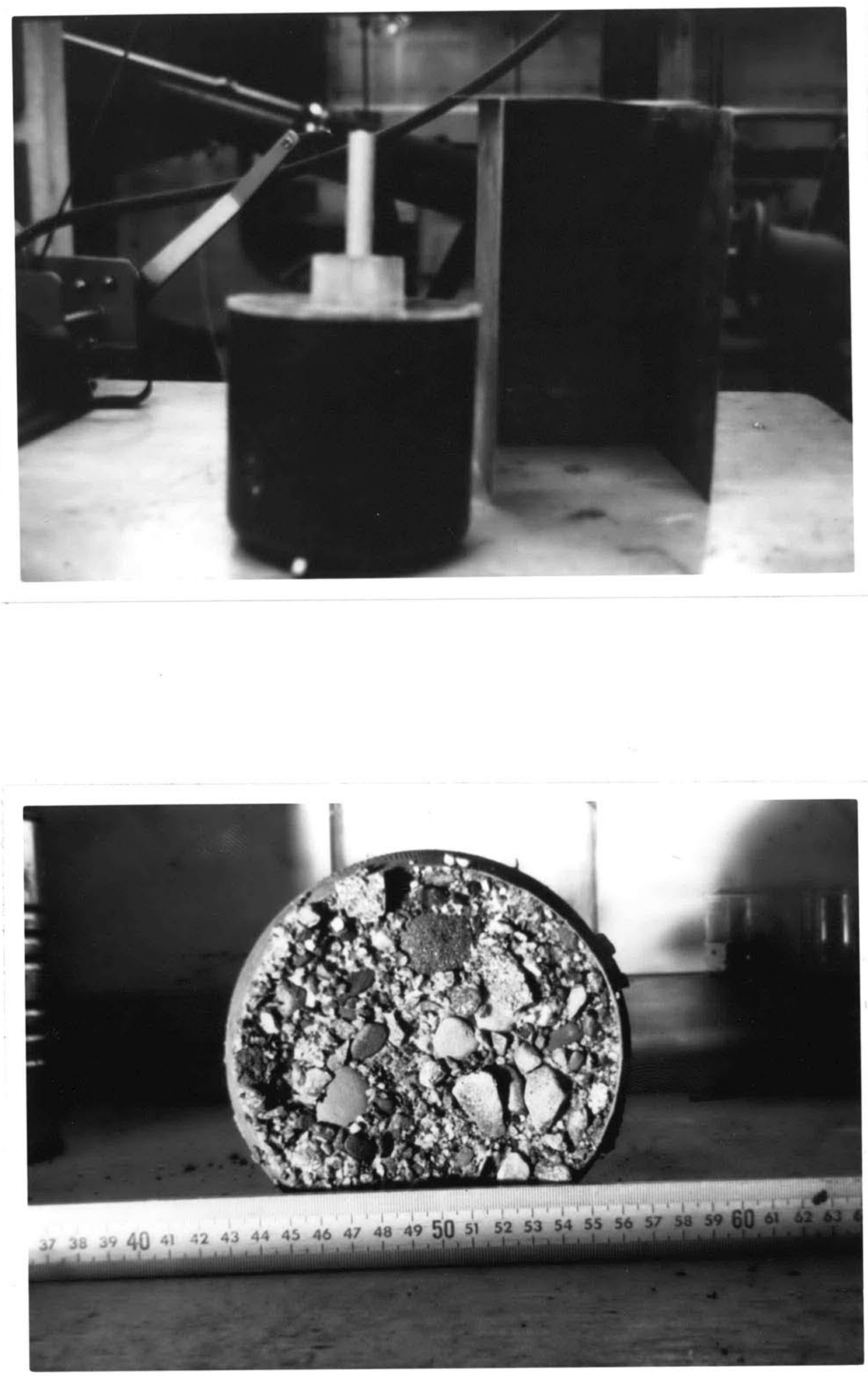

FIG. 8.-- Photographs of piston sampler

H7 was made in one set 9.5 minutes long. After each set, bed-surface elevations were measured with a point gauge as in the other runs. Sediment transported out of the channel was sampled once near the end of the first set and for 30 seconds out of every 2 minutes in the second set of Run H6, and 15 seconds out of every minute in Run H7. All of these samples were sieved and the heavies extracted. Bed samples of the surface and subsurface were taken after each run.

Extraction of Heavies

To fulfill the requirements of this study a rapid and accurate technique for extracting the three heavy-minerals was needed. The magnetite was separated using a strong magnet, but the best technique for the lead and tungsten was not as obvious. After exploring several possibilities unsucessfully, panning was considered as a possible technique for extraction. Useful discussion of the positive and negative aspects of panning are given by Smithson (1930), Ewing (1931), Mertie (1954), Theobald (1957), and Overstreet et al. (1968). Theobald (1957) has tabulated values for the average recovery of ten different heavies (densities from 3.0 to 5.4 g/cm^3) from panning. Average recoveries of from 18 to 100% were found for 45-100 mesh (0.35 to 0.149 mm) fractions of river gravels. Generally the recovery increased with increasing density, with the highest recoveries for rutile, zircon, and monazite. The much higher densities of lead and tungsten used here suggested that accurate separations by panning were indeed possible in this study. Thus panning was chosen as the method of extracting the lead and tungsten from the samples of this study.

In order to minimize errors and streamline the process as much as possible the following procedure for extraction of high-density grains was developed. First, all of the sizes greater than 1 mm were removed from the sample by sieving. The <1 mm fraction was weighed and split if necessary to between 50 and 100 grams. This part of the sample was then sieved at 0.5 ϕ intervals from 0.5 to 3.0 ϕ (0.707 to 0.125 mm). For each part of the sample retained on one of the five sieves the following procedure was followed. First the entire fraction of lights and heavies was weighed. Next the magnetite was separated by spreading out the fraction one grain thick on a large piece of paper. A strong magnet covered with a piece of paper was then used to extract the magnetite, which was weighed to the nearest 0.01 gram. The light grains were then removed by panning in a standard 6 in (15 cm) diameter aluminum pie tin. Panning was effective at removing nearly all of the lights. The sample was then dried and the last bit of lights were removed with a carefully controlled jet of air. In the one size fraction in which both lead and tungsten were present the spherical shape of the lead was used in the separation. A small quantity of the sample was spread out on a piece of sheet aluminum 15 cm square. By tilting the sheet slightly and tapping it gently the lead would roll off the sheet to give a nearly perfect separation between the lead and tungsten.

In order to refine the procedures and determine the magnitude of errors inherent in this technique, 1-kg samples containing exactly 1% each of magnetite, lead, and tungsten were made up and the heavies were extracted as above. The samples were each 1 kg in total weight and had 1% each of magnetite, lead, and tungsten. After several practice samples were done, ten samples were sieved and the heavies extracted and compared with the known quantity in each sample. Errors were within 5.3% for the magnetite, 3.4% for the lead, and 4.3% for the tungsten determinations. During actual sample determinations, all of the lights that were washed out of the pans were retained in a plastic basin. This material was sampled on several occasions to check that the quantities of heavies escaping detection were within the error limits noted above.

RESULTS

Introduction

Six of the eight runs listed in Table 4 (Runs L3 through H5) were made under steady conditions of water discharge and sediment feed; the results of these six runs are presented in groups in the following section. In each of the subsections, a general statement about the nature and purpose of the runs is followed by the main results on (i) visual observations of transport and deposition, (ii) transport samples taken at the channel exit, and (iii) bed samples. The other two runs were made under condtions of steady sediment feed (Run H6) or zero sediment feed (Run H7) but at a constant rate of overall degradation of the bed; these two runs are discussed separately in a later section.

For the sake of uniformity in comparing results from channels of two different widths, in the following sections the water discharge, sediment feed rate, and channel-exit transport rate are expressed per unit width of channel; hence the expressions unit discharge, unit feed rate, and unit transport rate used below.

Runs H1 and H2

General

Run H1 was the only run made in the larger flume in which heavies were in the sediment mix. (Other runs in the large flume are summarized in Part I.) Although the heavies did not reach equilibrium transport rates over the whole channel length

Table 4. EXPERIMENTAL CONDITIONS

Run#	Channel Width (m)	Flow Depth (m)	Fluid Discharge ($m^3/s \cdot m$)	Sediment Feed Rate ($kg/s \cdot m$)	Water Temp. (°C)	Bed Slope
L3	0.15	0.046	0.035	0.034	23.4-25.8	0.024
H1	0.53	0.046	0.035	0.034	10.2-12.6	0.019
H2	0.15	0.045	0.035	0.034	18.5-23.5	0.024
H3	0.15	0.074	0.067	0.098	21.6-25.2	0.015
H4	0.15	0.073	0.067	0.098	25.4-25.6	0.015
H5	0.15	0.069	0.089	1.073	25.4-25.5	0.021
H6	0.15	0.072	0.089	0.805	25.5	0.019
H7	0.15	0.074	0.089	0.000	17.5	0.019

in this run, much useful information was gained. The decision to feed sediment in these experiments was shown to be the correct choice for the following reasons. If the experimental system had been designed to recirculate sediment, all of the lead and tungsten would have been removed from the active layer of the sediment bed within a few hours and not transported at all thereafter, as shown by Brady and Jobson (1973, Fig. 23, p. 27). (The active layer is defined here to extend downward from the bed surface to the greatest depth of local erosion. It contains the sediment that is subjected to transport by the flow at one time or another during a long equilibrium run. The thickness of the active layer depends on the vertical scale of local erosion and deposition associated either with the passage of bed forms or with fluctuating overall aggradation and degradation of the bed about some long-term average bed elevation.) Another important lesson learned was that the 3,500 kg of sediment on hand was not nearly enough to complete a run with heavies in the large flume. In more than 43 hours of running time the lead and tungsten traveled only 2.5 m down the channel, so no lead or tungsten was transported out of the channel for the entire 43 hours.

With the knowledge gained from Run H1, Run H2 was made in the smaller flume with the same conditions of unit discharge and unit feed rate as in Run H1 in order to explore the mechanisms of transport of the heavies more fully. Run H2 lasted for 144.75 hours. The lights were transported in equilibrium from about 30 hours on. The magnetite began to be transported out of the channel at input rates at about 60 hours, the lead was first transported out of the channel at 139 hours, and the tungsten followed shortly thereafter, but not at equilibrium rates.

Since transport of the heavies is closely related to transport of the lights, a brief review of light-mineral transport will be given before presenting the data on heavy-mineral transport.

The bed in Runs H1 and H2 became armored due to the wide range of grain sizes in the sediment mix (see Fig. 13, part I). Also, transport-rate fluctuations were identified at periods of about 10 and 25 minutes. The shorter fluctuations were caused by long (0.5 to 3 m) and low (2-4 mm) bed-load sheets that migrated through the channel. These fluctuations in transport rate were mostly composed of the median-sized sediment of the mix, with coarser sizes peaking in transport rate before and finer sizes peaking in transport rate after the total transport rate had peaked. The longer-term fluctuations were identified from runs made in the larger flume and may be related to a process similar to the clast jams that were observed to cause variations on approximately the same time scale in the small flume (see Part I).

As mentioned above, lead and tungsten were transported only about 2.5 m in Run H1. In Run H2 they were transported the full 6 m length of the channel, but it took 140 hours. The reason that lead and tungsten moved so slowly is that concentrations composed of nearly 100% heavies needed to form at a location before the heavies would be transported downstream from that location. With time these 100% heavy-mineral concentrations merged to form a continuous layer. These heavy-mineral layers formed beneath a surficial layer of lights and are hereafter termed heavy sublayers. Observations from both Runs H1 and H2 demonstrated that except for small amounts of magnetite the heavies were transported only a short distance beyond the downstream end of the heavy sublayer.

In Run H2 a heavy sublayer began to form within the first few hours of the run. This layer first formed just downstream of where the sediment was fed and slowly extended down the channel. After full development, the heavy sublayer could easily be viewed just below the sediment surface through the transparent sidewall of the flume (Fig. 9). Heavy sublayers ranged from 2-5 millimeters in thickness. The upper contact was a sharp boundary, but the lower contact was diffuse. The sharpness of the upper contact was caused by the flow planing off the upper surface when the sublayer was exposed to the flow.

It was apparent that after full development this heavy sublayer existed everywhere beneath the active layer of low-density sediment. This fact was strikingly demonstrated by an erosion experiment, after the completion of Run H2, in which no sediment was fed while the water discharge was gradually increased. Nearly all of the low-density sediment on the bed surface was eroded away, leaving a continuous layer of heavies exposed on the bed with a few large low-density clasts (see Fig. 10).

FIG. 9.-- Photograph of heavy sublayer through flume sidewall, Run H2. Flow direction was left to right.

FIG. 10.-- Photograph of heavy sublayer after erosion experiment, Run H2

Heavy sublayers formed and prograded in the following way. At the beginning of a run no lead or tungsten and only a small quantity of magnetite were in transport. The heavy sublayer began to form at the upstream end of the channel just downstream of where the sediment was fed. Initially thin and nearly pure segregations of the heavies formed at the upstream end of the channel. Additional heavy-mineral grains were transported over these concentrated heavy-mineral areas and deposited downstream where no concentrated heavy accumulations had yet developed. After the formation of a concentrated heavy accumulation the transport of heavies past that point increased by growth of the heavy deposit in area and thickness until the transport rate downstream of that point was equal to the rate of supply from upstream. This observation was supported by samples of transport out of the channel taken during each set of the run: no lead or tungsten was detected in these samples until the heavy sublayer was observed to have prograded to the very end of the channel. By observing the position of the downstream edge of the heavy sublayer it was straightforward to determine the point farthest downstream to which the lead and tungsten had been transported.

The formation and progradation of a heavy sublayers can be represented as a three-part process (see Fig. 11). (1) Initially at a given location no heavies (except small quantities of magnetite) are in transport and the concentrations of the heavies in the bed are at original values. (2) The formation of highly concentrated deposits of heavies in an area begins when the downstream edge of the

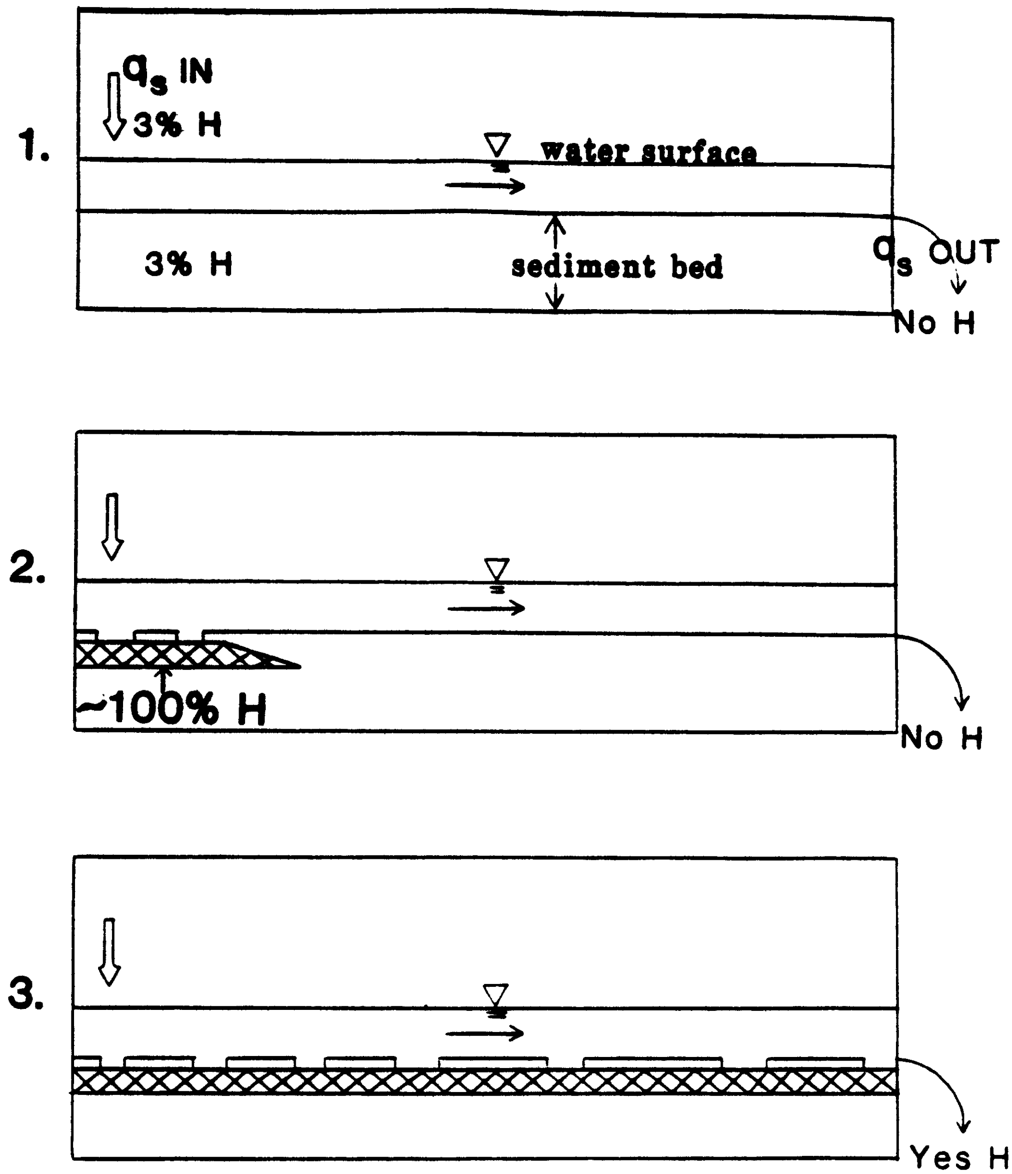

FIG. 11.-- Three phases in the formation of a heavy sublayer.

1. Initial conditions at the start of a run. The bed and feed sediment each contain 3% heavies by weight. No heavies, except small amounts of magnetite, are transported out of the channel.

2. The heavy sublayer begins to form at the upstream end of the channel. Transport of heavies occurs at their in-feed rates over the sublayer to the place downstream where the sublayer begins to thin and get patchy. At this location transport rates of the heavies begins to decrease downstream, reaching zero where there is no concentrated heavy layer present.

3. Eventually the heavy sublayer progrades over the entire channel length. Transport of heavies out of the channel occurs when the sublayer is exposed to the flow at the downstream end of the channel.

heavy sublayer approaches the area. In front of the heavy sublayer first accumulations of heavies form, which allow transport of heavies downstream from them at rates less than are being supplied from upstream. (3) The heavy-mineral accumulations thicken and merge to form a continuous layer such that transport downstream from that area equals the amount supplied from upstream.

The two higher-density heavies were transported only where parts of the heavy sublayers were exposed to the flow. Usually most of the layer was covered with low-density grains, with only small parts exposed. The shape of these exposed parts of the heavy sublayer was irregular and thus appeared from above the bed as patches of heavies on a bed of coarser low-density grains. These patches were just the surface exposures of the nearly continuous heavy sublayers. Patches ranged in size from 1 to 120 cm^2. The patches invariably occupied low areas on the bed (see Figs. 12, 13).

Small heavy-mineral patches representing exposed portions of the heavy sublayer were often observed to form in depressions in the lee of the large clasts; larger patches were commonly observed downstream of clast jams. The fact that heavy patches were confined to low bed elevations is part of the reason the heavies moved at such slow rates. The low elevation of the patches made them a prime location for low-density clasts to become deposited. This stopped transport of heavies from that location until the heavies were uncovered again. One factor that tended to prevent the patches from

FIG. 12.-- Photographs of heavy sublayer patches, plan view, Run H2 (continued next page).

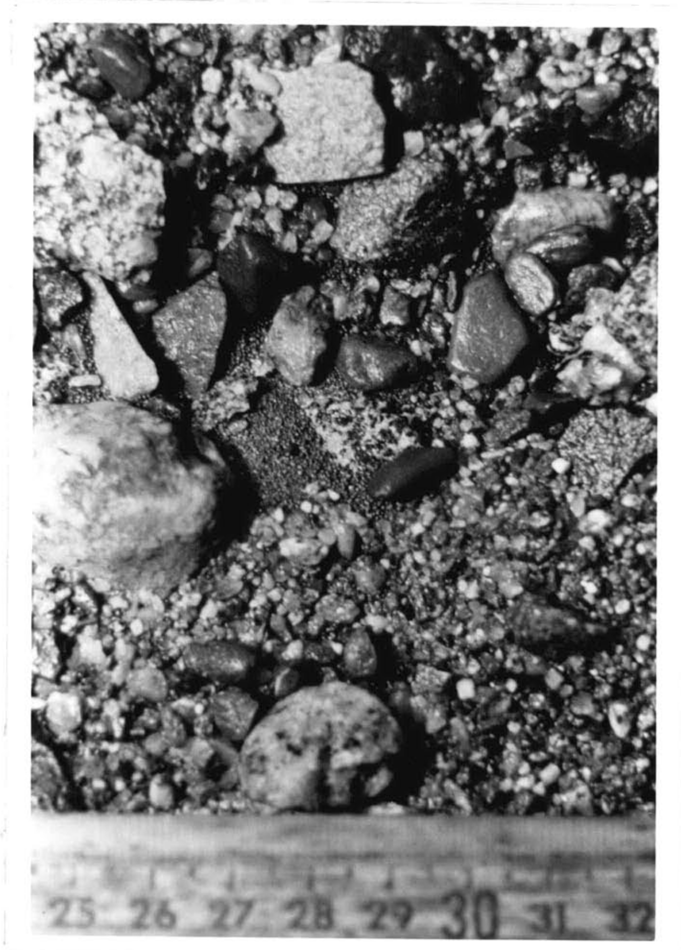

FIG. 12. (continued)

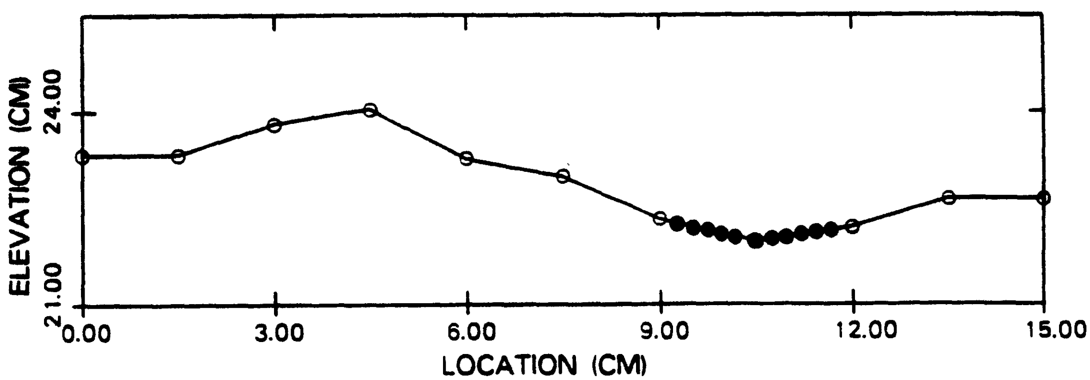

FIG. 13. -- Cross-sectional profile of bed perpendicular to flow direction, Run H2. Exposed patch of heavy sublayer is designated by the solid circles.

being covered by the lights was that their surface was much smoother than the surrounding coarsely armored bed of low-density grains, and many grains were transported over the patch without being deposited.

The two primary constituents of the heavy layers were lead and tungsten; magnetite was also present but in much smaller concentrations. As the heavy sublayer prograded downstream the first heavy accumulations to form downstream of the edge of the layer were observed to be composed only of lead and later to also contain tungsten. This was borne out by the transport samples taken at the end of the channel. These two heavies, however, were transported in very similar ways otherwise. Unlike lead and tungsten, some magnetite was detected in virtually all of the transport samples taken in Runs H1 and H2, although the rate of magnetite transport out of the channel in the early parts of the runs was much lower than the magnetite feed rates.

For a large percentage of the time at any one location the heavy sublayer was not exposed to the flow, so there was no heavy-mineral transport in that region of the bed. During some periods of the run, generally when the bed was aggrading, there were few or no exposures of the heavy sublayer. Overall aggradation of the bed isolated the heavy sublayer from the flow, and unless subsequent degradation reexposed the heavy sublayer a new heavy sublayer had to be formed in order for the heavies to be transported again from that area. This process was observed in the first part of Run H2, when the flume slope was substantially lower than the equilibrium value which caused the channel bed to aggrade in the early parts of the run. The successive layers of heavies shown in Figure 14 were formed as a result. After the channel slope in Run H2 had built up to the equilibrium value, aggradational and degradational periods of the channel were generally the result of the formation and destruction of clast jams. The periods of degradation after a large clast jam had broken were often the prime times when the heavies moved. At such times the heavies moved quite rapidly until the bed began to aggrade once again. The rates of movement of the heavy layer ranged from 2 to 12 cm/hr (mean = 4.3 cm/hr) when movement of the heavy front was averaged over individual 4-hour sets. Shorter-term rates of movement were very much faster during channel downcutting and near zero during general aggradational events.

Transport Samples

Three 30-minute-long sets of transport samples, each separated by one hour of running time, were taken near the end of Run H2. These three periods greatly increased the chances of sampling during both low-transport and high-transport intervals. The first sample set had a low mean transport rate and the second had a high mean transport rate, so sieving and extraction of heavies from samples was confined to the first two sample periods.

The samples were sieved, and the <1 mm fractions from each successive group of four samples were combined and the heavies extracted. The percentages of tungsten, lead, and magnetite

FIG. 14.-- Photograph of successive heavy sublayers in the upstream 1 m of the bed, Run H2. Flow direction was left to right.

were determined for each 2-minute sample. Figures 15 and 16 show the rates of transport of lead and magnetite and the total transport rate. Transport rates of tungsten (not plotted) were very low, but the small number of transport samples that contained tungsten and observations made during the runs suggest strongly that tungsten was transported very much like lead.

It is apparent from Figures 15 and 16 that the heavies tended to be transported at the highest rate when the total transport rate was low or decreasing. This pattern is similar to what was observed for the <1 mm low-density sediment in part I (see Figs. 15-17, Part I). Apparently the size of the lights and heavies was an important factor in the transport of <1 mm grains.

Bed Samples

The concentrations of magnetite, lead, and tungsten for bed-surface samples from Runs H1 and H2 are shown in Table 5. The sample taken at 1.5 m in Run H1 is the only one for which lead and tungsten were in active transport in that region of the bed. The samples from Run H2 illustrate some of the variation in the bed-surface grain sizes and densities at a given time. As noted in Table 5 the three samples were purposely taken at areas of the bed with zero, small, and large percentages of the bed surface covered with heavies. It is interesting to note that the sample taken over the larger area of exposed heavies is greatly enriched in lead, somewhat less

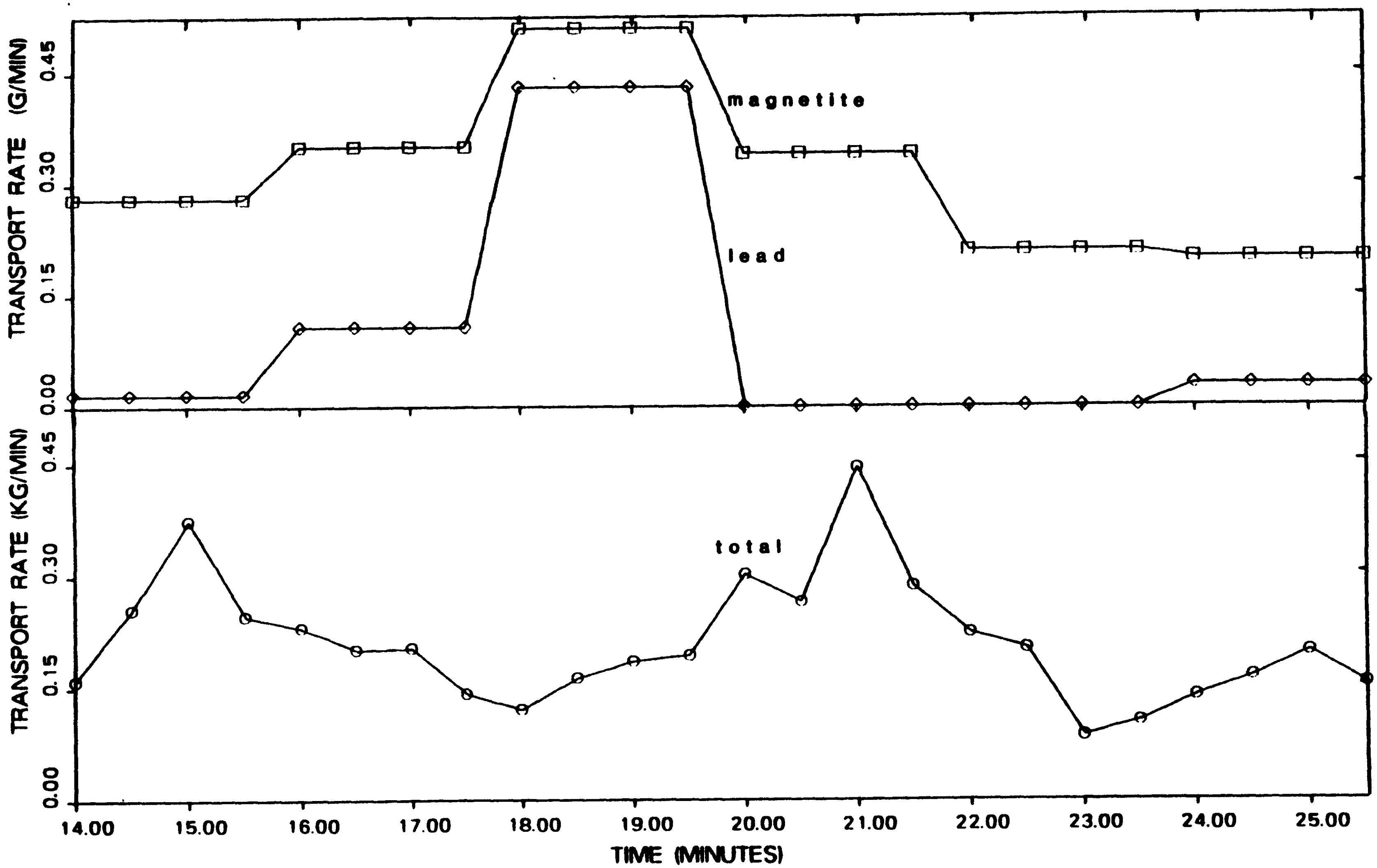

FIG. 15.-- Magnetite, lead, and total transport rates vs. time, Run H2, part 1

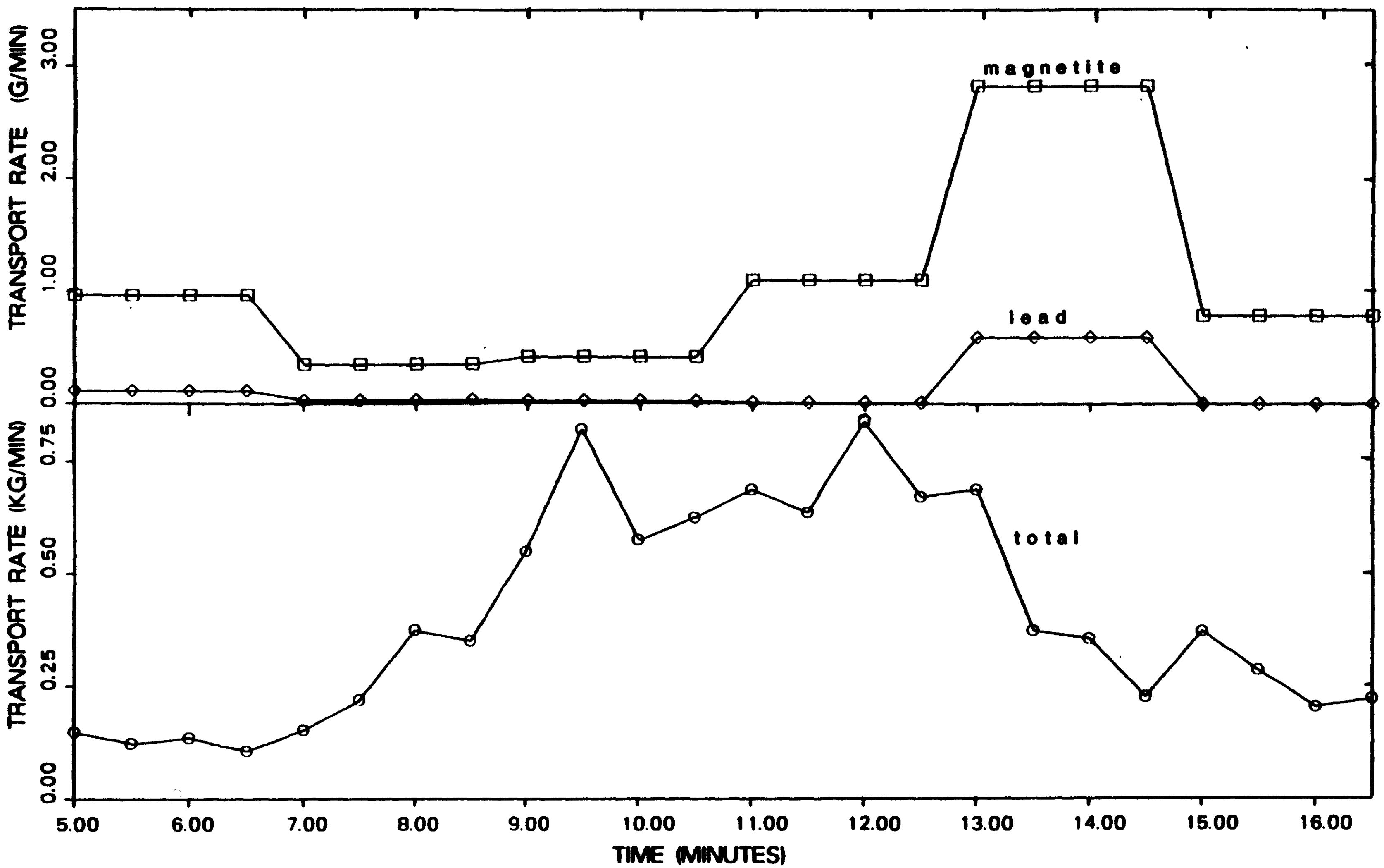

FIG. 16.-- Magnetite, lead, and total transport rates vs. time, Run H2, part 2

Table 5. PERCENTAGE OF HEAVIES IN BED-SURFACE SAMPLES, RUNS H1 AND H2

Location (m)			2nd layer down	Approx. percent of surface covered by heavies
Run H1				
	m	0.1	0.7	
1.5	l	0.4	1.1	0
	t	0.2	0.5	
	m	tr		
4.5	l	0.0		0
	t	0.0		
	m	tr	tr	
8.5	l	0.0	0.0	0
	t	0.0	0.0	
Run H2				
	m	1.9		
0.85	l	11.3		10
	t	7.9		
	m	0.2		
3.10	l	2.0		0
	t	2.1		
	m	1.0		
4.35	l	24.2		75
	t	8.1		

Note: The location is in meters from the upstream end of the channel. m - magnetite, l - lead, t - tungsten
tr - trace detected < 0.05%

enriched in tungsten, and even less enriched in magnetite. Possibly the lead is overenriched at the surface because it is coarser and better sorted than magnetite and tungsten, allowing grains of these other two heavies to be hidden in the spaces among the lead grains. Another observation from Table 5 is that magnetite is concentrated much less over its original value at the bed surface, or even not at all.

Table 6 shows the percentages of the three heavies from the vertical bed samples taken from Runs H1 and H2. These samples show the percentages of heavies concentrated in the heavy sublayer described above. Apparently concentrations of 15-30% in the upper 2.5 cm of the sediment bed are needed in order for the lead and tungsten to be transported under these conditions. Magnetite apparently needs to be concentrated far less than lead or tungsten. It is also obvious that lead and tungsten were transported less than 3 m in Run H1. The concentration of magnetite in the bed of Run H1 was probably at its equilibrium value in the upstream 5 meters of the channel. Lead and tungsten were present in the samples taken at locations 7, 8, and 9 of Run H1 not because they were transported to that distance but because these samples were thicker than the active layer and the heavies were extracted from the original unworked substrate.

The samples taken below the surface samples are interesting and informative. The concentrations of heavies in the samples taken below the surface slice in Run H1 at 1, 2, and 3 m and at all three locations in Run H2 show significant

Table 6. PERCENTAGES OF HEAVIES IN VERTICAL BED SAMPLES, RUNS H1 AND H2

Run H1

Location (m)		Sample # 0	1	2	3
	m	1.8	1.2	4.2	1.8
1.0	l	25.0	21.2	4.7	2.2
	t	24.1	15.0	3.0	1.8
	m	5.0	3.4	2.1	0.9
2.0	l	18.7	3.5	1.8	1.3
	t	7.5	1.3	0.8	0.9
	m	5.4	2.5	1.9	0.8
3.0	l	0.0	0.0	0.0	1.0
	t	0.0	0.0	0.0	0.8
	m	3.6	1.2	0.8	1.0
4.0	l	0.0	0.0	0.8	1.0
	t	0.0	0.0	0.7	0.9
	m	2.9			
5.0	l	0.0			
	t	0.0			
	m	1.5			
6.0	l	0.0			
	t	0.0			
	m	1.0			
7.0	l	0.0			
	t	tr			
	m	1.1			
8.0	l	0.1			
	t	0.1			
	m	1.0			
9.0	l	0.4			
	t	0.3			

(continued next page)

Table 6. (continued)

Run H2

Location (m)		Sample # 0	1	2	3
	m	1.3	3.4	2.1	0.8
1.5	l	15.6	13.8	3.0	1.3
	t	21.1	12.2	2.5	1.0
	m	1.7	1.0	1.2	
3.5	l	21.2	6.4	4.3	
	t	18.0	4.3	3.3	
	m	3.4	1.8	2.0	
5.5	l	27.4	5.3	5.3	
	t	2.9	1.2	1.9	

Note: The location is the distance in meters from the upstream end of the channel. Sample numbers refer to the 2.5 cm thick samples with 0 being the surface one. For the heavies: m - magnetite, l - lead, t - tungsten.
tr - trace detected < 0.05%

enrichment of all three heavies over their background concentrations (Table 6). This enrichment can be reasonably be explained for the three locations of Run H1 as follows. The data on bed elevation with time for Run H1 reveal that 9.1 cm, 7.8 cm, and 7.9 cm of net aggradation occurred over the course of the run at the 1, 2, and 3 meter locations, respectively. With reference to Table 6 these aggradation values show that the bed surface at all three locations existed at elevations within the three vertical sample intervals for a period of time. Thus there was at least the potential for the formation or beginning of formation of a heavy sublayer as described above. Furthermore the aggradation rate in Run H1 is shown in Table 7 to have decreased with time as the channel approached a steady state. The decreasing rate of deposition shown in Table 7 corresponds well with the greater concentrations of heavies upwards towards the bed surface (Table 6). Also the lowest sample levels at the 2 and 3 meter locations of Run H1 have concentrations equal to the background values. This can be explained by the fact that the bed surface was not located at the elevation of these samples except for a very short time.

For Run H2 the same line of reasoning can explain the enrichment of only some of the subsurface layers shown in Table 6. The thickness of net deposition for Run H2 is 4.14 cm, 2.71 cm, and 1.67 cm for locations 1.5 m, 3.5 m, and 5.5 m, respectively. For the layer directly below the surface sample at locations 1.5 m and 3.5 m the same processes inferred for

Table 7. AVERAGE AGGRADATION RATES FOR EACH SET, RUN H1

	Location (m) 1	2	3	
Set#				
1	0.5	0.4	0.4	cm/hr
2	0.5	0.4	0.3	
3	0.2	0.3	0.2	
4	0.3	0.2	0.2	
5	0.2	0.2	0.1	
6	0.1	0.1	0.1	
7	0.2	0.1	-0.2	
8	-0.1	0.2	0.0	
9	0.1	0.0	0.1	
10	-0.1	0.0	0.0	

Note: Values were averaged over each set, most of which lasted for 4.6 hours.

Run H1 can reasonably be assumed. However, the enrichment of the #2 and #3 samples (Table 6) at the two upstream locations and both lower samples at 5.5 m cannot be explained in this way. The only reasonable explanation appears to be that the heavies worked their way down through the interstices of the bed grains and thus become concentrated in the lower levels of the bed. According to Table 6, lead seems to be concentrated to a greater degree by this process than either tungsten or magnetite.

Run H3

General

In Run H3, which lasted for 32.3 hours, the feed rate was about three times greater than in Run H2, and the water discharge was nearly double. Equilibrium transport of the light minerals was attained at ten hours, and of magnetite, at 19 hours; lead and tungsten were first detected in transport samples out of the channel at 30 hours, although not at equilibrium rates.

The bed of Run H3 was armored with coarse grains (see Fig. 13, Part I), but the grain-size distribution of the bed surface was somewhat finer than in Run H2. The processes of transport of the lights in Run H3 were very similar to those in Runs H1 and H2. Transport was shown to vary at periods of six minutes, but no evidence for the longer-term fluctuations seen in Runs H1 and H2 was found. Long and low bed-load sheets analogous to those observed in Runs H1 and H2 were observed to cause the short-term variability in transport rate. The same pattern of variability of the different size fractions with time was observed in Run H3 as in Runs H1 and H2 relative to the peak in total transport rate: the peak in transport rate of the 4-16 mm fraction was earlier than that of the 1-4 mm fraction, which was at the same time as the peak in total transport rate, and that of the <1 mm fraction was later (see Fig. 17, Part I). The main difference between Runs H1 and H2 on the one hand and Run H3 on the other was that Run H3 showed no long-term fluctuations and the range of transport rates was much lower than in Runs H1 and H2 (see Table 3, Part I). The clast jams that were important for long-term fluctuations in Run H2 were much shorter-lived in Run H3 and did not have nearly as great an effect on the system as in Run H2.

Accumulations rich in heavies began to form within the first hour of Run H3. These deposits merged into a heavy sublayer, and as in Run H2 the surface exposure of the heavy sublayer was patchy. However, the patches tended to be larger and the frequency of their exposure was greater in Run H3 than in Run H2. The greater frequency of exposure was probably caused by lack of the long-term aggradation and degradation events observed in Run H2. The areas of the heavy patches had a wide range, but definitely tended to be larger than in Run H2. In fact, patches were observed to coalesce infrequently and form long (~1 m by 5 cm), sinuous, more or less continuous areas on the bed (see Fig. 17).

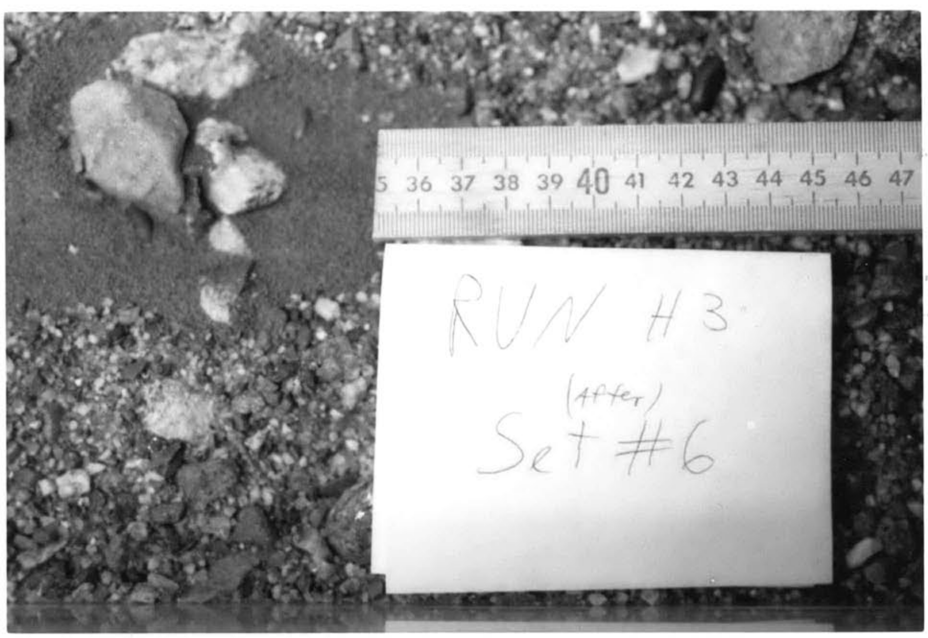

FIG. 17.-- Photographs of heavy sublayer patches, plan view, Run H3. Flow direction was left to right.

As in the earlier runs, lead and tungsten were transported through the system only after a heavy sublayer had been formed. Transport samples taken in each set confirmed that magnetite, before reaching its equilibrium transport rate, was transported out of the channel at a lower rate, but lead and tungsten were not transported out of the channel at all until the heavy sublayer of lead and tungsten reached the downstream end of the channel. Processes of covering and uncovering of heavy patches caused set-averaged migration rates of the heavy sublayer to range from 6.0 to 38.3 cm/hr, with a mean value of 20 cm/hr. The lack of long-term aggradation and degradation episodes caused the transport of the heavies to be steadier in Run H3 than in Run H2 but still in an absolute sense quite slow.

Transport Samples

For the last hour of Run H3 the transport was sampled in 30-second samples. The lack of substantial long-term variability in total transport rate meant that one period of sampling should have been sufficient to characterize the transport patterns. A number of samples from the hour-long sample string were sieved and the <1 mm sizes were combined into 2-minute samples. Figure 18 compares the total transport rate to that of magnetite and lead. (Tungsten transport rates were very small and not plotted; observations suggest that the mode of transport of tungsten was very similar to that of lead.)

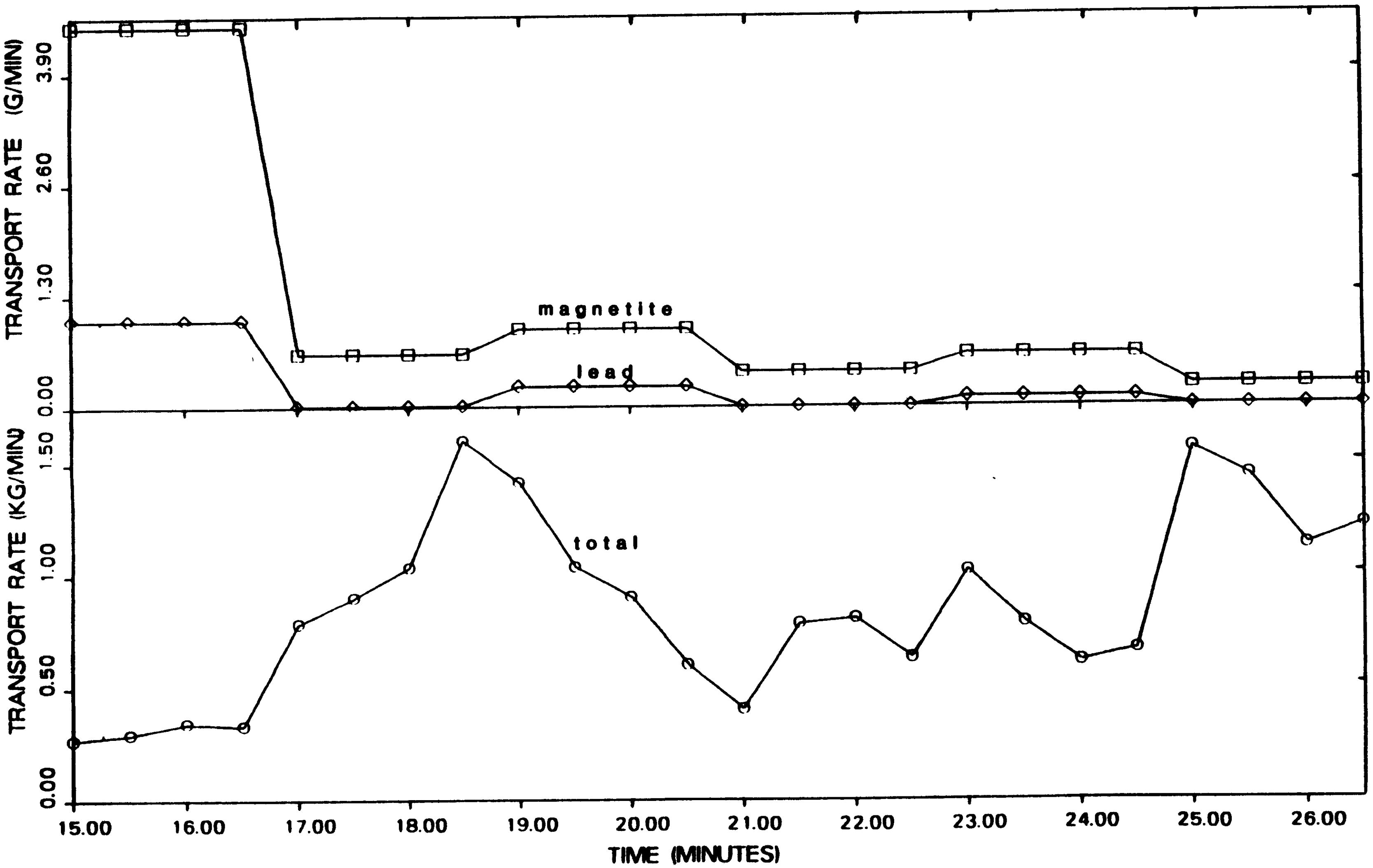

FIG. 18.-- Magnetite, lead, and total transport rates vs. time, Run H3

Figure 18 shows that lead and magnetite tended to peak in transport rate at times when the total transport rate was low or decreasing. This is very similar to the pattern for the <1 mm fraction of light grains (see Fig. 17, Part I).

Bed Samples

The concentrations of the three different heavies in the surface samples of Run H3 are shown in Table 8. The three samples illustrate the wide ranges of concentrations that are present on the bed surface at a given time. In the two samples that included heavy patches, the lead and tungsten were concentrated to several times their background levels but the magnetite was not concentrated at all. In most respects the concentrations of the heavies in the samples from Run H3 are very similar to those from Run H2 (see Table 5).

The percentages of the heavies in the vertical bed samples from Run H3 are shown in Table 9. Concentrations in the top sample are shown to be highest for lead, then tungsten, and then magnetite. The next layer below the surface at all three locations is also significantly concentrated in heavies over their background level. This cannot be explained by transport by the flow, because the bed-elevation data show that the bed surface was never lower than 1.4 cm below its final elevation. Thus the heavies must have worked their way down through the sediment, as was concluded for Run H2.

Table 8. PERCENTAGE OF HEAVIES IN BED-SURFACE SAMPLES, RUN H3

Location (m)			Approx. percent of surface covered by heavies
	m	0.8	
2.40	l	2.8	8
	t	3.9	
	m	0.6	
3.15	l	13.9	80
	t	6.7	
	m	0.1	
4.60	l	0.2	0
	t	0.2	

Note: Location is the distance from the upstream end of the channel in meters. For the heavies: m - magnetite, l - lead, t - tungsten.

Table 9.- PERCENTAGE OF HEAVIES IN VERTICAL BED SAMPLES, RUN H3

Location (m)		Sample # 0	1
	m	2.6	2.1
1.5	l	19.3	4.8
	t	17.0	5.3
	m	3.1	1.5
3.5	l	24.8	3.9
	t	15.5	3.4
	m	4.4	2.4
5.5	l	10.2	5.6
	t	2.0	1.8

Note: Location is the distance from the upstream end of the channel in meters. Sample numbers correspond to the 2.5 cm thick sample layers. The layer including the surface is #0. For heavies: m - magnetite, l - lead, t - tungsten.

Run H5

General

To expand the range of experimental conditions, Run H5 was made with a transport rate ten times greater and a water discharge 1.3 times greater than in Run H3. Run H5 lasted only for 2.3 hours. Because the transport rate was very high and the bed did not become armored (see Fig. 13, Part I), light-mineral transport reached a steady state within minutes. Due to technical difficulties with the flume, the run did not last long enough for lead and tungsten to be transported out of the channel. Nonetheless a heavy sublayer like those in the runs with lower transport rates was formed.

In addition to the lack of armoring, the processes of transport in Run H5 were also quite different from the other runs. Bed forms with a spacing of 60 cm and a height of 1 cm were observed (Fig. 20, Part I). These forms were composed mainly of grains near the median size of the sediment mix, with concentrations of large clasts located in the troughs of the forms just downstream of the crests. Migration rates of 3 cm/s were measured, but usually individual bed forms did not persist beyond 50 cm of migration distance. The range of variation in transport rate was much lower in this run than in the others (see Table 3, Part I). Possible periodic variations were observed for the 1-2 mm sizes of the sediment, with the 16-32 mm fraction peaking in transport rate before, and the <1 mm fraction peaking in transport rate after that of the 1-2 mm fraction. The other size fractions of the lights showed no periodic fluctuations in transport rate.

A heavy sublayer began to form within a few minutes of the start of Run H5. At a given location the heavy sublayer was exposed at the bed surface only when the low point or trough of a bed form was passing.

Sampling of the sediment transported out of the channel showed that magnetite was transported through the channel as in other runs but lead and tungsten were not. The speed of downstream extension of the heavy sublayer was measured to be 350 cm/hr on average.

Transport Samples

Transport was sampled for 15 seconds out of every 30 for a 30-minute period in Run H5. Partway through the sampling period, problems with the pumping system of the flume caused a gradual decrease in water discharge, resulting in aggradation of the bed. The difference between the feed rate and the average transport rate was 17%. It is not known exactly what effect this aggradation had on the collected samples, but the results and observations during this period relate well with measurements and observations made during the other parts of the run, in which the flow and bed surface were not changing. Therefore the results obtained from these samples are regarded as qualitatively correct.

The transport rates of magnetite and of the 1-2 mm size fraction are plotted against time in Figure 19. The run did not last long enough for lead and tungsten to be transported out of the channel, so no data are available on their

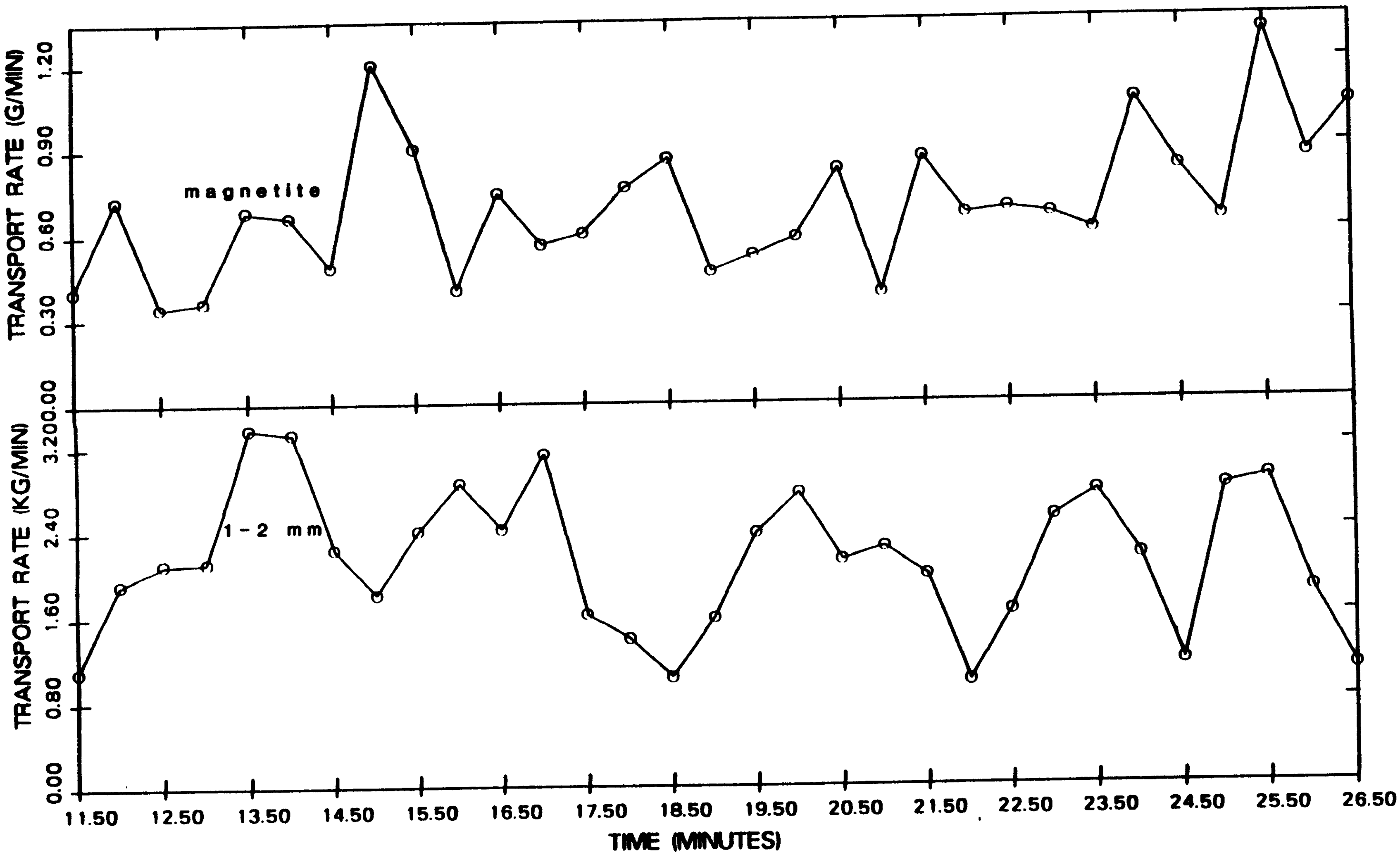

FIG. 19.-- Magnetite and 1-2 mm fraction transport rates vs. time, Run H5

short-term transport rates. The pattern shown in Figure 19 is for the transport rate of magnetite to peak after that of the 1-2 mm light fraction. This is most likely due to the magnetite being more exposed on the bed when the troughs of the bed forms passed a given location. This result corresponds exactly with what would be expected from observations of the transport of heavies during the run. It is highly probable that a similar result would have been obtained for lead and tungsten had they been in the transport samples. It is clear from the observations that the heavies moved only while exposed in the bed-form troughs. This indicates that the movement of the front of the heavy layer was controlled by bed-form migration. These observations lend more credence to the supposition that the data derived from the transport samples are qualitatively correct.

Bed Samples

Due to the above-mentioned problems with the flume during Run H5, no surface samples with heavies were obtained, but two samples 2.5 cm thick of the concentrated heavy-mineral layer were taken. The grain-size distribution of the surface lights is shown in Figure 13, Part I. The percentages of the heavies for these two samples are shown in Table 10. These samples show that a heavy sublayer similar to those formed in the other runs formed also in Run H5.

Table 10. PERCENTAGES OF HEAVIES IN BED SAMPLES, RUN H5

Location (m)		
	m	6.3
1.5	l	14.0
	t	10.6
	m	5.5
2.5	l	13.4
	t	11.7

Note: Location is the distance in meters from the upstream end of the channel. For the heavies: m - magnetite, l - lead, t - tungsten.

Run H4

The concentrations of the heavies, especially lead and tungsten, were many times higher in the sediment mix used in most of this study than natural background levels for materials of this density range. Values of the order of 1 ppm (0.0001%) have been cited as background levels for gold concentrations in rich placer deposits (see Minter, 1978; Fig. 8, p. 810). A special run (Run H4) was therefore made to study the effect of heavy-mineral concentration in the sediment mix on mode of heavy-mineral transport. The same unit discharge and unit feed rate were used as in Run H3 except that the concentrations of lead and tungsten (0.12% and 0.09%, respectively) were 0.1 times those used in Run H3. Run H4 was made in two sets each 10 hours long. With one-tenth the lead and tungsten, a heavy sublayer might be expected to take ten times as long to form if the same concentrations in the bed were necessary for transport as in Run H3. In Run H3 the heavy sublayer had advanced 1.8 m from the upstream end of the channel after 4 hours. If transport of the heavies was similar for the two runs we would expect the downstream edge of the heavy sublayer to have reached about 0.9 m after 20 hours. In Run H4 the downstream edge of the heavy sublayer had reached 0.8 m at the end of the 20 hours. Samples of transport out of the channel taken throughout the run showed no lead or tungsten.

After the run, vertical samples of the bed were taken from the upstream part of the channel. To avoid sampling the sediment that had not been affected by the flow, these samples were only 1.25 cm thick. This attempt was only partially successful. The percentages of the heavies in these samples are shown in Table 11. It is clear from these samples that a heavy sublayer did form in this run, but the values for the lead and tungsten are lower than those in the samples taken at the end of Run H3. This may be an unfair comparison, because the heavy sublayer in Run H4 may not have been fully formed when it was sampled. It is possible that the heavy sublayer was at a temporary stage, at which heavies were being transported at a rate less than their upstream feed rate. Thus it is possible that the values for the bed samples from Run H4 do not represent equilibrium values. A fair comparison might have been with samples taken at the comparable time in Run H3, but those samples were not taken. The near equality between the measured and predicted position of the downstream edge of the heavy sublayer formed in Run H4 supports the idea that at comparable times in Runs H3 and H4 the heavy sublayers were similar.

It seems reasonable to conclude that a heavy sublayer would form in this system irrespective of the concentration of the heavies in the feed sediment if given enough time. If we assume that the time needed to form a heavy sublayer in an alluvial channel varies linearly with the concentration of heavies in the sediment, we can estimate how long it would take for a heavy sublayer to form in this system if the

Table 11. PERCENTAGES OF HEAVIES IN 1.25 CM SAMPLES, RUN H4

Location (m)		
	m	2.2
0.5-0.6	l	6.8
	t	8.4
	m	2.6
0.6-0.7	l	4.3
	t	6.2
	m	3.4
0.7-0.8	l	5.3
	t	3.6
	m	3.8
0.8-0.9	l	0.7
	t	1.2
	m	2.5
0.9-1.0	l	tr
	t	0.3
	m	2.9
1.0-1.1	l	0.1
	t	0.1
	m	0.8
4.0-4.1	l	tr
	t	tr

Note: Location is the distance in meters from the upstream end of the channel. Key for heavies: m - magnetite, l - lead, t - tungsten, tr - trace < 0.05% detected.

concentration of lead was 1 ppm in the feed sediment: 10,000 hours, (= 417 days, = 1.14 years) of steady flow and sediment feed conditions. This exercise makes it clear why much higher background heavy-mineral concentrations are necessary in the laboratory than are present in the field. One final note regarding this subject is that according to W.E.L. Minter (1985, personal communication) gold layers of nearly 100% concentration are rare but indeed exist in the Witwatersrand paleoplacers.

Summary of Steady-State Runs

Heavy-mineral transport mechanisms show many similarities over the range of transport rates considered, but there are significant differences also.

It has been established that for the range of conditions studied a heavy sublayer forms as part of the process necessary for steady-state transport of the heavies. Data from sampling the top 2.5 cm layer of the bed show that the magnetite concentration is up to 5%, lead to 25%, and tungsten to 24%. There is significant variability in these values both among runs and in the same run at different locations. In any case it is clear that the lead and tungsten were concentrated to approximately the same extent, but magnetite was concentrated only about 0.2 times as much.

The mechanisms by which the heavies were transported in the various runs can be broken down into a short-term component, on the order of minutes, and a long-term component, on the order of tens of minutes. At all transport rates studied, short-term variations in the heavy-mineral transport rate were controlled by the bed forms developed in the low-density sediment. This control by the bed forms was manifested by the covering and uncovering of the heavies by the migrating forms composed of low-density sediment. In the three runs with the lowest transport rates, the passage of troughs or low points between the bed-load sheets was to a great extent correlated with episodes of transport of the heavies. This peak in transport of the heavies occurred at periods of 6-14 minutes, which was the time between the passage of troughs of successive bed-load sheets. Similarly the bed forms in Run H5 also restricted the movement of the heavies at a given location to the times when a bed-form trough was passing. The period between passage of these forms past a given point was determined to be about 3 minutes. Thus the bed forms in the low-density sediment controlled the exposure of the heavies to the flow and their pattern of transport rates at periods of minutes.

Variability in transport rates on the order of tens of minutes were present only in the runs with low transport rates. These longer-term processes, consisting in the formation and destruction of clast jams, were found to operate most strongly in Run H2, which had the lowest transport rate, and were not detected at all in the runs with the highest transport rates. At any given time in Runs H2 and H3 only portions of the heavy sublayer were exposed at the bed surface as irregularly shaped patches. These longer-term processes, which caused general aggradation and degradation periods on the bed, had the effect of reducing or increasing the areas of the bed in which heavy-mineral grains were exposed by covering them with low-density sediment during aggradation periods or uncovering them during degradation periods. This process was most extreme in Run H2: at times only very small areas of heavies were exposed, and other times much larger areas of heavies were exposed. Thus even though the mechanics of the gravel sheets were similar during periods of aggradation or degradation the quantity of heavies available for transport was less during aggradational periods. Figures 15 and 16 lend support to this idea, in that the rates of magnetite and lead transport were substantially higher for the sampling period with the higher average total transport rate in Run H2. This higher transport rate corresponded to a period of degradation of the channel, when more heavies were exposed at the surface. This effect was present but much reduced in Run H3 and appears to have been totally lacking in Run H5. In Run H5, which had the highest transport rate, the exposure of the heavies appears to have been a function only of the geometry and migration of the bed forms. The runs with lower transport rates, on the other hand, appear to have had an interplay between the processes controlling long-term fluctuations in the transport rate and shorter-term processes. The longer-term processes of aggradation and degradation control the proportion of the bed with heavies exposed, and the bed-load sheets control the short-term exposure of the heavies.

The pattern of the transport of magnetite was somewhat different from that of lead and tungsten, as is shown by the presence of at least some magnetite in all transport samples in all runs. The percentages to which magnetite was concentrated in the bed were much lower than for lead and tungsten.

Why was some magnetite in transport at all times? It is likely that this was because some of the magnetite tended to be transported in suspension at least part of the time (see Table 15). This is in contrast to the lead and tungsten, which were always transported as bed load. Magnetite in transport samples taken before magnetite transport had reached equilibrium were relatively enriched in the finer sizes relative to the feed sediment. All sizes of magnetite were in transport, although at a rate less than the feed rate, even before magnetite transport had reached equilibrium.

Transport of Heavies during Degradation

General

The steady-state runs made with heavies demonstrated that over the range of discharges and transport rates used the heavies (with the exception of small amounts of fine magnetite) are transported only after a heavy sublayer forms within the bed. To shed some light on the transport of heavies with a degrading bed, Runs H6 and H7 were designed to maintain a steady rate of degradation in the flume channel. The same water discharge as Run H5 was used in Runs H6 and H7. In Run H6 the same feed rate as Run H5 was used initially, while in Run H7 no sediment was fed at all. A degradation ratio of 4.8

for Run H6 was chosen on the basis of experience gained in gravel deposition experiments by Danna (1985) in a different apparatus in our laboratory. (Degradation ratio is defined here as 100 times the ratio of the mass of sediment eroded from the channel bed per unit time per unit area to the sediment transport rate in the channel, in mass per unit width. This represents the mass percentage of transported sediment acquired by the flow by erosion, per unit channel length. The units of degradation ratio are length^{-1}.) An initial trial of Run H6 demonstrated that for the chosen degradation rate the feed rate was too high. The feed rate was then reduced by 25% and the other conditions were not changed (see Table 4). In Run H7 the degradation ratio was 19.0, this was the maximum constant rate feasible for the system at these conditions, because all of the sediment in transport came from erosion of the sediment bed. Higher degradation ratios would have overloaded the flow with sediment, which an earlier trial run had shown to be an unworkable situation.

As was planned, conditions close to a steady rate of degradation were present in Runs H6 and H7. Figure 20 shows the bed-surface and water-surface elevations with time at the three measurement locations. The parallelism of the lines in Figure 20 shows that degradation was steady throughout Run H6. Upstream depths were slightly greater than downstream depths in Run H6 (7.4 cm vs. 7.1 cm) and in Run H7 (7.6 cm vs. 7.2 cm).

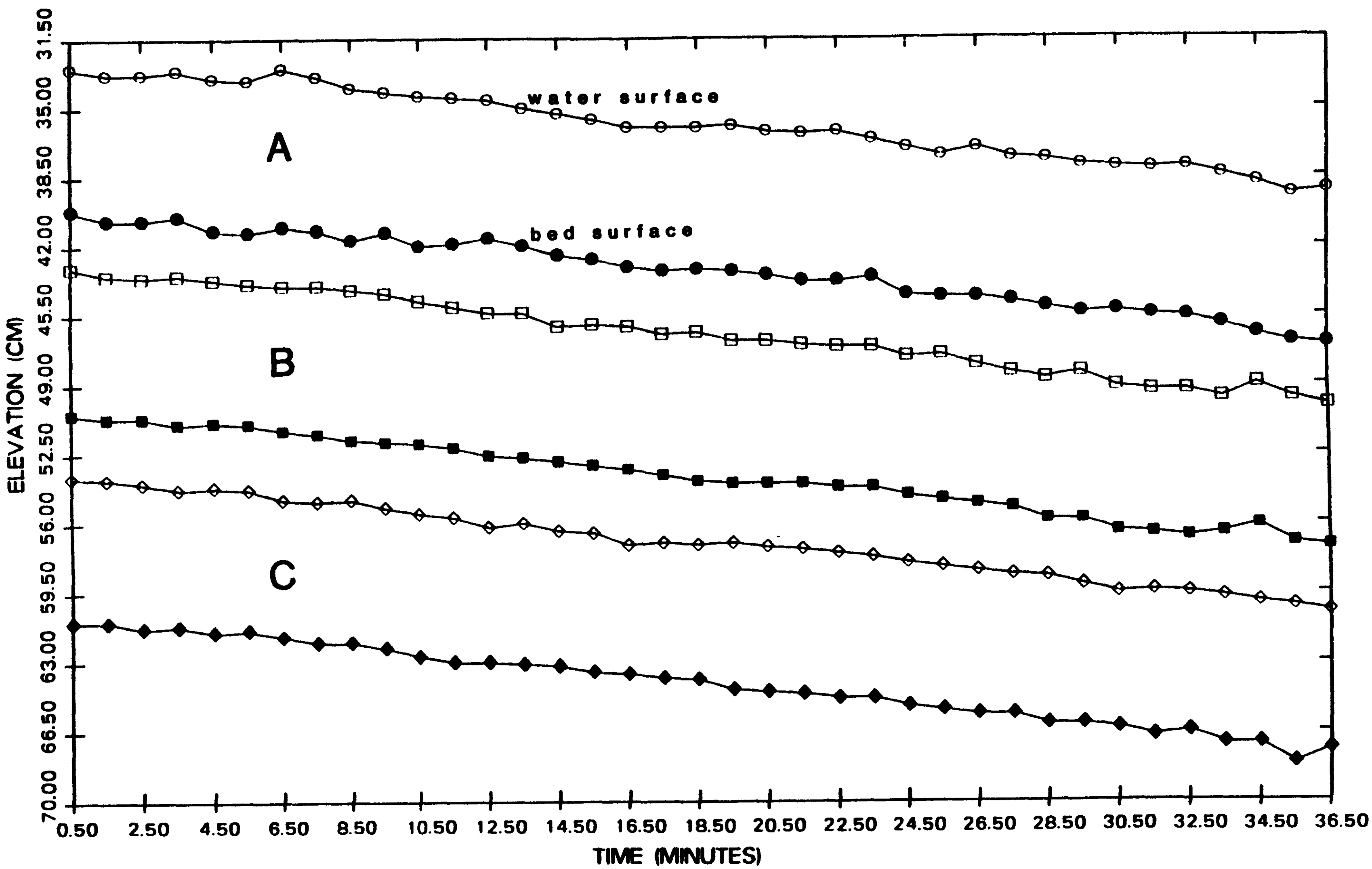

FIG. 20.-- Bed and water surface elevations vs. time, Run H6. Locations were (A) 1.5 m, (B) 3.5 m, and (C) 5.5 m from the upstream end of the channel. Solid symbols are the bed elevation and open symbols are the water surface elevation.

Bed forms similar to those in Run H5 were present in both runs. Figure 21 is a flow-parallel profile of the bed forms that was taken down the centerline of the channel at the end of Run H6. Spacing, height, and geometry of the bed forms were all similar to those of Run H5.

Bed Samples

Vertical samples of the bed sediment were taken at the end of both runs. The percentages of the three heavies in these samples are shown in Table 12. An abrupt decrease in the percentages of lead and tungsten is evident between the samples taken at 3.7 m and 4.2 m after Run H6. This abrupt change corresponds with observations of the bed after the run. The percentages of heavies in the downstream two samples are shown in Table 12 to have been concentrated by a factor of about 4 over background, which is the expected value if all of the heavies remained in the bed during degradation. No surface exposures of heavy minerals were observed in the downstream 2.3 m of the channel. The heavy sublayer in the upstream part of the channel was formed from the heavies concentrated during degradation of the bed plus the heavies contained in the feed sediment. Therefore any lead or tungsten in Run H6 downstream of 3.7 m came only from the heavies contained in the bed sediment. The percentage of heavies from two bed-surface samples taken in Run H6 are shown in Table 13. The concentrations of heavies contained in these two samples are consistent with the observations of the bed surface at the end of the run.

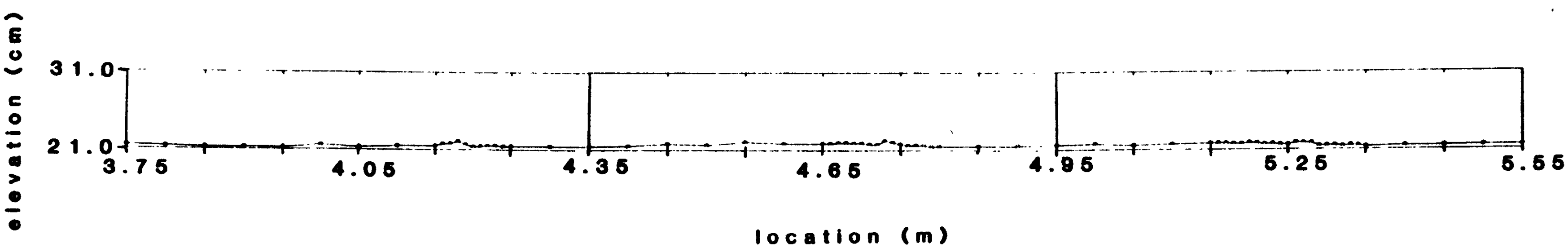

FIG. 21.-- Cross-sectional profile of bed forms parallel to flow, Run H6.
No vertical exaggeration.

Table 12. PERCENTAGES OF HEAVIES IN VERTICAL BED SAMPLES, RUNS H6 AND H7

Run H6

Location (m)		Sample # 0	1
	m	4.6	0.8
2.0	l	13.5	1.0
	t	14.1	0.9
	m	4.3	0.8
3.7	l	16.4	1.0
	t	13.0	0.8
	m	4.9	0.9
4.2	l	9.1	1.1
	t	4.4	0.8
	m	5.9	0.9
5.0	l	4.4	1.1
	t	3.7	1.0
	m	4.0	0.7
5.5	l	5.1	1.3
	t	3.8	0.9

Run H7

Location (m)		Sample # 0	1
	m	2.6	0.7
3.5	l	4.1	1.0
	t	3.7	0.9
	m	2.5	0.7
5.5	l	4.3	1.1
	t	3.5	0.9

Note: Location is the distance in meters from the upstream end of the channel. Samples were 2.5 cm thick with 0 as the surface sample. For heavies: m - magnetite, l - lead, t - tungsten.

Table 13. PERCENTAGES OF HEAVIES IN BED-SURFACE SAMPLES, RUNS H6 AND H7

Run H6

Location (m)			Approx. percent of surface area covered by heavies
2.7	m	3.9	50
	l	19.4	
	t	11.9	
5.2	m	0.1	0
	l	0.0	
	t	0.0	

Run H7

Location (m)			Approx. percent of surface area covered by heavies
2.5	m	tr	0
	l	0.1	
	t	tr	
4.0	m	0.1	0
	l	0.1	
	t	tr	

Note: Location is the distance in meters from the upstream end of the channel. Key for heavies: m - magnetite, l - lead, t - tungsten, tr - trace detected < 0.05%.

Since no sediment was fed in Run H7, the bed constituted the only source of heavy minerals. In Run H7 the increase in concentration of the heavy minerals came about solely from degrading 7 cm of the bed and was insufficient to form a heavy sublayer like the one that formed in the upstream 3.7 m of Run H6 for lead and tungsten, and apparently over nearly the entire channel length of Run H6 for magnetite. The percentages of heavies shown in Table 13 from two bed-surface samples taken at the end of Run H7 are consistent with the observed lack of a heavy sublayer at the end of Run H7.

Transport Samples

The sediment transported out of the channel during Runs H6 and H7 was weighed and sieved, and the heavies extracted. As expected from the data of Run H5 the variability in the total weight of sediment caught in the samples was low, with a coefficient of variation for the samples of 10%.

It is evident from Table 14 which shows the percentages of the three heavies caught in the transport samples of Runs H6 and H7, that lead and tungsten were transported only at very low rates for bed degradation ratios of 4.8 and 19.0. The magnetite transport rate was quite variable, and apparently increased with time during Run H6. This may have been because sediment was fed in Run H6 but not in Run H7. This point will be discussed in more detail in the next section.

Table 14. PERCENTAGES OF HEAVIES IN TRANSPORT SAMPLES, RUNS H6 AND H7

Run H6, Set 1

Sample #		
1	m	0.1
	l	tr
	t	0.0

Sample #	Run H6, Set 2		Run H7, Set 1	
1	m	0.3	m	tr
	l	tr	l	tr
	t	tr	t	0.0
2	m	tr	m	tr
	l	tr	l	0.0
	t	0.0	t	0.0
3	m	0.2	m	0.1
	l	tr	l	tr
	t	0.0	t	tr
4	m	0.1	m	0.1
	l	0.0	l	tr
	t	0.0	t	tr
5	m	0.5	m	tr
	l	tr	l	tr
	t	tr	t	tr
6	m	0.1	m	0.1
	l	tr	l	0.1
	t	0.0	t	tr
7	m	0.1	m	0.1
	l	tr	l	0.1
	t	tr	t	tr
8	m	0.1	m	0.1
	l	tr	l	tr
	t	tr	t	tr
9	m	0.7	m	0.1
	l	tr	l	tr
	t	tr	t	tr
10	m	0.3		
	l	tr		
	t	tr		

Note: Key for heavies: m - magnetite, l - lead, t - tungsten, tr - trace detected < 0.05%.

Analysis

Only very small quantities of lead and tungsten were transported out of the channel in both degradational runs. Magnetite was transported out of the channel in larger quantities in Run H6 than in Run H7 but still less than would be expected if the output transport rate had been equal to the feed rate. The probable reason for the greater concentration of magnetite in the transport samples of Run H6 when compared with those of Run H7 was that sediment was fed in Run H6 but not in Run H7. The supply of magnetite from both the bed and the sediment feed apparently caused magnetite to reach near-equilibrium concentrations in the bed of Run H6. The absence of sediment feed in Run H7 reduced the supply of heavies available for concentration, so the rate of transport of magnetite out of the channel was less in Run H7 than in Run H6.

Observations through the sidewall revealed that the heavy-mineral grains in the bed moved down through the interstices of the low-density grains as the bed degraded. Most grains moved down less than 2 cm, although some grains were observed 3 cm below the surface, or even deeper. This process caused the heavies to continually fall below the active surface of the bed. Presumably this would continue until concentrations of the heavies in the bed reached levels equivalent to those formed in the runs with steady flow conditions, at which time the heavies would begin to be transported through the system.

In summary, the conditions needed for transport of the three kinds of heavies during Runs H6 and H7 were essentially the same as during the steady-state runs. The formation of heavy sublayers was still necessary for transport of lead and tungsten. The case of magnetite was not clear in Run H6, but the results of Run H7 demonstrated (see Table 14) that the degrading bed did not enhance significantly the transportability of magnetite. As the bed surface degraded, the heavies were observed to filter down through the bed and become concentrated in the bed, leaving only small amounts in transport.

DISCUSSION

Transport of Heavies during Aggradation

In the first part of this investigation the transport of heavy minerals was studied under steady conditions of flow and sediment feed rate. The results of these experiments define a state toward which natural streams with similar conditions would tend if given sufficient time. Runs H6 and H7 dealt with the transport of heavies when the bed was being degraded. No runs were designed specifically with aggrading beds, because aggradation in the early parts of two of the steady-state runs yielded information on how the heavies behave in an aggrading regime.

The observation from the steady-state runs that is most applicable to the effect of aggradation on heavy-mineral transport in this system was that the heavies (especially lead and tungsten) must form a heavy sublayer in order to be transported. Except for small amounts of magnetite, no heavies were transported before this heavy sublayer developed. Undoubtedly the heavies are much less transportable than the lights. If some rate of aggradation is imposed on the system the heavies will not be transported from a given location until a heavy sublayer is formed. Whether a heavy sublayer is formed and how far it will extend down the channel are functions of the rate of supply of the heavies to the system and the rate of aggradation of the channel bed. Three different hypothetical runs, each with different values of aggradation ratio (defined, similarly to the degradation ratio, as 100 times the ratio of aggradation rate per unit area to the unit sediment feed rate) will be considered below. The aggradation ratio, and not the actual values of aggradation rate and heavy-mineral feed rate, is the most important factor in the results of the three hypothetical runs. The three cases related below consider aggradation ratios of 0.002, 0.06 and 0.4. The choice of 0.002 and 0.4 is arbitrary and values lower than 0.002 or higher than 0.4 would have demonstrated the same point. The value of 0.06 is the specific value for this system that allows the heavies to just be transported the 6 m length of the flume.

Case 1.--First an aggradation rate that is small relative to the heavy-mineral feed rate will be considered. An aggradation ratio of 0.002 will serve our purposes as an example, but as stated above any lower ratio would yield a similar result.

The concentration of lead and tungsten in the feed sediment is about 2% by weight. If we assume a mixture with equal concentrations of lead and tungsten by weight, the average density of the mix is 15.4 g/cm^3. Assuming equal porosities of heavies and lights, this means that the heavies are only about 0.36% of the sediment by volume. In our first hypothetical experiment the aggradation ratio is 0.002. Therefore over one meter of the channel the fraction of the sediment deposited is 0.002. We know from the steady-state runs that the heavies are much less easily transported than the lights and thus they will tend to be deposited before the lights. Also the heavies are not transported until they become concentrated near the location of the feed. Initially only heavies are deposited in the area where the heavies are fed to the channel. If the run is continued for a sufficiently long time the heavies are eventually transported the six meter length of the channel and into the tail barrel. Thereafter the sediment deposited is essentially 100% heavies over the entire channel length.

Case 2.--Next we consider an aggradation rate such that all of heavies fed to the channel are needed to maintain the aggradation rate. An aggradation ratio of 0.06 causes the heavies to just be transported the 6-m length of the channel if the run is continued for a long enough time. Very long times are necessary, because the transport rate of the heavies at a given cross section decreases down the channel as a greater percentage of the heavies fed into the channel goes into making the deposit.

Case 3.--Finally an aggradation rate that is large compared to the feed rate will be considered. The aggradation ratio is 0.4, and if the experiment is continued for a long enough time the heavies are transported less than one meter down the channel. The heavies are not transported past the one-meter mark because they all are needed to maintain the 0.4 aggradation ratio. For higher aggradation ratios the heavies are transported even shorter distances.

The three cases considered above demonstrate that for any aggradation ratio greater than 0.06 the heavies are transported less than 6 m. The aggradation during the first parts of Runs

H1 and H2 (Table 7), described above in the results section for these two runs, supports this conclusion.

It is evident from the three cases discussed above that channels with aggrading beds can in fact concentrate heavy minerals at or near the point where heavies are supplied. If the aggradation ratio is close to the ratio of the volume of heavies to the volume of lights being supplied to the system, a very rich placer deposit will form. Thus in a natural stream a very low aggradation rate would tend to concentrate heavies if a source of heavies is available. The deposits at points of abrupt valley widening (Crampton, 1937; Kuzvart and Bohmer, 1978; Hall, Thomas, and Thorp, 1985) may have been formed as a result of aggrading channels that were supplied with heavies from upstream.

Bedrock Placers

Concentrations of heavies at or near bedrock are very common in alluvial placers. In fact these deposits have been called axiomatic by Cheney and Patton (1967). Cheney and Patton suggest that bedrock concentrations in streams are caused by infrequent floods that scour the sediment in the valley down to bedrock. Others (e.g. Tuck, 1968; Karatashov, 1971) agree with Cheney and Patton's hypothesis, but give more details on how fluvial cycles of aggradation and degradation concentrate heavies at bedrock surfaces. Gunn (1968), on the other hand, believes that fluvial cycles of aggradation and degradation do not necessarily concentrate heavy minerals.

Gunn states that from his own experience heavy minerals readily move downwards through unconsolidated sediments if they are below the water table and are agitated in some way.

Both of the processes proposed by the above authors for the formation of bedrock placers operated in the runs of this study. In Runs H2 and H3 the infiltration of heavy grains through the bed was found to be the most likely explanation for the concentrations that developed in the bed below the level affected by the flow. The bed samples in Tables 6 and 9 show the enriched layers below the surface layer. The heavies were also concentrated by degradation in Runs H6 and H7 as the grains moved below the bed surface as it was lowered.

Although heavies were documented to have moved downwards a few centimeters through the bed in Runs H2 and H3, it is difficult to imagine this process operating to much greater depths in natural stream deposits. The large vertical variations in sediment mean sizes and distributions characteristic of fluvial deposits would in most cases prevent heavies from moving down more than a short distance because the size of the spaces between grains varies with grain size. Unless a fluvial deposit had a substantial thickness of the same coarse and well sorted light-mineral sediment, this process probably would not be effective. It is more likely that the heavies become concentrated by moving down through the interstices of the grains near the bed surface of a stream while degradation is occurring. This is precisely what was observed during Runs H6 and H7.

Thus both aggrading and degrading channels have the potential to concentrate heavies. If heavies are widely dispersed through large volumes of sediment, channels with degrading beds can concentrate the heavies into bedrock or false-bottom placers. Aggrading channels can form heavy-mineral concentrations if heavies are steadily supplied to the channel and the aggradation rate is not too high. These deposits, however, would tend to be more localized than those concentrated by degrading channels. It is also very likely that in many cases both aggradation and degradation acted in the same fluvial system at different times of its history. The concentrations of heavies that would be deposited from low and high aggradation and degradation ratios is summarized in Figure 22.

Heavy Sublayers

It is clear that in our experiments the heavies became highly concentrated in the bed before they were transported. These concentration factors over background were up to 6 for magnetite, 22 for lead, and 28 for tungsten. The <0.5 mm light fraction of the sediment was also concentrated by a factor of 3 over background in the bed (Fig. 23). The concentrations of the light fractions were determined from the bed samples of Run H1 that were downstream of the farthest location to which lead and tungsten had been transported. In the bed samples of the other runs that contained heavy sublayers, the lights were underrepresented in the sizes that contained heavies. Presumably the fine fractions of the lights did not need to

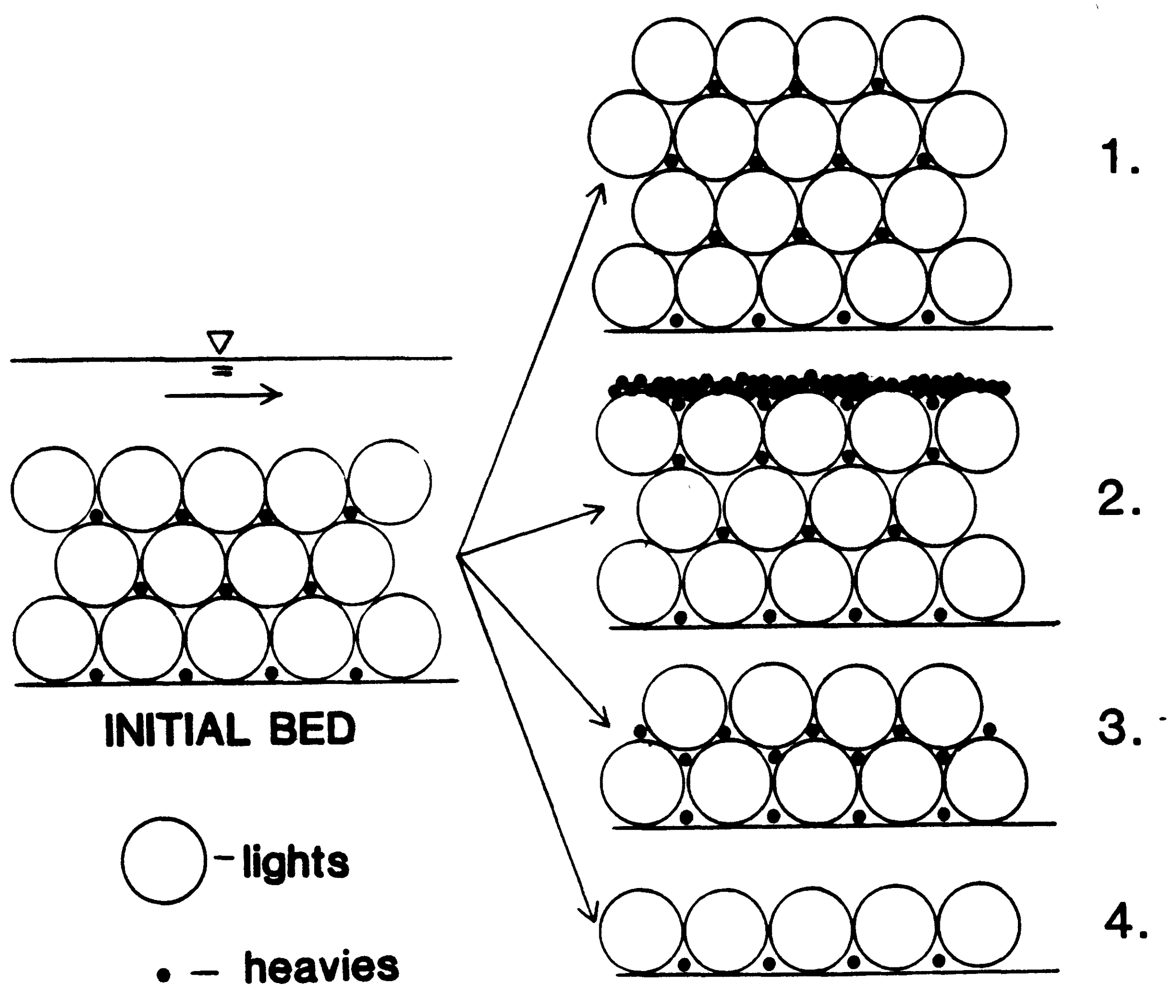

FIG. 22.-- Concentrations of heavies in the bed for high and low values of aggradation and degradation ratios.

1. High aggradation ratios yield a deposit with the same concentrations of heavies and lights as the sediment in transport.
2. Low aggradation ratios yield a deposit enriched in heavies. With increasing aggradation ratios the heavies are progressively less enriched in the deposit.
3. Low degradation ratios concentrate heavies in the bed. The heavies fall into the interstices between the light grains as the bed surface is lowered.
4. High degradation ratios erode heavies and lights in the same proportions as they are present on the bed. No heavies are concentrated on the bed.

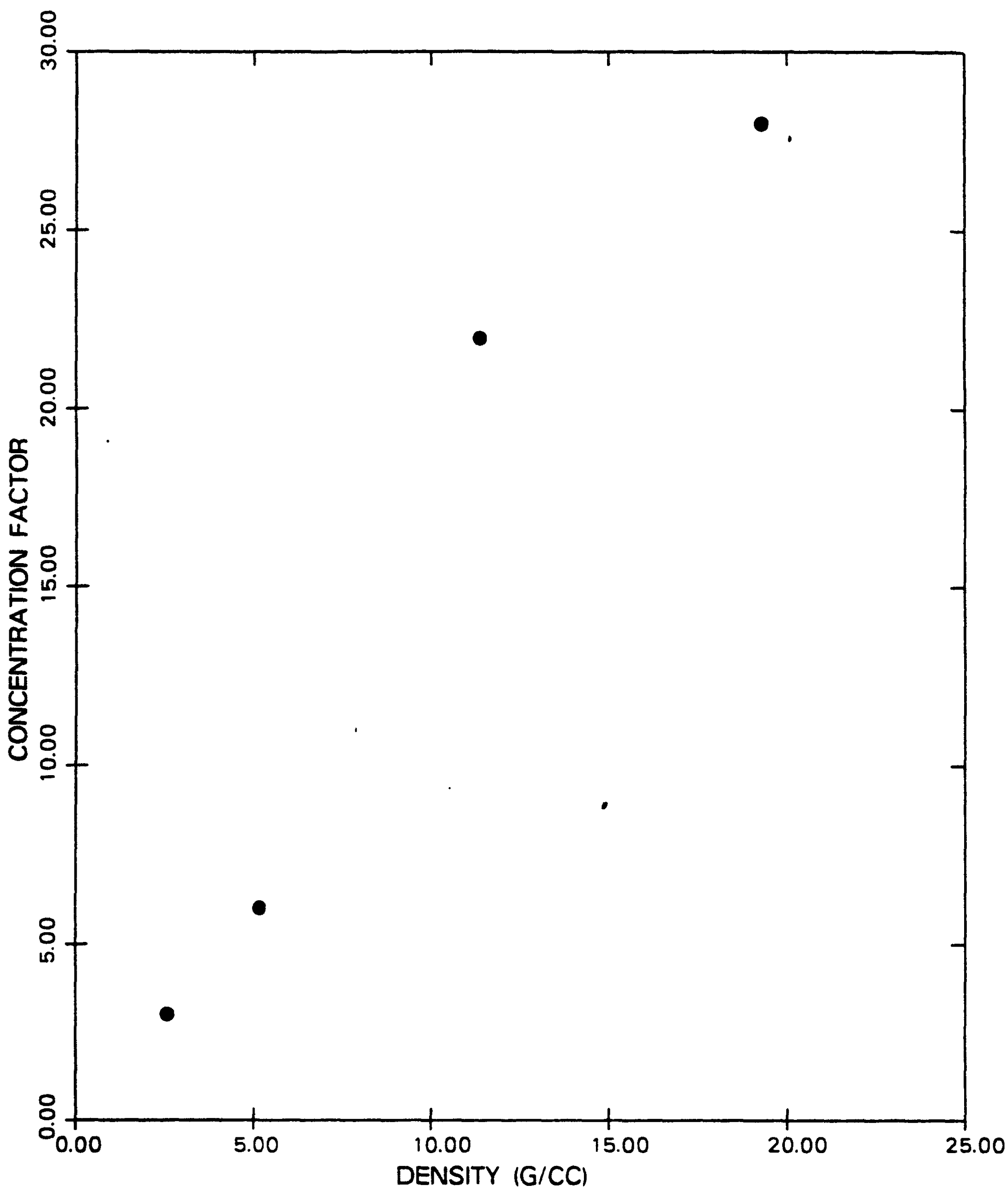

FIG. 23.-- Concentration factor vs. density. Concentration factor is defined as the ratio of the concentration of a given size-density fraction in a bed sample to the concentration of that fraction in the original sediment mix.

become concentrated in the bed after a heavy sublayer had formed.

Work by Miller and Byrne (1966), Slingerland (1977), Komar and Wang (1984), Z. Li and P.D. Komar (unpublished manuscript), and P.D. Komar and Z. Li (unpublished manuscript) on the initiation of motion of grains in sediments with a mixture of sizes is especially applicable to our data. These studies predict that sizes significantly smaller than the mean are more difficult to entrain than larger sizes. Miller and Byrne (1966) and Komar and coworkers determined that reactive angles of smaller grains resting on a bed of larger grains (see Fig. 24) are greater than for larger grains on the same bed. Figure 25, adapted from Miller and Byrne (1966) and Komar and Wang (1984), shows the relationship between the ratio of the critical shear stress for a given grain size to the critical shear stress of the mean grain size (τ_{ci}/τ_{cm}) and the ratio of a given grain size to the mean grain size (D_i/D_m). The general form of the equation for the plot shown in Figure 25 is

$$\tau_c = k(s-1)\rho g D \mathrm{Tan}\Phi \qquad (4)$$

where τ_c is the critical shear stress, k is a constant, s = ρ_s/ρ, ρ_s is the sediment density, ρ is the fluid density, D is the grain size, and

$$\Phi = e(D/K)^{-f} \qquad (5)$$

where Φ is the reactive angle of the grain, e and f are empirical constants related to shape, roundness, and sorting, respectively, and K is the roughness size of the bed, usually

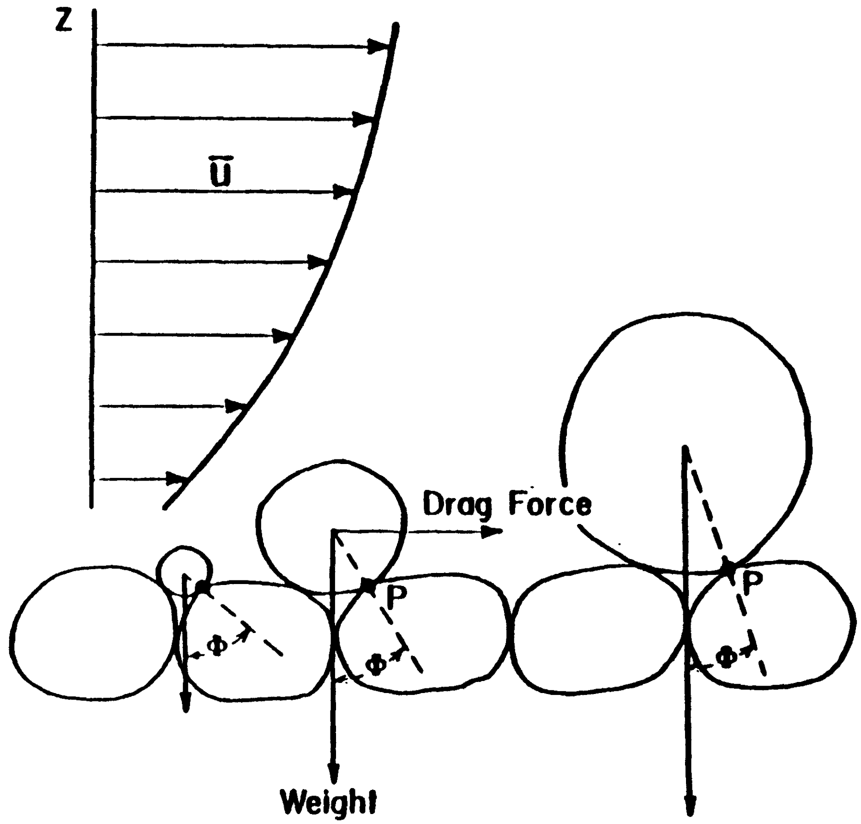

FIG. 24. -- Reactive angles for three different size grains on a bed of uni-size grains. As shown the reactive angle decreases with increasing grain size. (from Z. Li and P.D. Komar, unpub. manuscript)

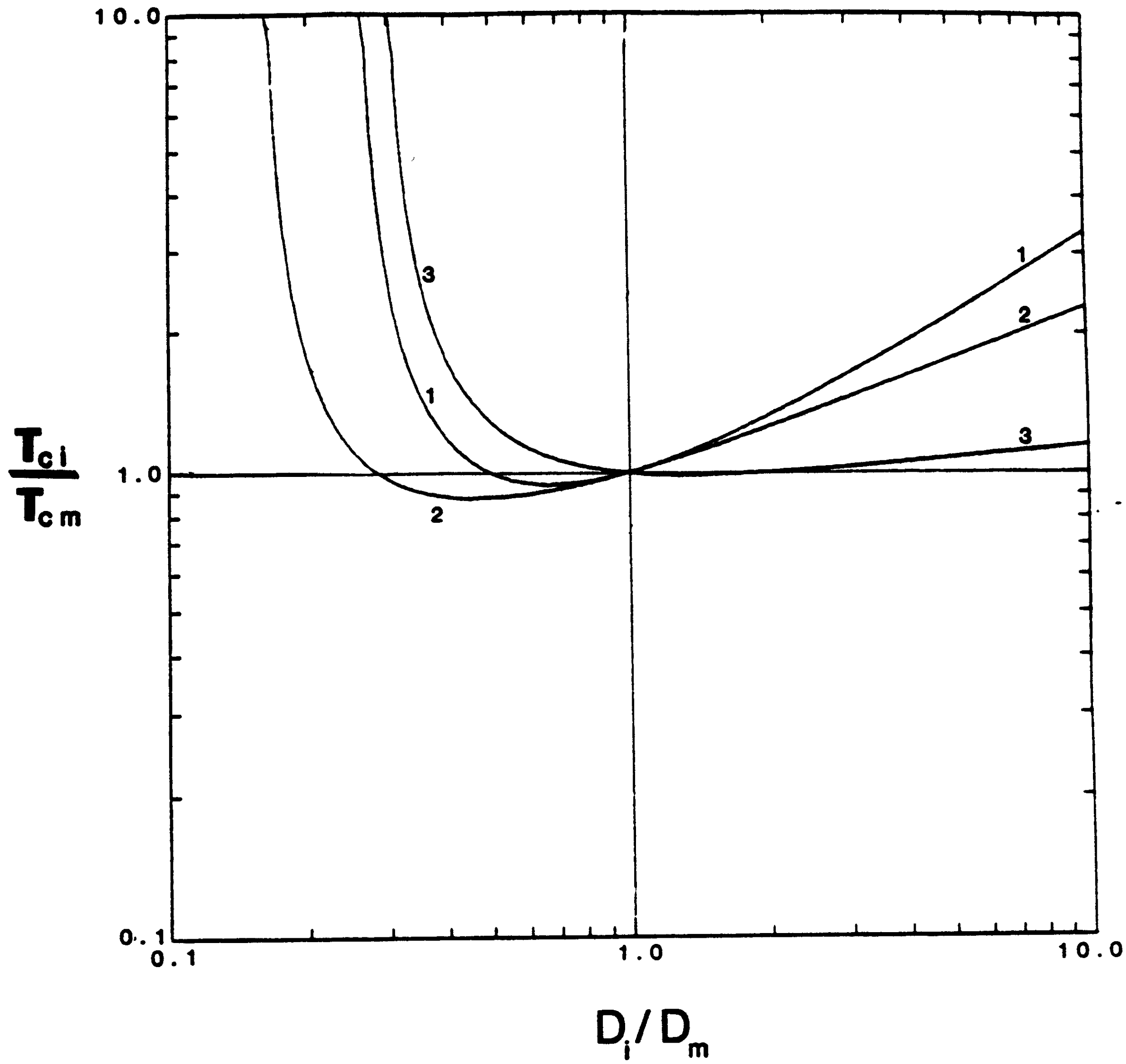

FIG. 25.-- Ratio of critical shear stress for the ith fraction to the critical shear stress of the mean size of the sediment (τ_{ci}/τ_{cm}) vs. the ratio of the size of the ith fraction to the mean size (D_i/D_m).

for 1 - e = 60, f = 0.3
2 - e = 30, f = 0.9
3 - e = 30, f = 0.6

taken as the mean grain size. Equation (4), from Komar and Wang (1984), was derived by equating the fluid and gravity forces on a grain; equation (5) is from Miller and Byrne (1966).

From equations (4) and (5),

$$\frac{\tau_{ci}}{\tau_{cm}} = \frac{k(s-1)\rho g D_i \tan(e(D_i/D_m)^{-f})}{k(s-1)\rho g D_m \tan(e(D_m/D_m)^{-f})} \qquad (6)$$

If we assume that k in equation (6) does not change for different grain sizes, equation (6) can be simplified to

$$\frac{\tau_{ci}}{\tau_{cm}} = \frac{D_i}{D_m} \frac{\tan(e(D_i/D_m)^{-f})}{\tan(e)} \qquad (7)$$

Equation (7) then equates the critical shear stress ratio, τ_{ci}/τ_{cm}, to the ratio of the grain sizes times the ratio of the tangents of the reactive angles of the ith fraction and the reactive angles of the mean size. The assumption that k in equation (6) does not depend on grain size has not been tested and is probably not correct because grains of different size rise to different heights above the bed into the boundary layer of the flow. The specifics of the boundary layer of flowing fluid close to a rough boundary are not well known, but the plot of critical velocity vs. grain size of Slingerland (1977, Fig. 5, bks=0.3 mm) includes the effect of the flow on the grains and shows the same general trend as shown in Figure 25. The shape of the curves in Figure 25 is probably correct, but the actual values may not be correct.

The values of the coefficients e and f used in equation (7) to generate the three curves shown in Figure 25 are approximately those obtained from the experiments of Miller and Byrne (1966) using sand-sized sediment and from the fitting of equation (4) to gravel-bed river data by P.D. Komar and Z. Li (unpublished manuscript). The values of e and f for curve 1 are 60 and 0.3, for curve 2 are 30 and 0.9, and for curve 3 are 30 and 0.6, respectively. Figure 25 illustrates the similarity of the resulting three curves despite the different values of e and f.

Comparing the data of this study with Figure 25 yields much insight into the processes acting on the bed during the runs. For grains smaller than the mean size the critical shear stress is seen to decrease slightly and then to increase rapidly with decreasing size. This is interpreted as being due to the higher reactive angles for small grains on beds of larger grains. For grains larger than the mean size the relative shear stress also increases, but at a much slower rate. This increase can presumably be explained by the increasing ratio of mass to the cross-sectional area as grain size increases even though the reactive angles continue to decrease.

All of the heavies used in this study had ratios D_i/D_m of 0.23 or less. Figure 25 predicts that at these values the shear stress for entrainment is at least ten times that of the mean, and for lower values of D_i/D_m the critical shear stress increases very rapidly. This prediction is supported by the data from our study. Initially in all runs the grains with $D_i/D_m < 0.2$ were transported at very low rates relative to their concentrations in the feed sediment or not at all. The grains in these size fractions were eventually transported at their equilibrium rates by becoming concentrated in the bed sediment. The factor by which < 0.5 mm fractions were concentrated is a function of their density as well as their size; generally the greater the density the greater the concentration in the bed (see Fig. 23). One minor exception to this generalization is that lead and tungsten were concentrated to a similar extent despite their large difference in density. Probably this is due to their different size distributions.

For transport of a sediment with a given imposed feed rate, size distribution, and density distribution the bed evolved so that the less easily entrained (and thus less easily transported) fractions became concentrated and the more easily entrained (and thus more easily transported) fractions became depleted relative to the original size and density fractions of the mix. These trends in the bed size distribution are shown in Figure 26. The bed sample that was essentially free of heavies in Figure 26 shows that the coarse and fine fractions are concentrated over their original values; the trend is similar but stronger for the other bed sample, which contained heavies.

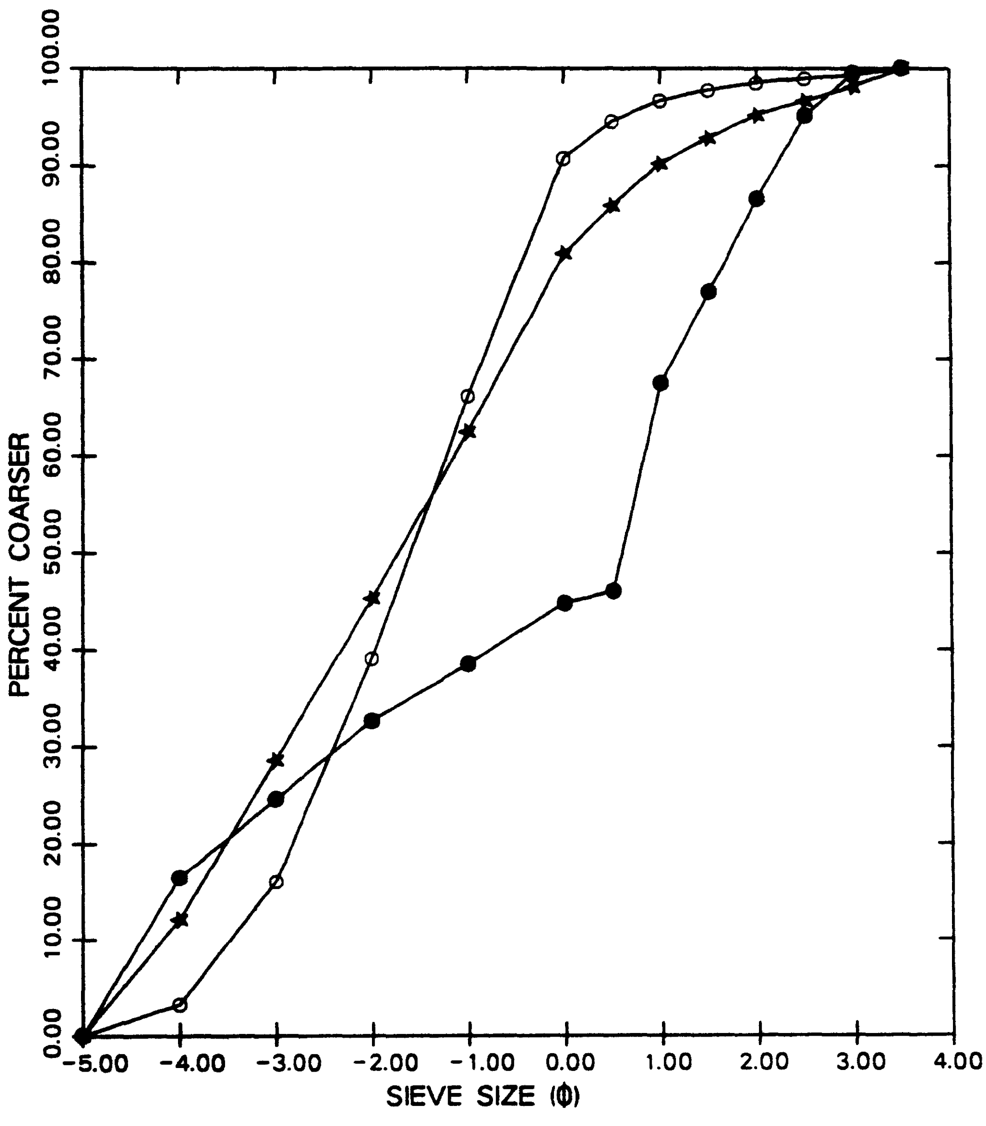

FIG. 26.-- Grain size distributions for 2.5 cm thick bed samples, Run H1.
o -- original mix
● -- bed with heavies
✶ -- bed without heavies

The values shown in Figure 25 are for one density. For the sizes of heavy minerals used in this study the critical shear stress for entrainment before heavy layers formed in the runs was very large. The way the system evolved in order for the heavies to be transported was for the heavies to form heavy sublayers. The lead and tungsten were transported when portions of these heavy sublayers were exposed to the flow. These heavy sublayers essentially created their own special environment on the bed, one in which the roughness size was controlled by the size distribution of the heavies rather than the size distribution of the lights. The shear stress necessary for entrainment of the heavies in the exposed patches was thus decreased such that the heavies could be transported. Threshold relations for the exposed portions of the heavy sublayers would be less than for heavies on a bed of larger lights, because the local bed roughness would be the mean size of the heavies rather than the mean size of the lights.

In all runs of this investigation the bed shear stresses that developed in order to transport the sediment at the imposed feed rate and size distribution was sufficient to transport the heavies once they became concentrated into heavy sublayers. This is apparent from the results of Runs L3 and H2, which were made under conditions the same in all respects except that one did not contain lead or tungsten in the sediment. The bed shear stress and the processes of transport of the light sediment were indistinguishable between Runs L3 and H2, indicating that the formation of a heavy sublayer in Run H2 did not significantly affect the processes of transport of the lights, which still dominated the system.

The results of our experiments as well as the entrainment relation in Figure 25 indicate that heavy sublayers must form for steady-state transport of heavies in systems similar to ours irrespective of the original concentration of the heavies in the sediment. This is an important result, because comparisons to natural systems might be suspect if the initial concentrations of heavies used in our experiments caused changes in the transport system that would not be present at lower concentrations. Apparently the important variables that controlled the transport of the heavies in this study were the size of the heavies relative to the mean size of the sediment (D_i/D_m) and the density of the heavies.

Applications to Natural Systems

The results of Runs H6 and H7 demonstrate clearly that heavies can be concentrated in an eroding bed. All three heavies were concentrated by moving down into the bed as the bed surface lowered. There is no reason why degradation cannot continue to much greater depths in natural systems. In fact, processes similar to those observed in Runs H6 and H7 are in all likelihood responsible for forming the bedrock and false-bottom placers common in natural deposits.

The processes by which heavies are transported in natural systems are not as straightforward as the processes by which heavies dispersed in a deposit can be concentrated. Unless the source of the heavy minerals is very near the river system and heavies are delivered to the channel through the formation of colluvial deposits, some mechanism for the transport of heavies not encountered in this study is needed. The transport of heavies of magnetite density and less is not as problematic as for denser heavies, because they need to be concentrated only to about 5% in the active layer to be transported. Also relatively low-density heavies, like magnetite, generally are more abundant naturally than higher-density heavies like gold. Even in a deposit like the Witwatersrand, which contains rich deposits of uraninite and gold, the background concentrations of these minerals are only a few parts per million (Minter, 1978). Only under extraordinary conditions do these very-high-density minerals ever reach concentrations that approach those formed in this study.

In some instances minerals of very high density, like gold, are not transported very far from their source. In these deposits the heavy minerals are generally present in small concentrations in source rocks in the valley walls of the streams. As sediment reaches the river through mass movements the heavies are concentrated during fluvial reworking of these sediments, which involves cycles of aggradation and degradation. Bedrock deposits and false-bottom deposits certainly can be formed in this way. Examples of placer deposits formed in this way include those of the Fairbanks, Alaska region (J.F.M. Simms, personal communication, 1985) and deposits in Costa Rica studied by Valls (1985). Kartashov (1971) discussed several examples of placer deposits in the USSR which he interpreted as having been formed in this way. In fact, Kartashov suggested a classification of placer deposits based on whether or not the heavies had been transported by fluvial processes. Kartashov termed these two types of placers, in which the heavies had and had not been transported, as allochthonous and autochthonous, respectively.

Heavy minerals in the placer deposits of the Precambrian Witwatersrand Group are known to have been transported at least 20 km (Minter, 1978) and probably considerably farther. The results of this study may not be directly applicable to these deposits, in that the grain sizes of the heavies may be different. The only detailed information of which we are aware on the size of the gold in the Witwatersrand is given by Nami (1983), who reports gold grain sizes ranging from 0.025 mm to 0.3 mm with a median size of about 0.07 mm. Although this size distribution overlaps that of the tungsten used in this study, it is significantly finer overall (compare Fig. 7 and Table 3). Data on the grain sizes of uraninite in the Witwatersrand placers is unknown to us. Mean grain sizes of the light fraction in the Witwatersrand range from gravel to sand (Minter, 1978). It is clear that the the sizes of the lights used in this study are certainly representative of sizes present in at least part of the Witwatersrand.

The possible mechanisms responsible for transport of the heavies of the Witwatersrand placers can be considered in light of what we know about heavy-mineral transport. If the size distribution for the gold given by Nami (1983) can be taken as representative of the deposit as a whole, and that is by no means a certainty, how would these smaller sizes act in our experimental system? First of all, the values of D_i/D_m for the median gold grain size of 0.07 mm would be 0.02 in our study. Referring to Figure 25, this value suggests that the shear stress needed for entrainment of this size would be very high. Once up in the flow, however, gold grains of this size could be expected to have been transported in suspension in the runs of this study, because values of u_*/w shown in Table 15 are substantially greater than one. However, this transport probably would not have taken place until a heavy sublayer had formed, because of the small values of D_i/D_m. This supposition is supported by the results of a study made by Brady and Jobson (1973) in which magnetite formed concentrated layers despite being transported in suspension (see Table 15). Brady and Jobson also showed that less than 10% of the magnetite in their original mix was in transport.

It is apparent from the values in Table 15 that 0.07 mm tungsten, or gold for that matter, probably would have been transported in suspension in our runs. Heavy patches probably still would have been necessary for transport of the finer heavies. Small amounts of the finer tungsten may have been in transport at most times of the runs, as was observed for magnetite, although the effect on transport of the size difference between the 0.07 mm tungsten and 0.125 mm magnetite

Table 15. VALUES OF u_*/w FOR VARIOUS SIZES AND DENSITIES OF HEAVIES

Tungsten

grain size (mm)	0.125	0.07
Run H2	0.98 (1.18)	2.20 (2.62)
Run H5	1.04 (1.26)	2.32 (2.81)

Lead

grain size	0.35
Run H2	0.44 (0.52)
Run H5	0.46 (0.56)

Magnetite

grain size (mm)	0.125	0.50
Run H2	3.24 (3.87)	0.57 (0.68)
Run H5	3.42 (4.14)	0.60 (0.72)

Values from Brady and Jobson (1973)

Magnetite

grain size (mm)	0.144	Bed phase
Run 1	1.52	dunes
Run 4	2.56	flat bed

Note: $u_* = (gRS_o)^{1/2}$, where g is the acceleration of gravity, R is the hydraulic radius, S_o is bed slope.
w is the fall velocity calculated from Figure 2.3 of Middleton and Southard (1984, p. 36).
Values in parentheses are u_*/w values in which sidewall corrected values of u_* (u_{*b}) were used. The correction technique used was that of Vanoni and Brooks (1957,p100)

would have is not clear. However, except for the possibility of small amounts of tungsten in transport the results of our steady-state runs probably would have been similar for finer sizes of tungsten. In natural systems, then, probably only very large floods with very rapid rates of erosion would entrain these grains if the lights were comparable to those used here. Heavies entrained by the flood would eventually be deposited, and the likelihood of reentrainment would be related to the sediment sizes and flow characteristics present where deposition occurred.

If the grain sizes where the heavies were deposited were similar to those used in our study, very high shear stresses would be needed for reentrainment. However, if heavies happened to be deposited on finer beds, conditions necessary for reentrainment would possibly be substantially different. Transport of heavy heavies in finer low-density sediment would possibly take place in the presence of large bed forms, which have been shown to affect the transport of heavies (4.5-5.2 g/cm^3) in sands (Brady and Jobson, 1973; Steidtmann, 1982).

Brady and Jobson (1973, Fig. 23, p. K27) showed that transport of 0.144 mm magnetite in 0.285 mm low-density sediment decreased steadily with time during plane-bed transport in a sediment-recirculating flume, but noted no such decrease in transport with time in runs in the same sediment in which dunes were present on the bed. The description of the processes of formation and migration of magnetite concentrations on the stoss side of ripples and during plane-bed transport given by Brady and Jobson is also very similar to the processes observed for heavy-mineral concentration and transport in this study. Steidtmann (1982) described results similar to those of Brady and Jobson (1973) from flume experiments in which deposits of 0.4 mm glass beads with densities of 2.5 g/cm^3 and 4.5 g/cm^3 were produced in an expanding-width channel (see Previous Work section, above).

Bed forms in the two studies discussed above clearly were important in the transport of sand-sized heavies with densities of 4.5 g/cm^3 to 5.2 g/cm^3 in sand-sized lights. Most likely the erosional and depositional aspects of ripple migration acted to keep the heavies in the active transport layer in the experiments of the two studies. It is probable that bed forms are also important in the transport of heavies with densities higher than magnetite for some range of sediment properties and flow conditions. This range of sediment and flow conditions over which bed forms might be important for the transport of "heavy" heavies is generally unknown at this time.

Formation of Placers

A possible mechanism of formation of bedrock and false-bottom placers has been demonstrated in this study. However, mechanisms for the formation of other kinds of placers can only be inferred. Basically mechanisms by which heavies are transported and concentrated are needed. It appears that only very rapid degradation will cause significant transport of heavies under the conditions used in this study. Even if heavies are entrained by a major erosive event, transport of the heavies ceases once the grain reaches the bed at the end of the event unless different conditions prevail at the point to which the heavies are transported. Beds made up of grains with a large mean grain size relative to the heavies would be likely candidates for deposition regardless of the process by which the heavies are transported. Thus heavy minerals that are transported during large erosive events will most likely be deposited in a variety of subenvironments within a fluvial system. The characteristics of the sediment in each subenvironment will determine whether the heavy minerals tend to remain in that location or be reentrained by weaker flows. Important factors affecting the ease with which heavies are entrained once they are deposited appear now to be (i) the size of the heavies relative to the mean size of the sediment bed and (ii) the presence or absence of robust bed forms.

A possible scenario for how placers are formed centers around the major flood events. After major flood events heavies are deposited in two broad groups of sites, those that allow reentrainment by weaker flows and those that do not. Heavies probably migrate gradually from sites where they are transportable to sites where they are untransportable in the interim between flood events. Eventually if given enough time transport of heavies ceases with the heavies concentrated in the sites that discourage transport. This entire process gets repeated at the next major flood.

The above sketch is very oversimplified in that a whole range of sites with varying degrees of susceptability to entrainment must exist, the magnitude of the flood events is a very important variable, and the sequences of events leading to the preservation of rich heavy segregations is not dealt with. In this study mechanisms of transport and segregation of heavies were determined for a gravel-bed channel. Further experiments are needed to expand the range of conditions over which the mechanisms of transport and concentration of heavies is known.

CONCLUSIONS

(1) For the range of conditions studied, a heavy sublayer must form before equilibrium transport of the heavy minerals is attained under steady conditions of sediment feed and water discharge. Factors of concentration in this study were up to 6, 22, and 28 over background levels for magnetite, lead, and tungsten, respectively. The two main factors that cause grains to become concentrated in the bed appear to be their relative size compared to the mean (D_i/D_m) and their relative density.

(2) For grains in the size range 0.125 mm to 0.500 mm, the concentration factors for the grains in the bed were directly related to the density of the grains. This trend was shown for grains of densities of 2.6 g/cm^3, 5.2 g/cm^3, and 19.3 g/cm^3 (see Fig. 23).

(3) The original concentration of the heavy minerals in the sediment was found <u>not</u> to be an important factor in the mode of transport of the heavy minerals in this system. There is likely to be some upper limit to heavy-mineral concentrations past which this is no longer true, but for heavy-mineral concentrations equal to or less than those used here, the steady-state transport conditions would be similar regardless of concentration. The main difference for the same sediment and flow conditions but with different concentrations of heavies probably would be the time required for a steady state to be reached.

(4) The pattern of the variations in transport rates of the heavies was controlled by the transport mechanisms of the low-density sediment. Rates of transport of the heavies peaked when the total transport rate was low. This was due to the increased uncovering of the heavy sublayers during the passage of bed-form troughs. In the runs with lower transport rates (0.03-0.09 kg/s·m) periods of aggradation and degradation on the bed at time scales of tens of minutes decreased the transport rate of the heavies during the aggradational periods and increased it during the degradational periods. These longer-term changes in heavy-mineral transport rate were caused by decreases in the exposed area of the heavy sublayer during general aggradation, and increases in the exposed area of the heavy sublayer during general degradation.

(5) Bed degradation in alluvial channels has been shown to be a plausible mechanism by which heavies can be concentrated. This process was determined to be the most likely mechanism in which bedrock and false-bottom placers are formed in natural streams.

(6) Aggradation of the sediment bed was found to prevent heavies from being transported to an appreciable distance (<6 m) except at low aggradation ratios (0.06 or lower for this study; aggradation ratio is defined as 100 times the ratio of the aggradation rate per unit area to the sediment feed rate per unit width). Rates of aggradation greater than the lower

limit cause all heavies to be deposited close to where they enter the system. Thus, in a channel with an aggrading bed potentially rich placer deposits can be formed at or very near the point at which the heavies enter the system.

REFERENCES

Adams, J., Zimpfer, G. L., and McLane, C. F., 1978, Basin dynamics, channel processes and placer formation: a model study: Eonomic Geology, v. 73, p. 416-426.

Aleva, G. J. J., 1985, Indonesian fluvial cassiterite placers and their genetic environment: J. Geological Society of London, v. 142, p. 815-836.

Bagnold, R. A., 1954, Experiments on a gravity-free dispersion of large solid spheres in a Newtonian fluid under shear: Proc. Roy. Soc. London, v. 225A, p. 49-63.

Bagnold, R. A., 1956, The flow of cohesionless grains in fluids: Proc. Roy. Soc. London, v. 265A, p. 315-319.

Bateman, A. M., 1950, Economic Mineral Deposits, 2nd ed., John Wiley and Sons, New York, 915 p.

Best, J. L., and Brayshaw, A. C., 1985, Flow separation--a physical process for the concentration of heavy minerals within alluvial channels: J. Geological Society of London, v. 142, p. 747-755.

Boggs, S., Jr., and Baldwin, E. M., 1970, Distribution of placer gold in the Sixes River, southwestern Oregon -a preliminary report: U.S. Geological Survey Bulletin 1312-I, 27 p.

Brady, L. L., and Jobson, H. E., 1973, An experimental study of heavy-mineral segregation under alluvial-flow conditions: U.S. Geological Survey Prof. Paper 562-K, p. K1-K37.

Buck, S. G., 1983, The Saaiplaas Quartzite Member: a braided system of gold- and uranium-bearing channel placers within the Proterozoic Witwatersrand Supergroup of South Africa, in Collinson, J. D., and Lewin, J., eds., Modern and Ancient Fluvial Systems, International Assoc. of Sedimentologists Special Pub. no. 6, p. 549-562.

Buck, S. G., and Minter, W. E. L., 1985, Placer formation and fluvial degradation of an alluvial fan sequence: the Proterozoic Carbon Leader placer, Witwatersrand Supergroup, South Africa: J. Geological Society of London, v. 142, p. 757-764.

Burroughs, W. A., 1982, Direct determination of hydraulic equivalence using fluorescent sand tracers in the beach nearshore zone, unpublished Ph.D. thesis, Syracuse University, 139 p.

Camm, G. S., and Hosking, K. F. G., 1985, Stanniferous placer development on an evolving land surface with special reference to placers near St. Austell, Cornwall: J. Geological Society of London, v. 142, p. 803-813.

Cheney, E. S., and Patton, T. C., 1967, Origin of the bedrock values of placer deposits: Economic Geology, v. 62, p. 852-853.

Clifton, H. E., 1969, Beach lamination: nature and origin: Marine Geology, v. 7, p. 553-559.

Crampton, F. A., 1937, Occurence of gold in stream placers: Mining Journal, v. 20, p. 3-4, 33-34.

Danna, J. G., 1985, Experimental study of clast orientation in gravels deposited by unidirectional flow, unpublished M.S. thesis, Massachusetts Institute of Technology, 84 p.

Dhamotharan, S., Wood, A., Parker, G., Stefan, H., 1980, Bedload transport in a model gravel stream: University of Minnesota, St. Anthony Falls Hydaulic Laboratory, Project Report No. 190, 75 p.

Eliseev, V. I., 1981, Placers of the coastal areas outside the U.S.S.R. and their genetic types: Lith. and Min. Resources, v. 15, p. 324-332.

Ewing, C. J. C., 1931, A comparison of the methods of heavy mineral separation: Geological Magazine, v. 68, p. 136-140.

Grigg, N. S., and Rathbun, R. E., 1969, Hydraulic eqivalence of minerals with a consideration of the reentrainment process: U.S. Geological Survey Prof. Paper 650-B, p. B77-B80.

Gunn, C. B. 1968, Origin of the bedrock values of placer deposits, Discussion: Economic Geology, v. 63, p. 86.

Hails, J. R., 1976, Placer deposits, in Wolf, K. H., ed., Handbook of Strata-Bound and Stratiform Ore Deposits, Volume 3, Supergene and Surficial Ore Deposits; Textures and Fabrics, Elsevier Publishing Co., Amsterdam, p. 213-244.

Hall, A. M., Thomas, M. F., and Thorp, M. B., 1985, Late Quaternary alluvial placer development in the humid tropics: the case of the Birim diamond placer, Ghana: J. Geological Society of London, v. 142, p. 777-787.

Hand, B. M., 1967, Differentiation of beach and dune sands using settling velocities of light and heavy minerals: J. Sed. Petrology, v. 37, p. 514-520.

Kartashov, I. P., 1971, Geological features of alluvial placers: Economic Geology, v. 66, p. 879-885.

Kogan, B. S., Noprasnikova, L. A., and Ryabtseva, G. I., 1975, Distribution and origin of local beach concentrates of gold as in one of the bays in South Primor'ye: Internat. Geology Rev., v. 17, p. 945-949.

Komar, P. D., and Wang, C., 1984, Processes of selective grain transport and the formation of placers on beaches: J. Geology, v. 92, p. 637-655.

Krapez, B., 1985, The Ventersdorp Contact Placer: a gold-pyrite placer of stream and debris-flow origins from the Archean Witwatersrand Basin of South Africa: Sedimentology, v. 32, p. 223-234.

Kuzvart, M., and Bohner, M., 1978, Prospecting and Exploration of Mineral Deposits: Developments in Economic Geology Vol. 8, Elsevier Publishing Co., Amsterdam, 431 p.

Lindgren, W., 1911, The Tertiary gravels of the Sierra Nevada of California: U.S. Geological Survey Prof. Paper 73, 226 p.

Lowright, R., Williams, E. G., and Dachille, F., 1972, An analysis of factors controlling deviations in hydraulic equivalence in some modern sands: J. Sed. Petrology, v. 42, p. 634-645.

McGowan, J. H., and Groat, C. G., 1971, Van Horn Sandstone, west Texas: an alluvial fan model for mineral exploration: Bur. Econ. Geol., Univ. of Texas, Austin, 57 p.

McIntyre, D. D., 1959, The hydraulic equivalence and size distribution of some mineral grains from a beach: J. Geology, v. 67, p. 278-301.

McQuivey, R. S., and Keefer, T. N., 1969, The relation of turbulence to deposition of magnetite over ripples: U.S. Geological Survey Prof. Paper 650-D, p. D244-D247.

Mertie, J. B., 1954, The gold pan: a neglected geological tool: Economic Geology, v. 49, p. 639-651.

Miller, R. L., and Byrne, R. J., 1966, The angle of repose for a single grain on a fixed bed: Sedimentology, v. 6, p. 303-314.

Minter, W. E. L., 1970, Gold distribution related to the sedimentology of a Precambrian Witwatersrand comglomerate, South Africa, as outlined by moving-average analysis: Economic Geology, v. 65, p. 963-969.

----------------, 1976, Detrital gold, uranium, and pyrite concentration related to sedimentology in the Precambrian Vaal Reef placer, Witwatersrand, South Africa: Economic Geology, v. 76, p. 157-176.

Minter, W. E. L., 1978, A sedimentological systhesis of placer gold, uranium and pyrite concentrations in Proterozoic Witwatersrand sediments: in Miall, A. D., ed., Fluvial Sedimentology, Canadian Soc. of Petroleum Geol. Memoir 5, p. 801-829.

----------------, and Toens, P. D., 1970, Experimental simulation of gold deposition in gravel beds: Transactions Geol. Soc. of South Africa, v. 73, p. 89-99.

Mosley, M. P., and Schumm, S. A., 1977, Stream junctions-a probable location for bedrock placers: Economic Geology, v. 72, p. 691-694.

Nami, M., 1983, Gold distribution in relation to depositional process in the Proterozoic Carbon Leader placer, Witwatersrand, South Africa, in Collinson, J. D., and Lewin, J., eds., Modern and Ancient Fluvial Systems, International Assoc. of Sedimentologists Spec. Pub. no. 6, p. 563-575.

Nelson, C. H., and Hopkins, D. M., 1972, Sedimentary processes and distribution of particulate gold in the northern Bearing Sea: U.S. Geological Survey Prof. Paper 689, 27 p.

Overstreet, W. C., White, A. M., Whitlow, J. W., Theobald, P.K., Coldwell, D. W., and Cuppels, N. P., 1968, Fluvial monazite deposits in the southeastern United States: U.S. Geological Survey Prof. Paper 568, 85 p.

Parker, G., Klingeman, P. C., and McLean, D. G., 1982, Bedload and size distribution in paved gravel-bed streams: American Society of Civil Engineers J. Hydraulics Div., v. 108, p. 544-571.

Reid, I., and Frostick, L. E., 1985a, Role of settling, entrainment and dispersive equivalence and of interstice trapping in placer formation: J. Geological Society of London, v. 142, p. 739-746.

-----------------------------, 1985b, Beach orientation, bar morphology and the concentration of metalliferous placer deposits: a case study, Lake Turkana, N. Kenya: J. Geological Society of London, v. 142, p. 837-848.

Reimnitz, E., and Plafker, G., 1976, Marine gold placers along the Gulf of Alaska margin: U.S. Geological Survey Bulletin 1415, 16 p.

Rittenhouse, G., 1943, Transportation and deposition of heavy minerals: Geological Soc. of America Bulletin, v. 54, p. 1725-1780.

Rubey, W. W., 1933, The size distribution of heavy minerals within a water laid sandstone: J. Sed. Petrology, v. 3, p. 3-29.

Schumm, S. A., 1977, The Fluvial System, John Wiley and Sons, New York, 338 p.

Sestini, G., 1973, Sedimentology of a paleoplacer: the gold-bearing Tarkwaian of Ghana: in Amstutz, G. G., and Bernard, A. J., eds., Ores in Sediments, Springer-Verlag, Berlin, p. 275-306.

Shepherd, R. G., and Schumm, S. A., 1974, Experimental study of river incision: Gelogical Society of Amer. Bulletin, v. 85, p. 257-268.

Shields, A., 1936, Anwendung der Ähnlichkeitsmechanik und der Turbulenzforschung auf die Geschiebebewegung: Preuss. Versuchanstalt für Wasserbau and Schiffbau, Berlin, Mitteilungen, v. 26, 26 p. (Transl.: W.P. Ott and J.C. van Uchelen, U.S. Dept. Agric. Soil Conserv. Serv. Coop. Lab. , Calif. Inst. Tech.)

Slingerland, R. L., 1977, The effects of entrainment on the hydraulic equivalence relationships of light and heavy minerals in sands: J. Sed. Petrology, v. 47, p. 753-770.

------------------, 1984, Role of hydraulic sorting in the origin of fluvial placers: J. Sed. Petrology, v. 54, p. 137-150.

------------------, and Smith, N. D., 1986, Occurrence and formation of water-laid placers: Earth Science Reviews (in press).

Smith, N. D., and Beukes, N. J., 1983, Bar to bank convergence zones: a contribution to the origin of alluvial placers: Economic Geology, v. 78, p. 1342-1349.

-----------, and Minter, W. E. L., 1980, Sedimentological controls of gold and uranium in two Witwatersrand paleoplacers: Economic Geology, v. 75, p. 1-14.

Smithson, F., 1930, The reliability of frequency-estimations of heavy mineral suites: Geological Magazine, v. 67, p. 134-136.

Stapor, F. W., 1973, Heavy mineral concentrating processes and density/shape/size equilibria in the marine and coastal dune sands of the Apalachicola, Florida, region: J. Sed. Petrol., v. 43, p. 396-407.

Stavrakis, N., 1980, Opaque heavy minerals of the Katberg sandstone, South Africa: Trans. Geol. Soc. S. Africa, v. 83, p. 17-21.

Steidtmann, J. R., 1982, Size-density sorting of sand-size spheres during deposition from bedload transport and implications concerning hydraulic equivalence: Sedimentology, v. 29, p. 877-883.

Theobald, P. K., Jr., 1957, The gold pan as a quantitative geological tool: U.S. Geological Survey Bulletin 1071-A, 54 p.

Thomas, M. F., Thorp, M. B., Teeuw, R. M., 1985, Palaeogeomorphology and the occurrence of diamondiferous placer deposits in Koidu, Sierra Leone: J. Geological Society of London, v. 142, p. 789-802.

Toh, E. S. C., 1978, Comparison of exploration for alluvial tin and gold, in Jones, M. J., ed., Proc. 11th Commonwealth Mining and Metallurgy Congress, Hong Kong, Trans. Inst. Mining and Metallurgy, p. 269-278.

Turner, B. R., and Minter, W. E. L., 1985, Diamond-bearing upper Karoo fluvial sediments in NE Swaziland: J. Geological Society of London, v. 142, p. 765-776.

Tuck, R., 1968, Origin of the bedrock values of placer deposits, Discussion: Economic Geology, v. 63, p. 191-193.

Valls, H. A., 1985, Occurrences and origin of heavy mineral placers in braided stream facies of the Agujas River, Osa Peninsula, Costa Rica, unpublished M.S. thesis, Pennsylvania State University, 164 p.

Vanoni, V. A., and Brooks, N.H., 1957, Laboratory studies of the roughness and suspended load of alluvial streams: California Inst. of Technology Sedimentation Laboratory, U.S. Army Engineer Division, M.R.D. Sediment Series no. 11, 121 p.

Wertz, J. B., 1949, Logarithmic pattern in river placer deposits: Economic Geology, v. 44, p. 193-209.

Wilcock, P. R., Southard, J. B., and Paola, C., 1985, Bed-load transport of individual fractions in mixed-size sediment, Abstract, Third International Fluvial Sedimentology Conference, Fort Collins, Colorado.

Yeend, W. E., 1974, Gold bearing gravel of the ancestral Yuba River, Sierra Nevada, California: U. S. Geological Survey Prof. Paper 722, p. 1-39.

BIOGRAPHICAL SKETCH

I was born in Evanston, Illinois on May 8, 1953, the third of eight children of Hans and Erma Kuhnle and grew up in Skokie, a suburb just north of Chicago. Throughout my childhood I can remember being fascinated by the natural wonders that my father took time to point out to us during our annual summer travels over parts of the United States. It was during these times that my fascination with natural phenomena grew.

I graduated from Niles North High School in June, 1971. Following high school I completed two years at Oakton Community College and then took a year off from school to work full time. During the year I spent away from school I decided to pursue a career in earth sciences. I began attending Northeastern Illinois University, Chicago, in the fall of 1974, and graduated from there with a B.S. in Earth Sciences in the spring of 1977. I next enrolled at the University of Illinois, Chicago and received a M.S. in Geological Sciences in January, 1981. While at UICC Norm Smith introduced me to many interesting aspects of sediment transport. After UICC Mari Kooiman and I were married. Since that time I have been a graduate student at MIT spending much time in the Experimental Sedimentology Laboratory of John Southard. John's infectious enthusiasm for sedimentology has never ceased to amaze me.

A large change in my lifestyle came about 2 years ago when a daughter, Alyssa, was born to Mari and me. We have rediscovered part of our youth through the eyes of Alyssa.

APPENDIX

The following two pages contain the Fortran computer program used to combine the total transport rate vs. time datasets of Runs L1, L2, and H1 from 30-second samples into 60-second samples, 90-second samples... all the way up to 75 minute samples. This program also calculated the mean and standard deviation for each of these "new" datasets. Values from this program were plotted in Figure 24 of part I.

```
CC THE NUMBER OF DATA POINTS **INUM** MUST BE THE FIRST THING
CC IN THE INPUT DATA.
CC FILEDEFS: 10=DATA INPUT
CC           20= OUTPUT
CC            6= SIGNOFF MESSAGE (PROGRAM IS FINISHED)
CC             (6 DOES NOT NEED A FILEDEF)
CC PROGRAM FOR CALCULATING STANDARD DEVIATIONS FOR SUCCESSIVELY
CC LONGER SAMPLING INTERVALS OF SEDIMENT TRANSPORT VS TIME DATA.
C THESE LONGER INTERVALS ARE CONSTRUCTED BY SUCCESSIVELY ADDING EVERY
CC 2 DATA POINTS, THEN 3 DATAPOINTS...TO INUM/2.  THE STANDARD DEVIATION
CC AND MEAN VALUE IS CALCULATED FOR EACH OF THESE 'NEW' DATASETS.
CC THE PRIMARY USE OF THIS PROGRAM IS TO FIND THE SAMPLE LENGTH
CC NECESSARY SUCH THAT ONE CAN BE CONFIDENT THAT THE VALUE OBTAINED IS
CC WITHIN 10% OF THE ACTUAL MEAN VALUE OF SEDIMENT TRANSPORT RATE.
      DIMENSION X(320), Y(320), YS(320), SD(200), RMEAN(200)
CC INUM= NUMBER OF DATA PAIRS IN DATASET.
      READ(10,*)INUM
CC READ IN DATASET INTO X AND Y ARRAYS.
      DO 10 I=1,INUM
   10 READ(10,*)X(I),Y(I)
CC CALCULATE AVERAGE DATA VALUE
      AV=0.0
      DO 20 I=1,INUM
   20 AV=AV+Y(I)
      BMEAN=AV/X(INUM)
      WRITE(20,*)'  RUNH3 DATA          '
      WRITE(20,123)BMEAN
  123 FORMAT(/,1X,'MEAN VALUE= ',F15.2,/)
CC CALCULATE STANDARD DEVIATIONS
CC FIRST THE SD FOR 30SEC SAMPLES (ORIGINAL DATA) IS CALCULATED
CC THEN SUCCESSIVELY LONGER SAMPLING LENGTHS ARE USED TO INUM/2.
CC STANDARD DEVIATIONS ARE STORED IN THE SD ARRAY.
CC  INUM2= TOTAL NUMBER OF REFORMATIONS TO BE DONE TO ORIGINAL DATASET.
      INUM2=INUM/2
      INT=0
CC MAIN LOOP- CALCULATES INUM/2 STANDARD DEVIATIONS
CC VARIABLE 'INT' = NUMBER OF DATA POINTS TO BE ADDED TOGETHER
CC TO FORM ONE VALUE FOR THE 'NEW' SET.
CC  INUB= NUMBER OF DATA POINTS IN REFORMED DATA SET
      DO 30 I=1,INUM2
      SI=0.0
      SI2=0.0
      INT=INT+1
      INUB=INUM/I
CC THE NEXT TWO LOOPS REFORM THE DATASET INTO EFFECTIVELY LONGER
CC SAMPLES; FROM TWICE AS LONG AS THE ORIG.TO 1/2 THE DATEASET LENGTH.
      DO 40 IJ=1,INUB
      JB=INT*IJ
      COL=0.0
      DO 50 JR=1,INT
      COL=COL+Y(JB)
      JB=JB-1
   50 CONTINUE
CC RETAIN REFORMED DATASETS IN YS-ARRAY FOR LATER USE(IE PLOTTING)
      YS(IJ)=COL
```

```
      SI=SI+COL
      SI2=SI2+COL**2
   40 CONTINUE
      RMEAN(I)=SI/FLOAT(INUB)
      SD(I)=SQRT((SI2-SI**2/FLOAT(INUB))/FLOAT(INUB))
   30 CONTINUE
CC MAKE DATA SUITABLE FOR PLOTTING SAMPLE LENGTH(MIN) VS. (SD/MN)*100.0
CC (STANDARD DEVIATION/MEAN)*100 = COEFFICIENT OF VARIATION.
      DO 73 I=1,INUM2
      TINT=FLOAT(I)/2
      PER=(SD(I)/RMEAN(I))*100.0
      WRITE(20,74)TINT,PER
 73   CONTINUE
 74   FORMAT(1X,F4.1,1X,F6.2)
CC PRINT OUT THE DATA:
C     WRITE(20,2)
C     WRITE(20,5)
C     WRITE(20,6)
C     DO 1000 I=1,INUM2
C     TINT=FLOAT(I)/2
C     PER=(SD(I)/RMEAN(I))*100.0
C     INU=INUM/I*I
C     PERU=FLOAT(INU)/FLOAT(INUM)*100.0
C1000 WRITE(6,3)TINT,RMEAN(I),SD(I),PER,INU,PERU
 999  WRITE(6,4)
    2 FORMAT(1X,'SAMPLE',3X,'MEAN ',3X,'STANDARD ',3X,'% SD   ',3X,'# PT
     1S',3X,'% PTS')
    3 FORMAT(1X,F5.1,F10.2,1X,F9.2,F10.2,2X,I5,6X,F7.2)
    4 FORMAT(' TH..TH.. THAT S ALL FOLKS!!!')
    5 FORMAT(1X,'LENGTH',3X,'VALUE',3X,'DEVIATION',3X,'TO MEAN',3X,'USED
     1 ',3X,'USED')
    6 FORMAT(2X,'(MIN)',4X,'(GM)',33X,'TO TOTAL PTS')
      STOP
      END
```